NOTE TO USERS

uOttawa

L'Université canadienne
Canada's university

FACULTÉ DES ÉTUDES SUPÉRIEURES ET POSTOCTORALES

uOttawa

L'Université canadienne
Canada's university

FACULTY OF GRADUATE AND POSDOCTORAL STUDIES

Lita E.C. McDonald

AUTEUR DE LA THÈSE / AUTHOR OF THESIS

M.Sc. (Microbiology and Immunology)

GRADE / DEGREE

Department of Biochemistry, Microbiology and Immunology

FACULTÉ, ÉCOLE, DÉPARTEMENT / FACULTY, SCHOOL, DEPARTMENT

The establishment of *in vivo* and *in vitro* models for Myoclonus Dystonia

TITRE DE LA THÈSE / TITLE OF THESIS

Dr. Dennis Bulman

DIRECTEUR (DIRECTRICE) DE LA THÈSE / THESIS SUPERVISOR

CO-DIRECTEUR (CO-DIRECTRICE) DE LA THÈSE / THESIS CO-SUPERVISOR

EXAMINATEURS (EXAMINATRICES) DE LA THÈSE / THESIS EXAMINERS

Dr. Rashmi Kothary

Dr. John Bell

Gary W. Slater

Le Doyen de la Faculté des études supérieures et postdoctorales / Dean of the Faculty of Graduate and Postdoctoral Studies

The establishment of *in vivo* and *in vitro* models for Myoclonus Dystonia

Lita E.C. McDonald

Thesis submitted to the
Faculty of Graduate and Postdoctoral Studies
In partial fulfillment of the requirements
MSc degree in Human and Molecular Genetics

Department of Biochemistry, Microbiology and Immunology
Faculty of Medicine
University of Ottawa

Your file Votre référence
ISBN: 978-0-494-49248-2
Our file Notre référence
ISBN: 978-0-494-49248-2

Table of Contents

Index of Figures

Index of Tables

Acknowledgments

I would like to thank the all of the Bulman laboratory members who were there between September 2004 and August 2006 for all of their support, advice and laughs. In no particular order Dr. David Grimes, Lemuel Racacho, Fengia Xiao, Fabin Han, Andrew Seto, Allison Grimsey, Ashley Byrnes, Graeme Cunningham, Kelly Westaff, Roubing Zou and all of the summer students including Marisa Rossi and Lam Pham. I also had a lot of assistance from the members of other labs of the OHRI. Again in no particular order Melissa Bowerman, Dina Shafey, Darren Yip, Steve Rennick, Marilyn Delorme, Joel Ross, Robert Lanthier and Dr. Robin Parks. I would especially like to thank Heather MacDonald for her help with everything from the cloning of the targeting cassettes, the screening of the ES cell clones to making sure that all the tissue culture supplies were in order; Yves De Repentigny for the blastocyst injection and mouse husbandry; and Dr. Josee Coloumbe for her unending patience in answering my questions and providing invaluable guidance and advice. I would also like to thank the members of my thesis advisory committee Dr. Rashmi Kothary and Dr. Ilona Skerjanc. My gratitude also extends to my supervisor, Dr. Dennis Bulman for his support during the course of my Master's. Not only did Dr. Bulman provide me with a bench space and the materials necessary to perform these experiments, but also excellent workout advice and motivation. I also owe thanks to my parents Patricia & Robert McDonald and my brother Daniel and my sister Heather. Lastly, I would like to mention my partner Mr. Austin Shih who provided me with much needed support, both emotional and in the form of a much needed technical support, during the course of this project.

Abstract

Myoclonus dystonia (DYT11, OMIM 159900) (MD) is a movement disorder characterized by bilateral alcohol responsive myoclonic jerks often seen in combination with dystonia. MD is inherited as an autosomal dominant trait with reduced penetrance upon maternal transmission. Patients with this disorder are not diminished in their intellectual capacity and have a normal life span. In 2001, mutations in the ε-sarcoglycan gene on human chromosome 7q21 were implicated in causing this disorder. Our laboratory identified a 2nd locus on chromosome 18p11 that co-segregates with this disorder, however, a disease causing mutation has not been identified. To establish the function of ε-sarcoglycan within the mammalian brain, I generated a conditional knock-out (CKO) mouse of *Sgce* and utilized bacterial recombineering to generate a cassette that contained a "floxed" exon 1 of ε-sarcoglycan. ES cells that had correctly incorporated the CKO targeting cassette were selected and used to generate 3 chimeric male mice by blastocyst injection or morula aggregation. Once germline transmission of the CKO allele has been established, these mice will be bred to Cre expressing mice to generate an *sgce*^{null}, and recapitulate the phenotype of MD patients. In addition, I also developed an *in vitro* model of MD using RNAi directed against ε-sarcoglycan in the mouse neuroblastoma cell line, N1E-115. Silencing of ε-sarcoglycan in this cell line resulted in a decrease in the neuronal nitric oxide synthase (nNos) and an increase in cell proliferation. This data will provide insight and direction during the characterization of the *sgce*^{null} mice.

Abbreviations

aa	amino acid
AD	autosomal dominant
Amp	ampicillin
AR	autosomal recessive
A/A	antibiotic antimycotic
BAC	bacterial artificial chromosome
β-gal	beta galactosidase
BLAST	basic local alignment search tool
bp	basepairs
Cam	chloramphenicol
°C	degrees celcius
CKO	conditional knock out
cm	centimeters
CMV	cytomegalovirus
DGC	Dystrophin Glycoprotein Complex
ddH_2O	double distilled H2O
dHPLC	denaturing high performance liquid chromatography
DMSO	dimethyl sulfoxide
Dpc	days post coitus
dNTPs	deoxy-nucleotide tri-phosphates
DMEM	Dulbecco's modified eagle medium
ES	embryonic stem
EST	expressed sequence tag
FBS	fetal bovine serum
FD	farady; unit of electrical charge
G418	geneticin
Gapdh	glyceraldehyde-3-phosphate dehydrogenase
Glu	glutamine
GFP	green fluorescent protein
Gy	Gray; unit of radiation
HRP	horseradish peroxidase
Kan	kanamycin
Kbp	kilo-basepairs
Kv	kilo-volts
lacZ	beta galactosidase gene
LB	Luria Burtani
LIF	leukemia inhibitor factor
loxP	locus of cross-over (x) in P1
MEF	mouse embryonic fibroblast
MEM	minimal essential media
min	minutes
ml	milliliters
MOI	multiplicity of infection
NaPy	sodium pyruvate

NCBI	National Centre for Biotechnology Information
NEAA	non-essential amino acids
Neo	neomycin
ng	nanograms
OHRI	Ottawa Health Research Institute
Oligo	oligodeoxyribonucleotide
OMIM	Online Mendelian Inheritence In Man
O/N	overnight
ORF	open reading frame
PAGE	poly-acrylamide gel electrophoresis
PCR	polymerase chain reaction
PBS	phosphate buffered saline
PMSF	phenylmethylsulfonyl fluoride
PTD	primary torsion dystonia
Q-PCR	semi-quantitative PCR
PVDF	polyvinylidene difluoride
RIPA	radioimmunoprecipitation
rpm	revolutions per minute
RT	reverse transcriptase
rt	room temperature
SDS	sodiumdodecylsulfate
sec	seconds
SGC	Sarcoglycan Complex
shRNA	short-hairpin RNA
siRNA	short-interfering RNA
TBST	Tris-Borate Saline Tween-20
Tet	tetracycline
TE	10 mM Tris-HCl pH 8.0, 0.1 M EDTA
TCAG	The Centre for Applied Genomics, Toronto, Ontario
tk	thymidine kinase
UTR	untranslated region
µg	micrograms
µl	microlitres
wt	wildtype
X-gal	5-bromo-4-chloro-3-indolyl-b-D-galactopyranoside

Chapter 1: Introduction

1.1 Dystonias

Dystonias are a heterogeneous group of disorders of which fifteen inherited forms have been described (Table 1). This group of neurological disorders is characterized by sustained involuntary muscle contractions that may affect the arms, legs, trunk, eyelids or vocal cords. The abnormal postures that describe dystonia are a result of concurrent contractions of agonist and antagonist muscles. Often the movements become worse during action, but may improve with the use of "sensory tricks", relaxation or sleep. Dystonic syndromes may be classified descriptively, etiologically or genetically (1). Dystonia may be focal; affecting only one body region i.e. writer's cramp (arm) or blepharospasm (eyes), or generalized; affecting more than one body region. Classification of dystonias is clinically important as it may have implications for prognosis, management and/or treatment. Usually, these disorders do not appear to interfere with normal lifespan and intelligence. Of the fifteen inherited forms of this disease, only six have had causative mutations described (2).

Dyt 1 (OMIM 128100) commonly known as early-onset torsion dystonia, is caused by mutations in the *TOR1A* (*DYT1*) gene on chromosome 9q24 (3). It is inherited as an autosomal dominant trait with variable penetrance. Torsin-A, the protein encoded by this gene, is a member of the AAA+ family of adenosine triphosphatases (AAA+ ATPases), and associated with diverse cellular activities (4). AAA+ ATPases induce conformational changes in their substrates such as unfolding, which may result in the dissociation of otherwise stable protein complexes or aggregates. Typically torsin-A

resides within the lumen of the endoplasmic reticulum (ER), ATP-bound torsin-A is recruited to the nuclear

envelope where it is thought to alter connections between the inner and outer nuclear membranes. Disease causing mutations have been found in the ATP binding domain of this protein that appear to alter nuclear envelope architecture (5,6). These changes are believed to disrupt neuronal communication in the basal ganglia resulting in abnormal movements and postures (3).

Dyt 3 (OMIM 314250) is also known as X-linked dystonia parkinsonism (XPD). XPD is associated with a disease-specific sequence change, 'DSC3', a C-to-T transition at base 797, in exon 4 of GenBank sequence (AJ549245.1). This change resides within the open reading of frame (ORF) of a not yet previously described 'multiple transcript system' composed of at least 16 exons. This multiple transcript system is now known as *DYT3*. There are a minimum of 3 different transcription start sites that encode 4 different transcripts. Two of these transcripts include distal portions of the TATA box-binding protein-associated factor 1 (*TAF1*) gene and are alternatively spliced. Three exons overlap with the inhibitor of growth, X-linked (*INGX*) gene and with a homolog of the cytokine-inducible SH2 protein 4 (*CIS4*) (605118), both of which are encoded by the opposite strand. The exon containing DSC3 is used by all alternative transcripts, making a pathogenic role of DSC3 in XDP likely (7).

Dyt 5 (OMIM 128230) is caused by mutations in the GTP cyclohydrolase 1 (*GCH1*) gene located on chromosome 14q22.1-q22.2, resulting in an autosomal dominant form of

Locus	Designation	OMIM	Clinical features	Age of onset	Mode of inheritance	Chromosome location	Protein
DYT1	AD early onset dystonia, IDT, Oppenheim's dystonia	128100	Early onset PTD starts in limb & often generalizes	<26 yrs	AD, ~30% penetrance	9q34	Torsin A
DYT2	autosomal recessive dystonia	224500	Early onset, generalized or segmental PTD	childhood to adolescence	AR	unknown	N/A
DYT3	X-linked parkinsonism (XPD),"Lubag"	314250	Segmental or generalized PTD with parkinsonism progressive neurodegenerative syndrome	Adult; ave. 35 yrs	X-linked	Xq31	'DSC3'
DYT4	torsion dystonia 4	128101	Whispering dystonia	13-37 yrs	AD	unknown	N/A
DYT5/GCH1	Segawa syndrome, Dopa-responsive dystonia (DRD)	128230	Most often dystonia with parkinsonism, treated with levodopa	usually childhood	AD, incomplete penetrance	14q22.1-q22.2	GCH1
DYT6	adolescent-onset PTD of mixed type	602629	Focal or generalized; cranial, cervical or limb dystonia	Late childhood ave. 19 yrs	AD	8p21-p22	N/A
DYT7	adult onset focal PTD	602124	Adult onset focal dystonia, & postural tremor	Adult, 28 to 70 yrs	AD, incomplete penetrance	18p11.3	N/A
DYT8/PNKD	paroxysmal non-kinesigenic dyskinesia (PNKD), Mount Reback Syndrome	118800	Attacks of dystonia, athetosis, chorea precipitated by hunger, caffeine, alcohol & emotional stress	childhood to early adulthood	AD, incomplete penetrance	2q35	MR1
DYT9/CSE	paroxysmal choreoathetosis with episodic ataxia & spacticity	601042	Involuntary movements & dystonia following exercise, stress and alcohol; spastic paraplegia between attacks	Childhood, 2-15 yrs	AD	1p13.3-p21	N/A
DYT10/PKC	paroxysmal kinesigenic choreoathetosis	128200	Attacks of dystonia/choreoathetosis brought on by sudden movements	Childhood, 6-16 yrs	AD, incomplete penetrance	16p11.2-q12.1 & 16q13-q22.1	N/A
DYT11	myoclonus dystonia, alcohol responsive dystonia	159900	Myoclonic jerks in combination with dystonia, responsive to alcohol	early childhood	AD, incomplete penetrance	7q21-q31	SGCE
DYT12	rapid-onset dystonia-parkinsonism	128235	Acute or subacute onset of generalized dystonia in with parkinsonism	childhood to adulthood	AD, incomplete penetrance	19q13	ATP1A3
DYT13	early and late onset focal or segmental dystonia	607671	Focal or segmental dystonia with onset either in the cranial-cervial region or in the upper limbs; mild course	early childhood to adulthood	AD, incomplete penetrance	1p36.13-36.32	N/A
DYT14	Dystonia 14	607195	Generalized dystonia and parkinsonism	Adult	AD	14q13	N/A
DYT15	Dystonia 15	607488	Highly similar to Dyt11, Myoclonus dystonia	Variable	AD, incomplete penetrance	18p11	N/A

Table 1 Inherited forms of dystonia

dystonia that affects women in a 4:1 ratio to men (8, 9). GCH1 catalyzes the conversion of GTP to D-erythro-7,8-dihydroneopterin triphosphate, the first and rate-limiting step intetrahydrobiopterin (BH4) biosynthesis. BH4 is an essential cofactor for 3 aromatic amino acid monooxygenases: phenylalanine, tyrosine, and tryptophan hydroxylases and is essential for the production of dopamine (8). Patients with this disorder are treated with exogenous levodopa, a precursor to dopamine, resulting in complete remission of their symptoms (9).

Dyt 8 (OMIM 118800) is alternatively known as Mount-Reback Syndrome, Paroxysmal nonkinesigenic dykinesia (PNKD), and Paroxysmal dystonic choreoathetosis (PDC). Mount and Reback (1940) described a five generation family from the southern United States affected by paroxysmal choreoathetosis. Several other families of British and Polish heritage that appear to have this form of dystonia have since been described (10, 11). Patients with this disorder suffer from attacks of dystonia that are a few minutes in duration, lasting only a few minutes, occur a few times a day and are not accompanied by unconsciousness. Precipitating factors for the attacks are alcohol, coffee, hunger, fatigue, and tobacco (12). Using positional cloning and a candidate gene approach, Rainer *et al* (2004) identified mutations in the myofibrillogenesis regulator gene (*MR-1*) on chromosome 2q33-35 (13).

Dyt 11 (OMIM 159900) is commonly known as Inherited Myoclonus Dystonia (IMD) or Myoclonus Dystonia (MD). MD is inherited as an autosomal dominant trait with reduced penetrance upon maternal transmission. Unlike levodopa responsive dystonias, MD has

no known treatment. However patients often find relief from their symptoms with the ingestion of alcohol (2, 14). This disorder is considered to be relatively mild. Patients usually begin to exhibit symptoms in the first or second decade of life and it is not associated with any other cognitive deficits or decrease in life span. Subtle psychiatric abnormalities such a obsessive compulsive disorder (OCD), anxiety and depression have been described in some families with MD (14, 15). In 2001, it was discovered that mutations in the epsilon sarcoglycan (*SGCE*) gene on chromosome 7q21 were responsible for approximately 40% of cases of MD (16, 17). In 2002, Grimes *et al* demonstrated that MD is genetically heterogeneous when they found linkage to a 17cM region on chromosome 18p11 in a large Canadian kindred (18).

Dyt 12 (OMIM 128235) is also known as rapid-onset dystonia-parkinsonism (RPD). Dyt 12 shows an autosomal dominant pattern of inheritance, sudden onset of combined dystonia and Parkinsonism with stabilization in less than four weeks, bulbar symptoms such as dysarthria and dysphagia. Bulbar and arm involvement is often more severe than leg involvement. Patients show moderate or no response to dopamine agonists, and have a normal brain MRI (19). In 2004, de Carvalho Aguiar *et al*, determined that missence mutations in the Na(+)/K(+)-ATPase alpha-3 gene (*ATP1A3*) cause DYT12/RPD. Mutations in this protein are thought impair enzymatic activity and disrupt the electrochemical gradient across the cellular membrane (20).

1.1 Myoclonus Dystonia (OMIM 159900):

MD is relatively rare genetic form of dystonia and is characterized by bilateral alcohol responsive rapid muscle contractions, myoclonic jerks that may involve the arms, legs and trunk and sustained muscle contractions, which is dystonia, resulting in abnormal postures. The age of onset, pattern of body parts affected, penetrance and responsiveness to alcohol are all variable (21). The prevalence of MD within the population is not known, likely due to under reporting and confusion with other forms of dystonia (22, 23). Other terms which have been previously used to describe this disorder include "hereditary essential myoclonus" (24), "familial essential myclonus" (25) and "alcohol responsive myoclonic dystonia" (26).

There have been several manuscripts published that have described MD beginning in the mid-twentieth century. In 1966, Daube and Peters described two families with hereditary essential myoclonus that had affected members occurred in at least four generations, with male-to-male transmission but some skipped generations (27). In 1967, Maljoudji *et al* described a French-Canadian family in which a father and five of his nine children showed onset of myoclonus in the first or second decade and a benign course without seizures, dementia, or neurological signs other than myoclonus (28). Nygaard *et al* 1999 described a large kindred with European and Native ancestry with alcohol responsive IMD. Within this family there were ten definitely affected individuals; four had both myoclonus and dystonia, five had myclonus alone and one had brachial dystonia only. The age of onset within this family was between four and fifteen years of age. Some of the affected family members reported seeking treatment for OCD, depression and anxiety

(21). A key feature of this disorder is the dramatic reduction of symptoms that some patients have with the ingestion of alcohol (2).

The first gene to be associated with MD was the D2 dopamine receptor (*DRD2*) when linkage and a missense mutation in this gene was reported in one family (29). However, additional screening of other MD families disproved this association (30). Linkage to chromosome 9q32-q34, the loci responsible for early onset torsion dystonia (OMIM 128100, DYT1), was ruled out in a Swedish kindred in 1990 and 1994 (26, 31). Linkage analysis using simple sequence repeat polymorphisms was performed on a large German family exhibiting IMD and excluded linkage to a number of different candidate loci included 9q32-q34, DYT1, and 5q31, a subunit of the gamma-aminobutyric acid A receptor, in 1996 (32). In 1996, Nygaard *et al* mapped the locus for MD in the large American kindred of European and Native American ancestry. The locus was mapped to a 28-cM region spanning the markers D7S802 and D7S1799 in 7q21-q31. The highest pair wise lod score was 3.91 at theta of 0.0 at both D7S657 and D7S796 (21). Later linkage studies further refined the locus to a 7.2-cM region (14, 33). Using a positional cloning approach, Zimprich *et al* (2001) identified five different heterozygous loss-of-function mutations in the gene for ε-sarcoglycan (*SGCE*), after they had mapped a refined critical region of 3.2 Mb in 7q21(16). A second locus the co-segregates with MD was described in 2002 on 18p11 (18). However, a disease causing mutation has not yet been identified.

Unlike some other forms of dystonia, there is no known acceptable treatment for the symptoms of MD. For example, patients with Dyt5 and mutations in the *GCH1* gene are successfully treated with exogenous levodopa. GCH1 catalyzes the conversion of GTP to D-erythro-7,8-dihydroneopterin triphosphate and is essential for dopamine production such that supplementation of ameliorates symptoms (9). Individuals with IMD do not show a response to this treatment and is a characteristic that may be used for clinical diagnosis. However, this disorder appears to be highly responsive to the ingestion of alcohol. This is not an acceptable therapy for this disorder as once ethanol ingestion has ceased, there is a rapid rebound of symptoms, often leading patients to chronic alcoholism (2, 26). It has been reported in some families that in addition to MD, there are also subtle psychiatric disorders present. These include OCD, depression, anxiety and psychosis. However, there does not appear to be any negative impact of MD on life span or intelligence (15). Interestingly, unlike some other movement disorders such as Parkinson's disease or Huntington's disease, there does not appear to be any gross morphological change in the structures of the brain that are responsible for the initiation, coordination and control of voluntary movements such as the cerebellum or substantia nigra (Dr. D. Grimes; personal communication).

Several studies found reduced penetrance in the offspring of affected females suggesting the possibility of maternal imprinting (26, 34-37). Human and mouse *SGCE* genes are located within imprinted regions of their respective genomes (38, 39). Grabowski *et al* (2003) utilized a defining feature of imprinted genes, differential methylated regions (DMRs) and bisulphate genomic sequencing to explain the parent of origin affects

observed in MD. CpG dinucleotides within the promoter region and exon 1 of *SGCE* in maternal and paternal uniparental disomy 7 (UPD7) lymphoblastoid cell lines demonstrated a corresponding parent-of-origin specific methylation pattern. The authors were able to conclude that *SGCE* is maternally imprinted. Despite strong evidence for the exclusive paternal expression of *SGCE* in all tissues, there are some cases in which the disease appears to be inherited from the affected mother (40).

1.2 Epsilon sarcoglycan

The *SGCE* gene: encodes the ε member of the sarcoglycan family of proteins, of which there are six members: α, Sgca (OMIM 600119); β, Sgcb (OMIM 600900); δ, Sgcd (OMIM 601411); γ, Sgcg (OMIM 608896); ε, Sgce (OMIM 604149) and ζ, Sgcz (OMIM 608113). These transmembrane proteins come together to form two distinct, hetero-tetrameric complexes that are thought to stabilize the dystrophin glycoprotein complex (DGC). In striated and cardiovascular muscle, the sarcoglycan complex (SGC) is composed of α, β, δ and γ sarcoglycans. In smooth muscle, this complex is composed of ε, β, γ and ζ sarcoglycan (41, 42). An SGC complex has been described in the retina and peripheral nervous system that is composed of β, γ, δ, and ε sarcoglycans (43). However, to date, no SGC has been described in the central nervous system. The limb girdle muscular dystrophies (LGMD) are a specific sub-type of muscular dystrophy that results from mutation of α, β, γ and δ sarcoglycan genes (44). No disease, neuromuscular or otherwise, has been attributed to ζ-sarcoglycan. Interestingly, patients with LGMD do

not appear have a neurological phenotype and conversely patients with MD do not demonstrate involvement of the vascular or striated muscles.

All of the sarcoglycans are single pass glycosylated transmembrane proteins. α-sarcoglycan and ε-sarcoglycan are type I transmembrane proteins, C-terminus facing the cytosol, with hydrophobic signal sequences present on their N-terminal. These two genes share nearly identical intron-exon boundaries and the proteins are 44% identical and 62% similar at the amino acid (aa) level and likely arose during a gene duplication event. This homology extends for the whole length of the molecules with some areas being more highly conserved than others. The regions of the proteins that share particularly high levels of identity are in the extracellular domain (aa 168-191) and the transmembrane domain (aa 283-325). The expression of α is restricted to cardiac and skeletal muscle, whereas ε is expressed in nearly all tissues (45).

γ, δ and ζ-sarcoglycan are also highly related as they share identical intron-exon boundaries and 70% identity at the amino acid level and it is likely that they arose during a gene duplication event. These type II transmembrane proteins are weakly related to β–sarcoglycan with most of the similarity occurring at the location of the cysteine residues located at the C-terminal. The exact function of each of the sarcoglycans within the different SGC's has remained somewhat elusive, although sarcoglycan-null mice have been able to provide some insight into the role of the SGC (41). It is believed that in the striated muscle SGC, the presence of δ-sarcoglycan is essential for the expression

of the other sarcoglycans on the cell surface. However, there is no evidence to suggest that the presence of the other sarcoglycans is not required for this event to occur (44, 46).

The assembly of the SGC at the cell membrane in muscle follows a discrete step-wise process, during which β and δ-sarcoglycans play a critical role. β and δ-sarcoglycan come together to form a core complex, followed by recruitment of γ and then the α sarcoglycans. This heterotetramer is then trafficked the cell surface (47). In the absence of δ-sarcoglycan, the remaining sarcoglycans are unable to assemble within the endoplasmic reticulum (41). In muscle, mutations in one of the sarcoglycans has been shown to disrupt the assembly of the SGC, leading to its absence from the cell surface and LGMD (48, 49). This, however, does not appear to be true for Sgce as the absence of the SGC complex within the skeletal muscle has not been reported in MD patients. In fact, it has been demonstrated that overexpression of ε-sarcoglycan can actually compensate for the lack of SGCA in the mouse model for LGMD type 2D (50). The SGC is also responsible for maintaining the presence of sarcospan (SSPN) (OMIM 601599) at the sarcolemma, as this protein is not present in the muscle tissue of LGMD patients (51).

The *SGCE* gene is located on human chromosome 7q21, in a region of synteny with mouse chromosome 6A1 (52). *SGCE* is composed of 12 exons spanning approximately 70.9Kbp. Exons 8 and 11 are subject to tissue specific alternative splicing (53) (Figure 1). The mouse, human and rat e-sarcoglycan proteins are 437 amino acids in length with a predicted molecular weight of 45 kDa (45). There is a processed pseudogene located

on human chromosome 2q21 that appears to have several exons, however an open reading frame is not present (52). The mouse ε-sarcoglycan protein is 95.9% and 98.2% identical to the human and rat proteins respectively (54). There is a conserved N-terminal signal sequence which targets ε-sarcoglycan to the cellular surface membrane. The extracellular domain contains an asparagine residue, which is presumably the site of glycosylation, and 4 conserved cysteine residues (55). It has not yet been elucidated if these cysteine residues are required for intra or intermolecular interactions. There are 6 potential phosphorylation sites in the C-terminal intracellular domain of ε-sarcoglycan which are conserved between rat, mouse and human. It is likely that they play a role in cell matrix adhesion, as this is the case for the closely related α-sarcoglycan (56).

The temporal and spatial expression pattern of ε-sarcoglycan is distinct from both the closely related α-sarcoglycan and the other sarcoglycans. ε-sarcoglycan is the most widely expressed of all the sarcoglycan proteins as it has been found to be present throughout development and in almost all tissue types examined. The protein expression of ε-sarcoglycan is highest within the central nervous system (CNS) and the lung, although protein and *SGCE* mRNA have also been detected in the heart, liver, kidney and skeletal muscle. ε-sarcoglycan has been detected as early as embryonic (E) day 12 in rat embryos, with expression peaking at E20 and dropping off rapidly towards adulthood (54). In adult rats and mice, it has been found that the areas of highest expression were those that are known to have dense neuronal packing such as the cerebellar molecular layer, the cerebral cortex and the hippocampus (53, 54). More in depth studies of the expression pattern of ε-sarcoglycan within the mammalian brain have shown that

Figure 1: The genomic organization of the *Sgce* gene in mouse.

The 3' and 5' untranslated regions are blue and the translated exons are in red. Exon 1 of the gene *paternally expressed gene 10* (*Peg10*) is green. Nucleotide distances are indicated for between exon 1 of *Peg10* and *Sgce* and between exon 1 and exon 2 of *Sgce*. Those exons of *Sgce* that are known to be alternatively spliced are indicated by a *.

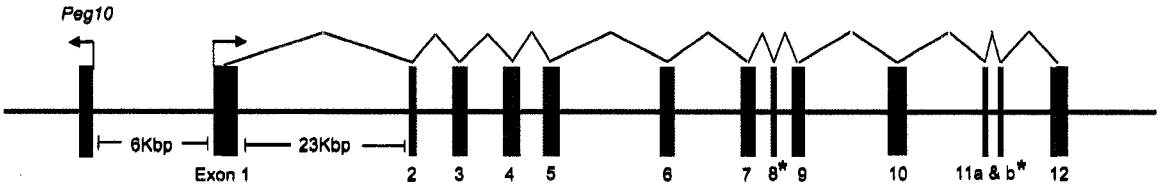
Peg10
6Kbp
23Kbp
Exon 1
2
3
4
5
6
7
8*
9
10
11a & b*
12

expression is especially high in the mitral cell layer of the olfactory bulb, the Purkinje cell layer in the cerebellum and the monoaminegic neurons in the mouse midbrain (57). Subcellular fractionation experiments have indicated that □-sarcoglycan is found in presynaptic and postsynaptic regions of neurons (53).

ε-sarcoglycan has been found to be present in the serotoninergic neurons of the dorsal raphe nucleus (57). Patients with OCD, one of the psychiatric symptoms that often accompanies MD, are known to have reduced serotonin transmission in this area of the brain (58). The monoaminergic neurons of the mouse brain also show high level of expression of ε-sarcoglycan and their function appears to be disrupted in mice deficient for ε-sarcoglycan. This was determined by measuring the concentrations of different neurotransmitters within the brains of these mice (57, 59). Many other types of movement disorders have been attributed to defects in this subset of neurons such as Parkinson's disease and patients with mutations in the *GCH1* gene (DYT5) (8, 60).

1.3 The Dystrophin Glycoprotein Complex (DGC)

Components of the DGC include dystrophin (OMIM 300377), dystrobrevin (OMIM 601239) and sarcospan (OMIM 601599) among others. The DGC links the actin cytoskeleton to the extra-cellular matrix and is critical to the stability of the muscle fiber membranes (44). The DGC can be broken down into three subcomplexes (1) the cytoplasmic proteins such as utrophin, dystrophin and syntrophin (2) the membrane spanning α and β dystroglycans and (3) the sarcospan-sarcoglycan complex (Figure 2).

Figure 2: The dystrophin glycoprotein complex within muscle.

The dystrophin glycoprotein complex (DGC) is composed of dystrophin which links the intracellular actin cytoskeleton (purple) to the transmembrane components of the DGC. In addition to its well characterized role in providing structural stability to the sarcolemma, it also has functions in signal transduction and providing scaffolding to proteins involved in signaling such as nitric oxide synthase (Nos). The sarcoglycan complex (SGC) is believed to stabilize the DGC. In smooth muscle the SGC is a heterotetramer composed of ε, β, γ and ζ sarcoglycan and in cardiac and. Adapted with modification from Wheeler *et al* (2003) (44).

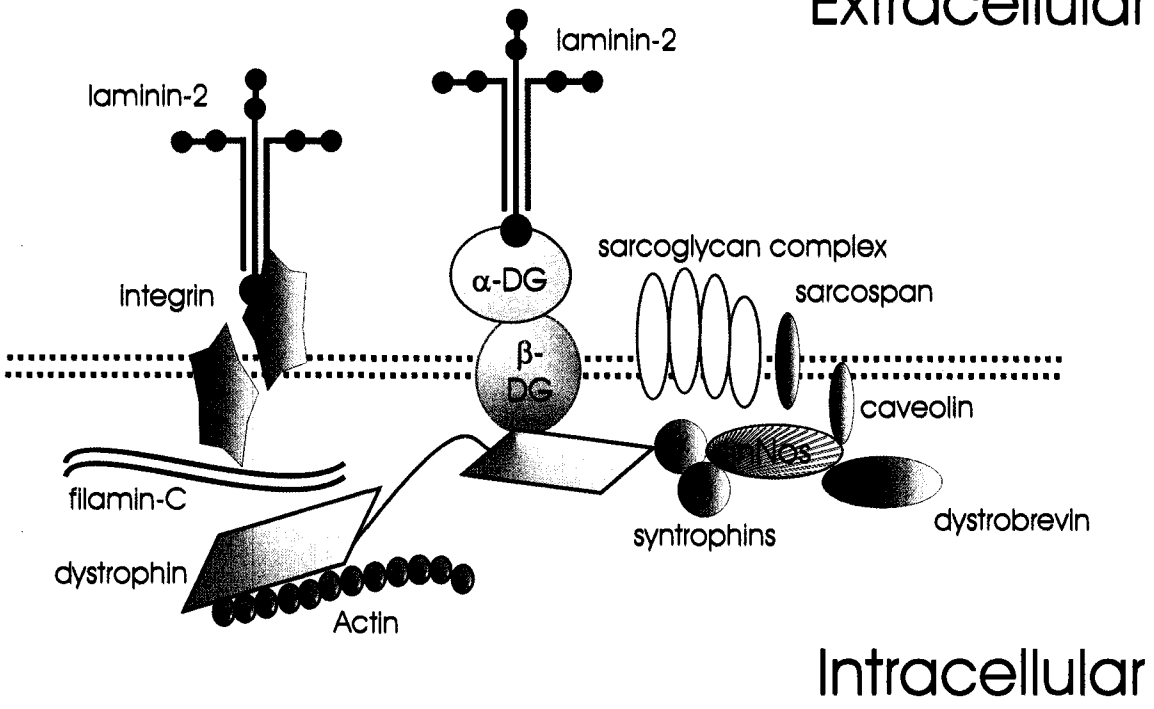
Extracellular
laminin-2
laminin-2
sarcoglycan complex
α-DG
sarcospan
integrin
β-
DG
caveolin
nNOs
filamin-C
syntrophins
dystrobrevin
dystrophin
Actin
Intracellular

Mutations in some of the components of the DGC, including the sarcoglycan proteins (other than ε and ζ) results in a family of disorders known as the muscular dystrophies. The most common of which is Duchenne muscular dystrophy (DMD), which results from mutations in the dystrophin gene on the X chromosome. The muscular dystrophies are characterized by progressive muscle degeneration resulting in weakness and elevated levels of blood creatine kinase. The loss of dystrophin results in the destabilization of the entire DGC, including the SGC. This results in the mechanical link between the sarcolemma and the extracellular matrix being compromised. Conversely, the loss of the sarcoglycans also results in the disruption of the entire DGC complex at the sarcolemma (61).

The DGC has important functions in the establishment and maintenance of the architecture of the CNS, in addition to its role in maintaining the structural integrity of the sarcolemma. Abnormal motor behavior and cerebellar defects have been reported in both DMD patients the *mdx* mouse and mice lacking α and β-dystrobrevin. For DMD patients and the *mdx* mouse, these abnormalities include mild cognitive impairment, decreased motor coordination and impairment in passive avoidance reflex (62, 63). The abnormalities associated with the absence of α and β dystrobrevin include alterations in the structure and function of the inhibitory cerebellar synapses (64). The 50% reduction of the $GABA_A$ channel in DMD patient and the *mdx* mouse model indicates an important role for the DGC in clustering and stabilization of this receptor (65). In addition to its role in the synapse, the components of the DGC are also required for the function of astrocytes to maintain the pial and perivascular basal laminas (66). In the peripheral

nervous system, dystrophin 116 (DP116) and the dystrophin homologue, utrophin (UTRN) are anchored by a unique sarcoglycan-dystroglycan complex (67). UTRN has conserved actin and dystroglycan binding and has been found to be upregulated in DMD patients (68). As UTRN is found within the CNS, it seems plausible that it may play an important role in the stabilization of neurotransmitter receptors in cooperation with DP116.

Gamma-aminobutyric acid, GABA, is the major inhibitory neurotransmitter in the mammalian CNS, and acts by binding to the $GABA_A$ receptor. It has been demonstrated that the alpha-6-subunit of the $GABA_A$ receptor has a distinct role in cerebellar motor control (69). In 2005, a study examining alcohol dependence found linkage to this receptor subunit in two distinct populations: one of Finnish decent and one of Southwestern Native American decent (70). Other neurological disorders have been attributed polymorphism within the subunits of the $GABA_A$ receptor; these include bipolar disorder (71), autism (72), the symptoms, including OCD, which accompany Prader-Willi and Angelman syndromes (73) and juvenile myoclonic epilepsy (74). Although there is significant overlap in the phenotype of patients with MD and those with mutations in the subunits of the $GABA_A$ receptor, no link has been found between the two.

The DGC functions to anchor proteins involved in signaling, such as neuronal nitric oxide synthase (nNos). nNos is one of three isoforms of nitric oxide synthases (Nos), in addition to inducible Nos (iNos) and endothelial Nos (eNos). Nitric oxide (NO) and L-

citruline are the products of nNos as it breaks down L-arginine and O_2 in the presence of nicotinamide adenine dinucleotide phosphate (NADPH) (75). NO acts as a paracrine signaling molecule to regulate a diverse range of functions such as fluid balance (76), contraction and development of muscle (77, 78) and the proliferation and differentiation in the central nervous system (79). nNos is absent from the muscle of patients with DMD and is either absent or significantly decreased in patients with LGMD (80, 81).

In neurons, nNos is anchored in the post-synaptic density through its interaction with the post synaptic density protein 95 (PSD-95) and nitric oxide synthase interacting protein (NOSIP) (82). These in turn function to tether nNos to a complex containing N-methyl-D-aspartic acid (NMDA) subtype of glutamate receptor (83). The activation of the NMDA receptor by glutamate results in an increase in the intracellular Ca^{2+} concentration, which in turn activates nNos through calmodulin (CALM). nNos also interacts with another synaptic protein, C-terminal PDZ ligand of nNOS (CAPON), which complexes with synapsin (SYN1) to mediate neurotransmitter release (84). Furthermore syntrophin-1 (SNT1) binds nNos to the neuromuscular junction in addition to directly binding to dystrophin (85, 86). The interaction between nNos and the NMDA receptor indicates that the DGC may play a role in excitatory transmission (87). *In vitro* cultured neurons derived from *mdx* mice have significantly more cytoplasmic Ca^{2+} when compared to wildtype controls. This increase in Ca^{2+} in addition to reduced nNos may result in dystrophin deficient neurons being particularly sensitive to metabolic offenses resulting in defective synaptic transmission and neuronal death (63).

nNos also plays an important role in regulating the proliferation of neurons *in vivo* and *in vitro* (88-90). During development, the expression of nNos is relatively transient within the mammalian brain and triggers the switch of neuroprogenitor cells (NPCs) from proliferation to differentiation (88). Conversely the inhibition of NO synthesis increases the proliferation rate of NPCs (89). Although the exact target(s) of NO signaling have yet to be determined it is known that NO acts in a concentration dependent paracrine fashion, as it is produced by a cell, neighboring cells exit the cell cycle in response. *In vitro*, nNos expression and NO signaling are required for neurite growth factor (NGF) induced differentiation of PC12 cells (90).

In the brain, NO is involved in activity dependent neurotoxicity , suggesting that there may be a link between NO production and cognitive impairment in individuals with DMD (91). In the musculature of patients with DMD there appears to be defects in the regulation of vasoconstriction and this may be attributed to the loss of sarcolemma nNos activity. This defect in controlling blood flow is thought to contribute to focal necrosis in the muscle of these patients (92). Moreover, it has been reported that supplementation of L-arginine, the substrate of nNos, has been shown to improve *mdx* muscle function (93).

Animals deficient in nNos are known to have behavioral abnormalities in addition to being resistant to neural stroke damage following an ischemic event and having a significant decrease in the number of immature neurons in the olfactory epithelium (79, 94, 95). Although the expression of NOS enzymes is ubiquitous, the highest levels of expression of nNos1 in the mammalian brain are the olfactory bulb and the granule cells

of the cerebellum (79, 96). Coincidentally, these are two of the areas that show high levels of expression of ε-sarcoglycan, although a link between MD and altered nNos expression in the brains of these patients has not yet been made (54, 57).

My hypothesis is that ε-sarcoglycan plays a role in determining neurona architecture in the mammalian CNS and that mutation of this gene perturbs neuronal wiring. By generating an *in vivo* model for MD, I hoped to be able to be able to provide a means of studying the molecular biology of this molecule in a biologically relavent context. I chose to design a conditional knock out (CKO) of exon 1 of *Sgce*. To provide preliminary data to assist in the molecular characterization of the CKO mouse, I also sought to generate an *in vitro* model of MD using RNAi against *Sgce* in the mouse neuroblastoma cell line, N1E-115.

Chapter 2: Establishment of an *In vivo* model for Myoclonus Dystonia

2.1 Materials & Methods

2.1.1 Bacterial Culture and Reagents

E.coli strains DY380 and EL350 and plasmids, pL253, pL451 and pL452 (Table 2) were gifts from Dr. Neal Copeland of the National Cancer Institute (NCI), Frederick, Maryland (97). *E.coli* strains DY380 and EL350 were maintained in Luria Burtani (LB) broth or solid media with the appropriate antibiotics at 32°C unless otherwise indicated. DH5α competent cells (Invitrogen, Carlsbad, CA) were maintained on LB-broth or solid media with appropriate antibiotics at 37°C unless otherwise indicated. Antibiotics were added to a final concentration of 12.5 μg/μl Chloramphenicol (Cam), 12.5 μg/ml Tetracycline (Tet), 25 μg/ml Kanamycin (Kan), and 100 μg/ml Ampicillin (Amp) (Sigma-Aldrich,Oakville, ON) when required.

2.1.2 Identification of the bacterial artificial chromosome (BAC) clone

Three BAC clones of the RPCI-22 (129S6/SvEvTac) mouse BAC library were obtained from The Centre for Applied Genomics (TCAG), Toronto, Ontario, RP22-220M1, RP22-237K16 and RP22-218N16, which had been screened by hybridization of the *Sgce* mouse cDNA to an arrayed BAC library. DNA from each clone was isolated using the GenElute Plasmid Mini-Prep Kit (Sigma-Aldrich, Oakville ON) and sent to TCAG to be sequenced in their DNA sequencing facility. The data was analyzed using DS Gene (Accelrys, San Diego, CA) and aligned to the mouse genome build 35.1 available on the National Centre for Biotechnology (NCBI) database (http://www.ncbi.nlm.nih.gov/). The genomic

Bacterial Strain	Genotype
DH10B	F- *mcrA* D (*mrr–hsdRMS–mcrBC*) φ*80dlacZ ΔM15 ΔlacX74 deoR recA1,endA1 araD139* Δ(*ara, leu*)*7649 ga/Uga/KrspLnupG*
DY380	DH10B [cI857 λ (*cro-bioA* < > *tet*]
EL350	DH10B [cI857 λ (*cro-bioA* < > *araC-P*BAD*cre*]
DH5α	F- φ80d*lacZ*ΔM15 Δ(*lacZYA-argF*) U169, *deoR*, *recA*1, *endA*1, *hsdR*17(rk-, mk+), *phoA*, *supE*44, λ-, *thi*-1, *gyrA*96, *relA*1
Selection Cassettes	
pL451	*FRT–PGK–EM7–NeobpA–FRT–loxP*
pL452	*loxP–PGK–EM7–NeobpA–loxP*
Other Plasmids	
pL253	pBluescript with modified *MC1-TK*
pLM103	retrieval vector with AB and YZ homology arms
pLM104	upstream targeting cassette *CD-loxp-PGK-EM7-NeobpA-loxp-EF*
pLM105	downstream targeting cassette *GH-loxp-FRT-PGK-EM7-NeobpA-FRT-IJ*
pLM106	pLM 103 following targeting with pLM104 and Cre excision of *PGKNeo*
pLM108	CKO targetting cassette
pLM109	CKO targetting cassette following CRE mediate excision of exon 1
237K16	Mouse BAC clone containing *Sgce*; from RPCI-22(129S6/SvEvTac) Mouse BAC Library

Table 2 Recombineering reagents

E.coli strains and plasmid vectors utilized or generated during recombineering experiments. The genotype of the bacteria and plasmids is also given.

sequence corresponding to the *Sgce* gene and surrounding region was downloaded from the NCBI database. This sequence was used for primer design and alignment of sequence data obtained from other experiments.

2.1.3 Cloning of the retrieval and mini-targeting vectors

Polymerase chain reaction (PCR) primers used to amplify the AB and YZ homology arms (Figure 3) for the retrieval vector were designed with *SpeI/HindIII* and *HindIII/NotI* restriction sites, respectively, using the Primer 3 webtool (http://frodo.wi.mit.edu/cgi-bin/primer3/primer3_www.cgi) to facilitate cloning into the pL253 vector. The primer sequences used for all PCR experiments are located in Table 3. The two arms were PCR amplified from the BAC clone RP22-237K16 using the following reagents: 10 mM Tris-HCl pH8.3, 0.5 M KCl, 0.15 mM $MgCl_2$, 25 mM dNTPs, and 0.8 μM of each forward and reverse primer, 1 μl of TAQ DNA polymerase and 70 ng of BAC DNA. Amplification conditions were: (1) 95°C for 5 min; (2) 95°C for 30sec; (3) 61°C for 30sec; (4) 72°C for 30sec; (5) 72°C for 2 min with steps 2 through 4 being repeated for 30 cycles. The resulting PCR products were sequenced to confirm identity using the Big Dye 3.1 Cycle Sequencing kit (Applied Biosystems, Foster City, CA). The AB and YZ PCR products were using the GFX PCR DNA and Gel Band Purification Kit (spin columns) (Amersham Biosciences, Fairfield, CT) and digested with either *SpeI* and *HindIII* or *HindIII* or *Not I* restriction enzymes respectively (Sigma-Aldrich, Oakville, ON). The digested PCR products were again purified by spin column and quantified by gel electrophoresis by comparison of band intensities to the Highranger 1 kb DNA Ladder (Norgen Biotek, St Catherines, ON).

Target	Primer Name	Sequence 5' to 3'
AB homology arm	Sgce-A-Not1F	ATAAGCGGCCGCTCCCCTGCCATAACCATCTG
	Sgce-B-Hind3R	GTCAAGCTTGAAATAGGGGGCTTTTGCTC
YZ homology arm	Sgce-Z-Spe1R	TCTACTAGTGGTATAGGCTGCCAAAGAG
	Sgce-Y-Hind3F	GTCAAGCTTTGCCATGCACTTCTGTGAGG
GH homology arm	Sgce-G-Not1-Xho1-F	ATAAGCGGCCGCCTCGAGCTGTCCGAAGCTCAT GTGTC
	Sgce-H-EcoR1-R	GTCGSSTTCGCATAGAGCGGGACTAGCAC
IJ homology arm	Sgce-I-BamH1-F	ATAGGATCCCCTCACAGCACCCCTCTTT
	Sgce-J-Sal1-R	GTCGTCGACTCAACCAGATCCCAGAGAAAATG
CD homology arm	Sgce-C-Sal1-F	GTCGTCGACCCACCATCATGCAGATAG
	Sgce-D-EcoRV-EcoR1-R	GTCGAATTCGATATATCCGAACGAGCAAATGAAA CGG
EF homology arm	Sgce-E-BamH1-F	ATAGGATCCGTACGCTGAAGCGCATGAAG
	Sgce-F-Not1-R	ATAAGCGGCCGCCTGCAAAGTGACTGGCTCTG
T7 Promoter	T7 Promoter Primer	TAATACGACTCACTATAGGGAGA
T3 Promoter	T3 Promoter Primer	ATTAACCCTCACTAAAGGGA
SP6 Promoter	SP6 Universal Primer	CGATTTAGGTGACACTATAG

Table 3 Primer sequences for PCR amplification of homology arms and sequencing

The primers designed for the generation of the CKO targeting cassette. Please see Figures 3 to 5 for diagrams of corresponding homology arm sequences. The T7, T3 and SP6 promoter primers were used for DNA sequencing throughout the construction of the CKO targeting cassette to confirm the identity of the various PCR products and vectors that were produced.

The pL253 vector contains the *MC1-TK* gene for negative selection in mouse embryonic stem (ES) cells (99). The pL253 plasmid was digested with *NotI* and *SpeI* restriction enzymes and treated with ExoSAP-it, exonuclease I-Shrimp alkaline phosphatase (Amersham Biosciences, Fairfield, CT). The linearized plasmid was then purified by spin column and quantified by gel electrophoresis as previously described. The ligation of the homology arms into the pL253 vector was performed at 16°C overnight (O/N) in a 10μl reaction containing 1U of T4 DNA ligase (Invitrogen, Carlsbad, CA), and 1μl of 10X ligation buffer as supplied by the manufacturer. The ligation reactions were then transformed into DH5α competent cells according to the manufacturer's protocol. DNA from Amp^r resistant clones was screened for the correct cloning of the homology arms by restriction digest with *HindIII*, *NotI* and *SpeI*. This plasmid was then designated as the retrieval vector.

Two mini-targeting vectors were designed to place floxed-neomycin resistance cassettes 5' and 3' of exon 1 of *Sgce*. The homology arms for each of the two cassettes; CD and EF, GH and IJ were amplified by PCR from the BAC clone RP22-237K16 using the same conditions as described above for the homology arms of the retrieval vector (Table 3). Each of the homology arms was sequenced to confirm its identity. The CD and EF homology arms were digested with *SalI/EcoRI* and *BamHI/NotI* respectively and the GH and IJ homology arms were digested with *NotI/EcoRI* and *SalI/BamHI* respectively. Following digestion by the appropriate enzymes, the PCR products were purified and quantified as previously described.

To generate the 5' targeting cassette, the pL452 plasmid was digested with *BamHI* and *EcoRI* restriction enzymes to excise the *loxP-PGKNeo-loxP* cassette. Both the pL451 and pL452 plasmids were obtained from Dr Neal Copeland. To generate the 3' targeting cassette, the pL451 plasmid was digested with *EcoRI* and *BamHI* restriction enzymes to excise the *loxP-frt-PGKNeo-frt* cassette. The digested products were subject to gel electrophoresis; the band corresponding to the cassette was excised, purified by spin column and quantified by gel electrophoresis as previously described. Each of the homology arms and their respective *PGKNeo* cassettes were ligated into the pBluescript as described above.

2.1.4 Electroporation of BAC clone RP22-237-K16 into DY380 E.coli

BAC DNA from *E. coli* that contained the clone RPCI22-237K16 was collected using the GenElute Plasmid Mini-prep Kit (Sigma-Aldrich, Oakville, ON). The DNA was resuspended in 50 µl of 10 mM Tris-HCl pH8.0, 0.1 mM EDTA (TE) buffer. *E. coli* strain DY380 was grown in 5 ml of LB-Tet-broth O/N at 32°C in a shaking incubator. The next morning, DY380 O/N cultures were subcultured 1:20 into 25 ml of LB-Tet-broth and grown at 32°C in a shaking incubator until the culture reached an optical density (OD) 600 nm of 0.6. OD measurements were taken after 3hrs and then every half hour until the cultures reached the desired confluency. The culture was then cooled quickly in an ice water bath for approximately 10 min and 12.5 ml was transferred to one of two pre-chilled glass conical tubes with rubber adapters. The tubes were then centrifuged at 4000 rpm for 10 min at 4°C and the supernatant was discarded. The

bacterial cell pellet was then resuspended in 1ml of ice-cold autoclaved ddH_2O, transferred to a 1.5 ml microfuge tube and centrifuged at 4000 rpm for 5 min at 4°C. The previous step was repeated two more times for a total of three washes with ice-cold ddH_2O. After discarding the supernatant from the final wash, the cells were resuspended in 50 µl of ice-cold ddH_2O.

Twenty micrograms of the BAC clone RPCI22-237K16 that had been freshly prepared was added to the 50 µl DY380 cells and mixed with gentle flicking. The mixture was transferred to a pre-chilled 0.2 cm gap Gene Pulser / Micropulser electroporation cuvette (Bio-Rad Laboratories, Hercules, CA) and subject to electroporation at 175 Kv, 25 µFD and 200 ohms. The bacteria were allowed to recover for 1hr at 32°C in SOC-broth and were plated onto LB-Cam/Tet plates. These were then placed at 32°C and allowed to incubate O/N. Colony PCR to amplify the AB homology arms was used to confirm the presence of RP22-237K16 in the Cam^r/Tet^r clones. One clone was chosen that contained RP22-237K16 and was utilized for recombineering experiments.

2.1.5 Recombineering to generate Gap-Repaired Retrieval vector

One DY380 clone that was confirmed to carry RP22-237K16 by PCR was grown as described above to an OD600 nm of 0.6 in 25 ml of LB-Cam/Tet. Ten milliliters of the culture was transferred to a clean 250 ml Erlenmeyer flask and incubated at 42°C for 15 min in order to induce the expression of the λ Red recombination proteins. The remaining 15 ml culture was returned to the 32°C incubator to act as an "un-induced" control. Following the 15 min incubation, both of the flasks were then transferred to an

ice water bath and cooled as quickly as possible while shaken gently for 10 min. The bacteria were then collected by centrifugation in pre-chilled glass centrifuge tubes, with rubber adaptors, at 4000 rpm for 10 min at 4°C. The bacterial cell pellet was then washed a total of 3 times with 1 ml of ice-cold ddH_2O, and centrifuged again at 4000 rpm at 4°C in order to remove any traces of media.

Following the final centrifugation, the bacterial cell pellet was resuspended in 50 µl of ice-cold ddH_2O. Twenty nanograms of *HindIII* digested, linearized, retrieval vector was added to the bacterial mixture (Figure 3). The bacteria and DNA mixture was then transferred to a pre-chilled electroporation cuvette, subjected to electroporation at 175 Kv, 25 µFD and 200 ohms, removed from the cuvette and allowed to recover in SOC-broth for 1hr at 32°C in a shaking incubator. After the recovery period, the induced and un-induced samples were plated onto LB-Amp/Tet plates and were incubated at 32°C overnight. Amp^r/Tet^r clones were selected for plasmid DNA collection and streaked out onto LB-Amp/Tet plates for single colony isolates (SCI's).

The GenElute Plasmid Mini-prep Kit was used to collect and purify the gap repaired plasmid. Approximately, 200 ng of plasmid DNA was digested with *EcoRI* and the digest fragment sizes were resolved by gel electrophoresis. Due to the possibility of rolling replication and the generation of long concatamers, the gap repaired plasmid, renamed pLM103, was transformed into DH5α bacteria according to the manufacturer's protocol.

Figure 3: Gap-repaired mediated retrieval of 10.9Kbp genomic DNA from BAC.

The AB (light green) and YZ (purple) homology arms were PCR amplified from the BAC clone RP22-237K16 and cloned into the *MC1-TK* containing plasmid using primers A, B and Y, Z. This plasmid was then linearized using *HindIII* to create a double strand break for gap repair. A 10.9Kbp fragment was subcloned into the linearized retrieval plasmid via homologous recombination to generate the gap repaired plasmid pLM103.

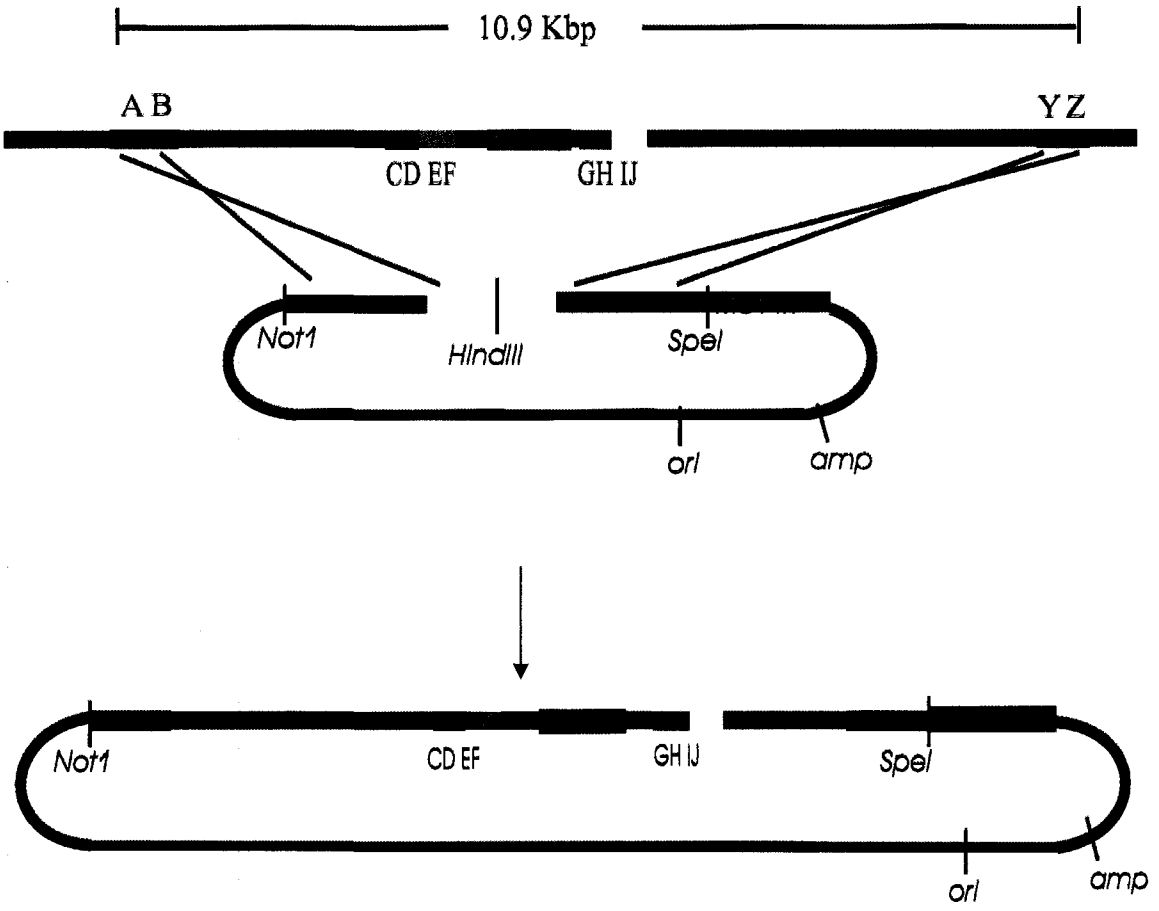
10.9 Kbp
A B
Y Z
CD EF
GH IJ
Not1
HindIII
SpeI
ori
amp
Not1
CD EF
GH IJ
SpeI
ori
amp

2.1.6 Targeting of the first loxP site into pLM103

The 3' mini-targeting cassette was constructed such that it would introduce a *loxP* site 1000 bp upstream of exon 1 of *Sgce* as described above. The 3' mini-targeting cassette was digested with *NotI* and *SalI* to excise the *loxP-PGKNeo-loxP* cassette and the CD and EF homology arms. The digest products were subject to gel electrophoresis and the corresponding band was excised and purified by spin column. DY380 cells that contained pLM103 were prepared in the same manner as was described for recombineering to generate the gap repaired retrieval plasmid. Thirty-five nanograms of the purified 3' mini-targeting cassette was transformed into the pLM103 containing bacteria by electroporation using the same conditions as previously described. Bacteria that had undergone recombination to integrate the 3' mini-targeting cassette into pLM103 were Amp^r/Kan^r, conferred by the presence of the *PGKNeo* gene and the Amp resistance cassette on the vector backbone. During recombination a mixed population of targeted and non-targeted plasmids results and it was necessary to purify the mixed population of plasmids by retransformed into DH5α bacteria and selection with Kan only.

The excision of the *PGKNeo* cassette was achieved by electroporation of 5 ng of the targeted plasmid DNA into *E.coli* EL350 using the same conditions as described above, in which Cre expression had been induced by arabinose and selected on Amp or Kan. Amp^r colonies were plated onto Kan plates and allowed to incubate O/N at 32°C. The excision of the *PGKNeo* cassette was confirmed by restriction digest with *EcoRI*. This plasmid was designated pLM106 (Figure 4).

Figure 4: Targeting of 3' *loxP* and Cre mediated excision of the *PGKNeo* cassette

(**A**) The 5' mini-targeting cassette was constructed by ligating the CD (dark green) and EF (pink) PCR products, amplified using primers C,D and E,F, on either side of the floxed *PGKNeo* cassette within pL452. An *EcoRV* site was included in the mini-targeting cassette to assist in diagnosing gene targeting in ES cells.

(**B**) The excised targeting cassette was transformed in to recombination competent DY380 cells containing pLM103.

(**C**) Amp^r/Kan^r recombinants had the floxed *PGKNeo* cassette inserted 1000bp 5' of exon one.

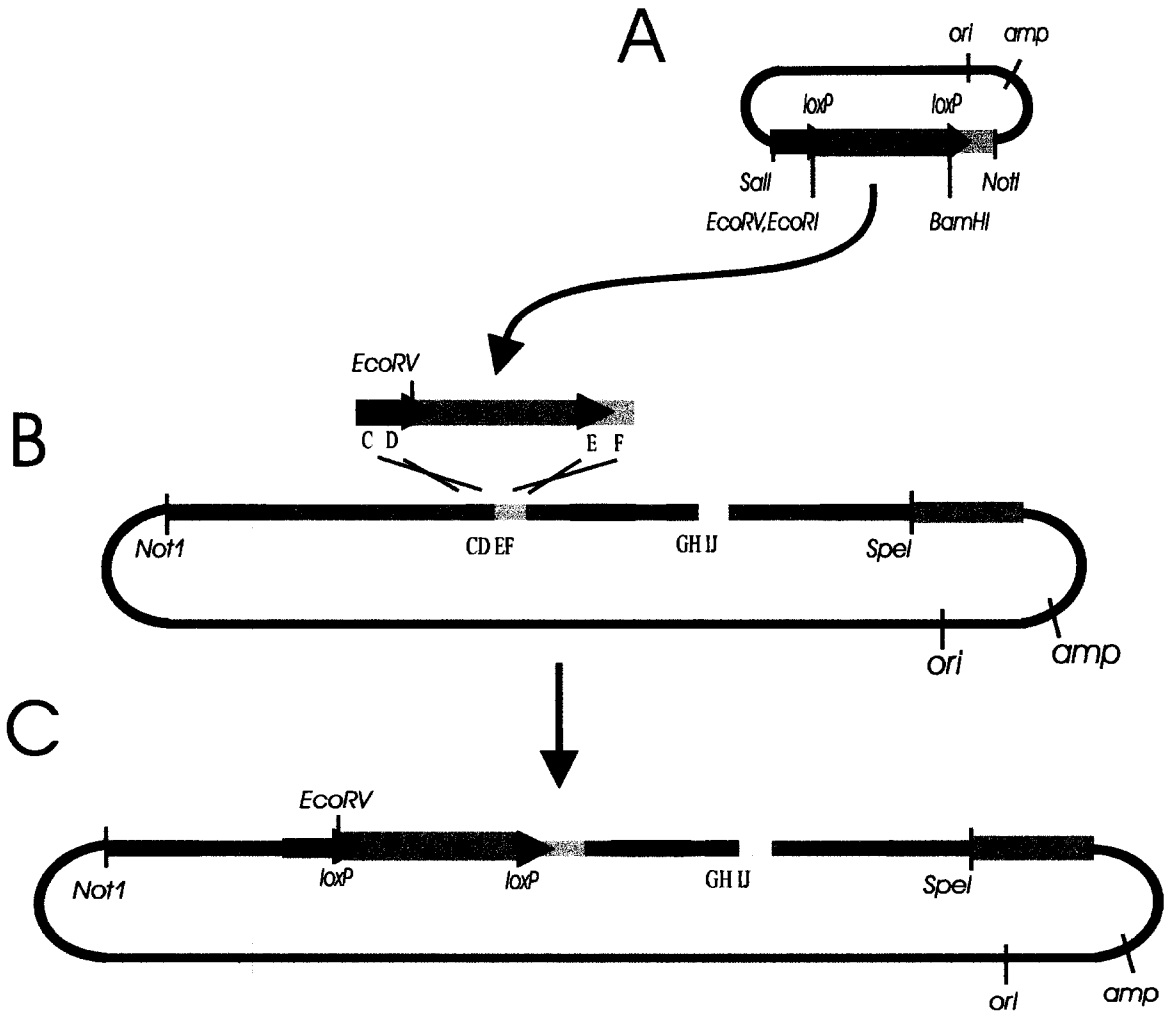
A
ori
amp
loxP
loxP
SalI
NotI
EcoRV,EcoRI
BamHI
B
EcoRV
C D
E F
Not1
CD EF
GH IJ
SpeI
ori
amp
C
EcoRV
Not1
loxP
loxP
GH IJ
SpeI
ori
amp

2.1.7 Targeting of the second loxP site into pLM106

The 5' mini-targeting cassette was designed such that it would integrate approximately 300 bp downstream of exon 1 of *Sgce* as described above. The *loxP-frt-PGKNeo-frt* cassette was excised by digestion with *NotI* and *SalI* and purified by gel electectrophoresis and spin column. DY380 cells that contained pLM106 were prepared in the same manner as described above to generate the gap repaired retrieval plasmid. Bacteria that contained pLM106 were transformed with 100 ng of the purified 5' mini-targeting cassette by electroporation as previously described and selected for on LB-Amp/Kan plates. To purify the mixed plasmids, DH5α cells were transformed and selected for with Kan. To confirm that the second targeting had been successful, plasmid DNA from these colonies were screened by digestion with *EcoRI.* This plasmid was designated pLM108; the conditional knockout (CKO) targeting cassette (Figure 5).

2.1.8 Preparation of pLM108 for electroporation into mouse ES cells

To obtain enough pLM108 of sufficient purity and quantity for the targeting experiments in ES cells, it was necessary to do large scale cesium chloride (CsCl) buoyant density gradient centrifugation preparations. The concentration and purity of each preparation was confirmed by gel electrophoresis and digestion with *EcoRI.* Approximately 1 mg of plasmid was obtained from each preparation and stored at -80°C in TE. One-hundred micrograms of pLM108 was digested with *NotI* and purified by spin column and resuspended in 1X phosphate buffered saline (PBS). The concentration of the digest product was determined by gel electrophoresis versus a standard DNA ladder, *HindIII* digested λ DNA (Sigma-Aldrich, Oakville, ON).

Figure 5: Targeting of 5' *loxP* site

(**A**) The 3' mini-targeting cassette was constructed by ligating the GH (dark red) and IJ (light yellow) PCR products, amplified using primers G,H and I,J, on either side of a *loxP-frt'd PGKNeo* cassette within pL451. A *XhoI* site was included the mini-targeting cassette to identify Cre mediated recombination between the *loxP* sites that would flank exon 1.

(**B**) The excised mini-targeting cassette was transformed into recombination competent DY380 cells that contained pLM106. Amp^r/Kan^r recombinants had the *loxP-frt'd PGKNeo* cassette inserted 300bp 3' of exon 1.

(**C**) The completed CKO targeting cassette; pLM108

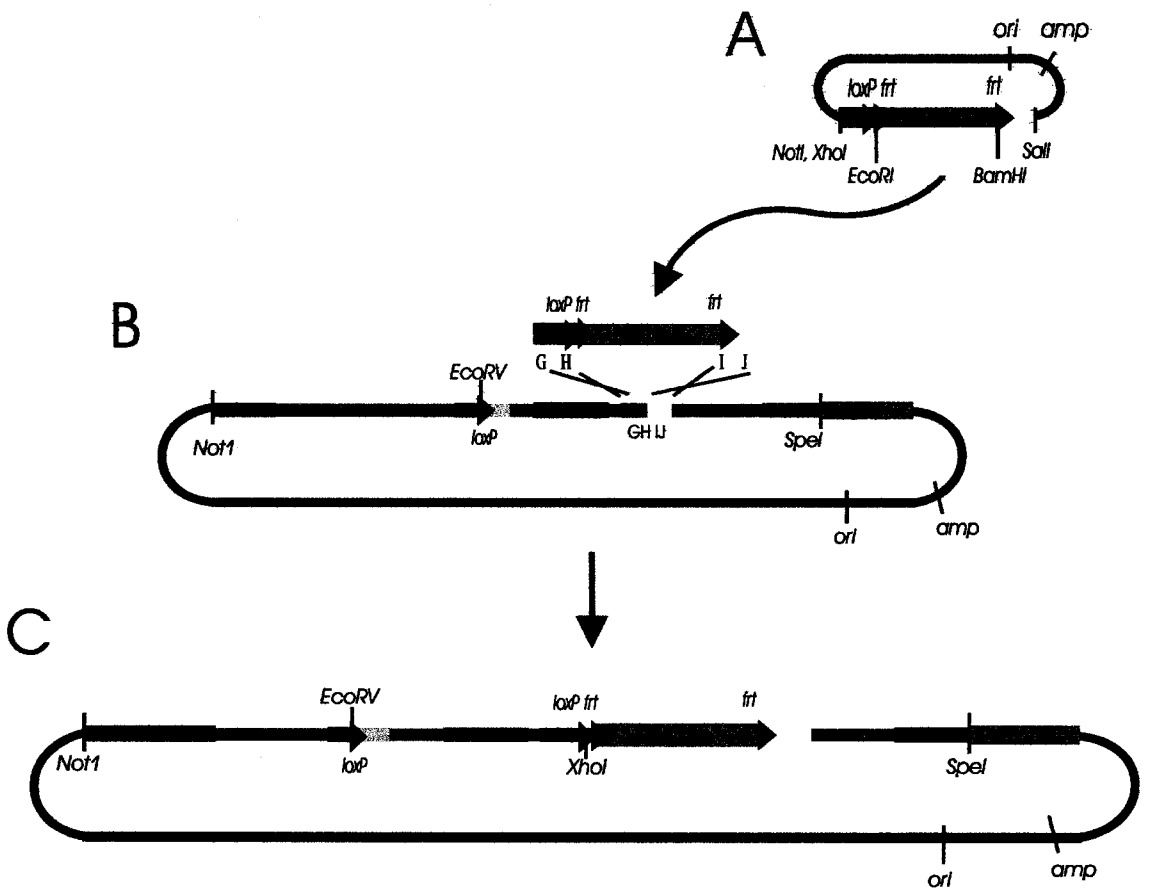
A
ori
amp
loxP frt
frt
NotI, XhoI
EcoRI
BamHI
SalI
B
loxP frt
frt
G H
I J
EcoRV
loxP
GH IJ
Not1
SpeI
ori
amp
C
EcoRV
loxP frt
frt
Not1
loxP
XhoI
SpeI
ori
amp

2.1.9 ES tissue culture reagents and conditions

Both J1 (129S4/SvJae) and V6.5 (129S4 x C57BL/6) ES cells were a gift from Dr. Micheal Rudnicki, Ottawa Health Research Institute (OHRI). The ES cells were maintained in ES complete medium containing Dulbecco's modified eagle medium (DMEM) with glucose, 1X glutamax (glu), 1X non-essential amino acids (NEAA), 1X sodium pyruvate (NaPy), 1X antibiotic/antimycotic (A/A), 0.1 M β-mercaptoethanol (all from Sigma-Aldrich, Oakville, ON) 15% toxicity tested fetal bovine serum (FBS) (Hyclone, Logan, UT) and murine leukemia inhibitory factor (LIF) (Chemicon International Inc, Temecula, CA). Drug resistant 4 (DR4) live mouse embryonic fibroblasts (MEF) were obtained from Dr Josee Coloumbe of the laboratory of Dr. Micheal Rudnicki and maintained in MEF medium containing DMEM with glucose, 1X glu, 1X NaPy, 1X NEAA, 1X A/A and 10% FBS. The HEK293 cell line was a gift from Dr. Robin Parks and were maintained in minimal essential media (MEM) with glucose, 1X glu and 10% FBS. All cell lines were maintained at a temperature of 37°C and 5% CO_2. Gelatin coating of plates for MEF and ES cell culture was achieved by pipetting 5 ml of a 0.1% w/v gelatin (Sigma-Aldrich, Oakville, ON) 1X PBS solution per 10 cm dish, swirling the dish until the entire surface was coated and removal of the excess solution prior to plating cells.

2.1.10 Preparation of feeder mouse embryonic fibroblasts

Frozen vials containing $1X10^6$ DR4 MEF's were thawed and transferred into a 15 cm tissue culture dish (Falcon, BD Biosciences, San Jose, CA) containing MEF medium and allowed to grow until the cells reached 90% confluency. The MEFs were then split into

eight 15 cm dishes and grown for another 3 to 4 days until the cultures were approximately 90% confluent. The cells were then trypsinized (Sigma-Aldrich, Oakville, ON) and pelleted in a 50ml conical tube (Falcon, BD Biosciences, San Jose, CA) with MEF medium, counted using a hemacytometer, and exposed to 30 Gy of gamma-irradiation. The cells were then frozen in 10% dimethyl sulfoxide (DMSO), 20% FBS in DMEM at a concentration of $2.5X10^6$ cell aliquots for later use. One vial of frozen feeder MEF's (feeders) was used to seed two 10cm tissue culture dishes (Corning Life Science, Corning NY).

2.1.11 Toxicity testing of serum

One vial of feeders was thawed into two 10 cm dishes that had been coated with 0.1% gelatin, in ES complete medium. One vial of approximately $2X10^6$ J1 ES stem cells was then thawed and seeded into one of the two feeder containing dishes; the other dish was discarded. After 48hrs, another vial of feeders was thawed into six 65 mm gelatin coated dishes (Falcon, BD Biosciences, San Jose, CA). The dish of J1 ES cells was then split equally into each of the 65 mm dishes. After 24 hrs the media was changed to one of five different media that had been prepared containing concentrations of Hyclone FBS (Hyclone, Logan, UT) ranging from 10% to 30%. The media was changed every 24 hrs and the dishes were split when the ES cells appeared to reach a confluency of approximately 60%. The cells were observed daily for 7 days to determine if there appeared to be any toxicity associated with increasing concentrations of serum i.e. changes in morphology and differentiation.

2.1.12 β-Gal staining of ES cells transfected with pRP2044

One 10 cm plate of 90% confluent HEK293 cells was obtained from Dr Robin Parks and one 10 cm plates with 60% confluent J1 ES cells, including feeders, were trypsinized and collected in 50 ml conical tubes. The cells were centrifuged at 2000 rpm for 5 min and re-suspended in 5 ml of room temperature 1X PBS. This step was repeated 3 times to remove all traces of media. Following the final centrifugation, the cell pellet was re-suspended in 700 µl of ice-cold 1XPBS and placed inside a pre-chilled 0.4 cm gap Genepulser / Micro-pulser electroporation cuvette (Bio-rad Laboratories, Hercules, CA). Thirty micrograms of the plasmid pRP2044, which contains a *lacZ* reporter gene, was added and mixed with the cells by gentle flicking. The cells were then subject to electroporation with 240 V and 500 µFD and allowed to incubate on ice for 20 min then removed from the cuvette by washing with room temperature media. The HEK293 cells were plated onto one 10 cm dish and the ES cells were plated onto one 10 cm gelatin coated dish that had been seeded with feeders.

The following day, the media was removed and the cells were washed two times with 1X PBS. One milliliter of fixing solution (0.2% glutaraldehyde, 2% formalin, 2 mM $MgCl_2$ in PBS) was added to each plate and swirled to ensure that it covered the entire surface. The plates were then incubated at room temperature for 5 minutes before the fixing solution was removed and the plates washed twice with 1X PBS. Six milliliters of β-gal staining solution (5 mM $K_4Fe(CN)_6$, 5 mM $K_3Fe(CN)_6$, 2 mM $MgCl_2$ in 1X PBS) was prepared by adding 50 µl of a 20 mg/ml X-gal stock solution per ml of β-gal staining solution. Three milliliters of the X-gal staining solution was then added to each 10 cm

plate and allowed to incubate overnight at room temperature. Images of the staining were then taken using a Zeiss Axioplane Microscrope and images were captured using an Axiocam Rawpro camera (Carl Zeiss Inc, Oberkochen, Germany). The images were processed using Adobe Photoshop V7.0 software (Adobe Systems Inc, San Jose, CA)

2.1.13 RNA collection from ES cells

One vial of passage 19 J1, and passage 23 J1 Clone B3 ES cells were thawed and each plated into one 10 cm gelatin coated dish that had been seeded with feeders and allowed to recover for 24 to 48 hrs. Once the ES cells had reached approximately 50% confluency, the dishes were trypsinized until all of the ES cell colonies had completely dissociated and then replated into one 10 cm dish that had not been coated with gelatin. The dish was then allowed to incubate at 37°C and 5% CO_2 for 15 min to allow the feeder cells to reattach. The media containing mostly unattached ES cells was removed and placed in a 50 ml conical tube. The density of the ES clones was determined using a Bright-line Hemacytometer (Hausser Scientific, Horsham, PA), and $1X10^5$ cells was plated per 35 mm gelatin coated dish (Falcon, BD Biosciences, San Jose, CA) without feeders. The following day, the cells were trypsinized and collected by centrifugation at 2000 rpm for 5 min. The cells were then lysed in 300 µl of Tri-Reagent (Sigma-Aldrich, Oakville, ON) and total RNA was isolated according to the manufacturer's protocol. The RNA was quantified by spectrophotometry and frozen at -80°C for long term storage. One microgram was then subject to random-primed RT-PCR using the following protocol; 1 µg of RNA and 1 ng of random hexamers were mixed, incubated at 70°C for 10 min then cooled quickly on ice. The 20 µl RT-PCR contained 10 mM diothiothreitol

(DTT), 5 ng/μl of dNTPs and 200 U of Superscript II Reverse Transcriptase (Invitrogen, Carlsbad, CA). The reactions were incubated at 42°C for 45 min and 95°C for 10 min and stored at -20°C until required.

The first strand cDNA was subject multiplex PCR to detect the presence of the *Sgce* mRNA and the *Gapdh* mRNA. Primers were designed to detect the transcript of the house-keeping gene, murine glyceraldehyde-3-phosphate dehydrogenase (*Gapdh*), NM_001001303 and of *Sgce*, BC012665. To be sure that only the mRNA transcript would be detected, the cDNA sequence for each gene was downloaded from the NCBI database and primer pairs were selected that were located within different exons using the Primer 3 program. The PCR protocol that was used to amplify the *Sgce* and *Gapdh* PCR products is as follows: 10 mM Tris-HCl pH8.3, 0.5 M KCl, 0.15 mM $MgCl_2$1, 25 mM dNTPs, 0.35 pmol Gapdh forward/reverse primers, 1.35 pmol Sgce forward/reverse primers, 2 μl random-primed cDNA, 1 μl of TAQ DNA polymerase and ddH_2O to a total volume of 30 μl. The amplification conditions were (1) 95°C for 5 min; (2) 95°C for 30 sec; (3) 55°C for 30 sec; (4) 72°C for 30 sec; (5) 72°C for 2 min with steps 2 through 4 being repeated for 30 cycles.

2.1.14 Transfection of ES cells with linearized CKO targeting cassette

One vial of low passage V6.5 or J1 ES cells was seeded onto one 10 cm gelatin coated dishes that had been seeded with feeders. The following day the ES cells were passaged into three 10 cm gelatin coated plates with feeders and allowed to reach approximately 60% confluency. Once the ES cells had reached the desired confluency, the cells were

trypsinized and collected into a 50 ml conical tube. The cells were subject to centrifugation and washing steps as described above. After the final centrifugation, the cells were re-suspended in 700 µl of ice-cold 1x PBS and 35 µg of *NotI* digested, linearized pLM108 was added. The ES cells and pLM108 was then transferred to a pre-chilled 0.4 cm electroporation cuvette and subject to electroporation as described above. Following electroporation, the cells were allowed to incubate on ice for 20min. Ten milliliters of room temperature (rt) ES complete medium was then used to remove the ES cells from the cuvette and the cells were distributed equally amongst five 10 cm dishes that had been seeded with feeders. The following day, the media was switched to "selection media" with LIF, which contained 2 µM Ganciclovir (Sigma-Aldrich, Oakville, ON) and 400 µg/ml of G418 (Sigma-Aldrich, Oakville, ON).

2.1.15 Selection of Ganciclovir and G418 resistant clones

After 4 days in selection media, significant cell death of non-resistant colonies was observed; however, selection was maintained for another 2 to 4 days. After approximately 6 to 8 days, large colonies were visible. Colonies that appeared to be minimally differentiated were isolated and cultured in 24 well tissue culture dishes with feeders (Falcon, BD Biosciences, San Jose, CA). As each individual clone reached 60% confluency, it was passaged in duplicate 6 well tissue culture dishes (Falcon, BD Biosciences, San Jose, CA). One set of 6 well plates was reserved to isolate genomic DNA for Southern Blot analysis, while the other set was used to grow clones to 60% confluency and frozen for long term storage in liquid nitrogen in 10% DMSO, 20% FBS in DMEM.

2.1.16 Screening of Ganciclovir and G418 resistant clones

In order to obtain the maximum amount of DNA, the duplicate 6 well plates (Corning Life Science, Corning, NY) that were to be used for DNA isolation were allowed to overgrow in selection medium; differentiation was not-important as the DNA collected would not reflect any change in this status. After several days, 0.5 ml of lysis buffer (100 mM Tris-HCl pH 8.5, 5 mM EDTA, 0.2% SDS, 200 mM NaCl and 100 μg/ml of Proteinase K (Sigma-Aldrich, Oakville, ON)) was added to each well. Genomic DNA was isolated by ethanol (EtOH) precipitation and 10 μg of DNA from each clone was digested with either 50 U of *XbaI* or *BglII* restriction enzymes (Sigma-Aldrich, Oakville, ON). The digests were then used for Southern blotting experiments with a 0.8Kbp probe that was 1.8 Kbp 5' of the 5' *loxP* site or a 500 bp probe immediately adjacent to the 3' arms of the CKO targeting vector.

2.1.17 Expansion of correctly targeted clones

Those clones that appeared to carry the correctly targeted CKO cassette were thawed and plated into 10 cm gelatin coated plates in the presence of feeders. The clones were then passaged into six 10 cm dishes with feeders and allowed to grow to 60% confluency and then frozen for long term storage in liquid nitrogen as previously described.

2.1.18 Preparation of CKO ES clones for blastocyst injection or morula aggregation

One vial of each clone was thawed into one 10cm gelatin coated plate with feeders and allowed to recover and grow for 24 to 48 hrs. The clones were then passaged 1 in 4 or 1 in 6, depending on the rate of growth, onto one 10 cm plate with feeders. After the clones had reached approximately 60% confluency, the cells were trypsinized and re-plated into a 10 cm dish that had not been coated in gelatin. The culture was incubated for 15 min at 37°C to allow the feeders to re-attach then the media containing mostly un-attached ES cells was removed. The ES clones were maintained in selection medium containing LIF for 48hrs prior to blastocyst injection or morula aggregation experiments.

2.1.19 Collection of 8-cell to morula stage embryos for morula aggregation

CD1 2.5 day post coital (dpc) white female mice (Charles River Laboratories, Wilmington, MA) were sacrificed by cervical dislocation and the oviducts were removed by cutting the fat pad just above the ovary and the oviduct uterus junction. Fat and connective tissue were removed from the oviduct as well as the ovary and the infundibulum was found to be located proximal to the location of the ovary. A 30G needle (flushing needle) (BD Biosciences, San Jose, CA) was prepared by removing the point by rubbing it on a whet stone. The flushing needle attached to a 1 cc syringe (BD Biosciences, San Jose, CA) was then inserted into the infundibulum and approximately 100 µl of M2 medium (Sigma-Aldrich, Oakville, ON) was used to flush out the embryos. The embryos were then transferred by pipette to M16 medium (Sigma-Aldrich, Oakville, ON) and allowed to incubate at 37°C and 5% CO_2 until needed.

2.1.20 Aggregation of morula stage embryos with CKO ES cell clones

Thirty-five millimeter aggregation plates were prepared with 14 drops of M16 medium overlaid with embryo tested mineral oil (Sigma-Aldrich, Oakville, ON) and incubated at 37°C and 5% CO_2 for 30 min. In each drop of M16 medium, 6 "aggregation depressions" were made using a darning needle (BLS, Budapest, Hungary). To remove the zona pellucida from the embryos, they were incubated in Acid Tyrode's solution for 2 to 3 min until the zona pellucida visibly dissolved. The embryos were then transferred individually to an "aggregation depression" in the aggregation plate and aggregates of 5 to 10 ES cells were added to each embryo. The aggregations were allowed to incubate overnight at 37°C and 5% CO_2. The following day the blastocyst stage embryos were transferred into the uterus of 2.5 dpc pseudo-pregnant CD1 females; approximately 10 embryos per uterine horn.

2.2 Results

2.2.1 Generation of the CKO targeting cassette

The 3 BAC clones obtained from The Centre for Applied Genomics (TCAG), Toronto, Ontario, RP22-220M1, RP22-237K16 and RP22-218N16 were end sequenced using flanking T7 and SP6 promoter sites. The sequences were compared to those contained in the mouse genome build 35.1 available on the NCBI database by BLAST search. Only one clone, RP22-237K16, aligned the region surrounding *Sgce* on mouse chromosome 6A1. The sequence of *Sgce* and flanking regions was downloaded from the NCBI database and all primers and sequence alignments were based on this genomic sequence. To subclone by homologous recombination it was necessary to transform RP22-237K16 into the recombination competent *E. coli* DH10B derived strain, DY380. The DH10B strain is one of the few strains of *E.coli* that are readily transformable with BAC DNA. The recombination functions present in DY380 are encoded on a defective lambda prophage integrated into the chromosome. The recombination genes; *exo*, *bet* and *gam* are expressed from the λ P_L promoter, which is under the control of the temperature sensitive λc1857 repressor. At 32°C the expression of these proteins is undetectable; however at 42°C, their expression is strongly induced and functions to protect and recombine the linear DNA targeting cassette with its substrate sequence (97).

Homologous recombination mediated by gap repair was utilized to subclone a 10.9 Kbp fragment from RP22-237K16 into a pBluescript based vector, pL253, containing a modified *MC1-TK* cassette. The AB and YZ homology arms were approximately 500 bp

long, a size which is thought to have optimal retrieving efficiency, correspond to sequences 4 Kbp 5' and 6 Kbp 3 of exon 1 of *Sgce* and thus mark the end points of the fragment to be subcloned. The PCR primers used to amplify these homology arms introduced restriction sites that allowed for directional cloning of the PCR products into pL253. The common *HindIII* restriction site between primers B and Y was used to linearize the retrieval vector and create a DNA double strand break for gap repair (Figure 6a). After inducing the expression of the λ Red recombination proteins by heat shock, recombination between the homology arms and the BAC DNA generated a circular plasmid containing the target DNA. This circularized plasmid was propagated in bacteria and Amp^r was used to select the circular products. The process of recombineering was highly efficient as greater that 55 Amp^r clones were obtained. Of the 10 clones screened by restriction digest with *EcoRI*, all were correctly constructed. The plasmid was designated as pLM103 (Figure 6b, lane 2).

Recombination and repair proteins (Rec) B, C and D are inhibited during the gap repair process. In their absence, ColEI derived plasmids such as pBluescript, and therefore pL253, will replicate by rolling circle replication creating plasmid mutlimers. To prevent this from occurring, the gap-repaired plasmid was transformed in DH5α cells and Amp^r clones were selected. One clone was screened by *EcoRI* digest to ensure that it had not rearranged and was frozen in glycerol for storage at -80°C. All plasmids constructed were transformed into DH5α cells for long term storage.

Figure 6: Restriction digest patterns of retrieval vector and plasmids generated during the construction of the CKO targeting cassette.

(**A**) The retrieval vector was constructed by directional cloning of the AB and YZ homology arms into the vector pL253 using *NotI*, *SpeI* and *HindIII* restriction enzymes. Lane 1: Highranger 1kb DNA Ladder. Lane 2: The linearized retrieval vector following digestion with *HindIII*. Lane 3: Following digestion with *NotI* and *SpeI* to excise the AB and YZ homology arms together. Lane 4: Following digestion with *HindIII*, *NotI* and *SpeI* to excise the AB and YZ homology arms separately. Lane 5: Digestion of pL253 with *NotI* and *SpeI* prior to cloning of the AB and YZ homology arms.

(**B**) Digestion with *EcoRI* was used to follow the construction of the CKO targeting cassette at each step. Lane 2: The gap-repaired retrieval plasmid containing the 10.9Kbp genomic insert; pLM103. Lane 3: Targeting of the 3' floxed *PGKNeo* cassette. Lane 4: Cre mediated excision of the *PGKNeo* cassette leaving behind one *loxP* site; pLM106. Lane 5: Targeting of the 5' *loxP-frt'd-PGKNeo* cassette; pLM108. Lane 6: Cre mediated excision of intervening DNA between the 3' and 5' *loxP* sites, including exon 1 of *Sgce*. Lane 7: *HindIII* digested λ DNA ladder

A

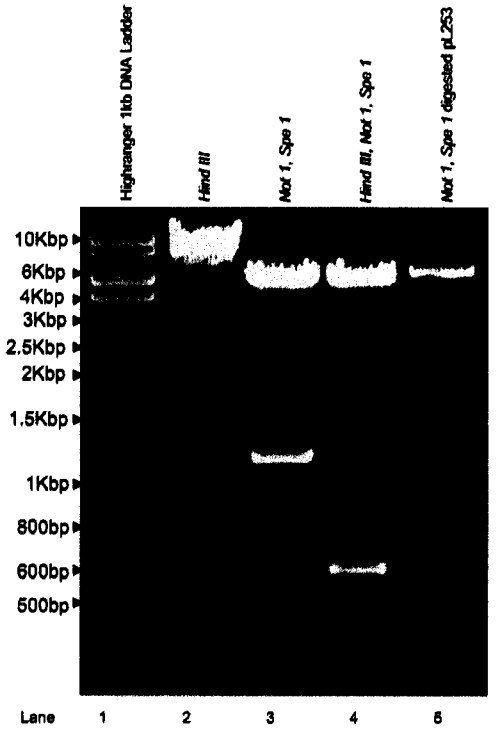
Highranger 1kb DNA Ladder
Hind III
Not 1, Spe 1
Hind III, Not 1, Spe 1
Not 1, Spe 1 digested pL253
10Kbp
6Kbp
4Kbp
3Kbp
2.5Kbp
2Kbp
1.5Kbp
1Kbp
800bp
600bp
500bp
Lane 1 2 3 4 5

B

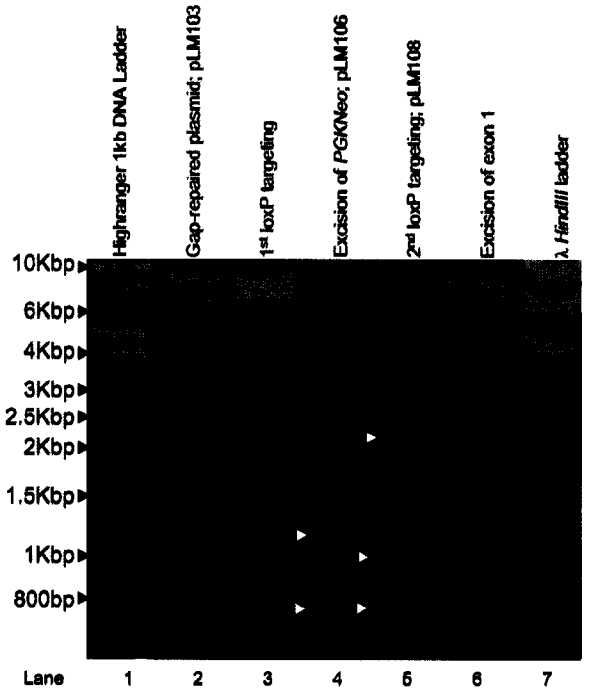
Highranger 1kb DNA Ladder
Gap-repaired plasmid; pLM103
1st loxP targeting
Excision of PGKNeo; pLM106
2nd loxP targeting; pLM108
Excision of exon 1
λ HindIII ladder
10Kbp
6Kbp
4Kbp
3Kbp
2.5Kbp
2Kbp
1.5Kbp
1Kbp
800bp
Lane 1 2 3 4 5 6 7

The next step in the generation of the CKO vector was the cloning of the 5' mini-targeting cassette. The homology arms required for the 5' mini-targeting cassettes were PCR amplified from the BAC clone RP22-237K16. Each set of primers, CD and EF introduced restriction sites, *SalI* and *EcoRV/EcoRI* or *BamHI* and *NotI* respectively. These restriction sites served two purposes; the first was to permit the directional cloning of each 500 bp PCR product on either side of a floxed *PGKNeo* cassette from the plasmid pL452, *loxP-PGKNeo-loxP*, and the second was to screen for correctly constructed clones with *EcoRI*. The *loxP* sites are the 34 bp recognition sequences for the Cre recombinase; when Cre is expressed, the DNA lying between the two *loxP* sites is excised leaving behind one *loxP* site. The *Neo* gene in pL452, which confers resistance to Kanamycin in bacteria and G418 in eukaryotic cells, is expressed from a hybrid *PGK-EM7* promoter. This promoter allows expression in both mammalian and bacterial cells respectively. The homology arms were designed for homologous recombination between themselves and the target DNA in order to introduce a *loxP* site 1000 bp 5' of exon 1 of *Sgce*. These PCR products were cloned sequentially into the pL452 vector on either side of the *loxP-PGKNeo-loxP* cassette. Five Kan^r colonies were selected and screened by restriction digest and sequencing to confirm that they were correctly constructed. This plasmid was designated pLM104. The floxed *PGKNeo* cassette and the flanking homology arms were excised from pLM104 by digestion with *NotI* and *SalI* followed by gel purification of the corresponding band.

Thirty-five nanograms of the purified cassette was transformed into DY380 bacteria that contained gap-repaired plasmid, pLM103, and had been either induced by heat shock or

uninduced for the λ Red recombination proteins. Approximately 5000 Amp^r/Kan^r resistant clones were obtained from the induced DY380 cells whereas only 15 were obtained from the uninduced control. DNA was obtained from 10 of the induced clones and screened for correct integration of the 5' mini-targeting cassette by *EcoRI* digestion, as there was an additional recognition site for this enzyme from the restriction site included in Primer D (Figure 6b, lane 3). All of the clones appeared to have the correct digest fragment pattern; however, there was a mixed population of targeted and non-targeted plasmids present. DH5α cells were then transformed with 1 ng of DNA from one of the clones and selected for Kan^r. As most cells will receive only one plasmid, those that took up the targeted plasmid would be both Amp^r/Kan^r whereas those that took up the non-targeting plasmid wouldn be Amp^r/Kan^s. Empirically, it was determined that this retransformation process eliminates plasmid multi-mers and selects for plasmid monomers. Ten Kan^r clones were selected and screened by *EcoRI* digestion; all of which contained only the correctly targeted plasmid.

In order to remove the *PGK-Neo* cassette from the subcloned plasmid, it was necessary to transform 1 ng of the targeted plasmid into EL350 cells. EL350 *E.coli* is derived from DY380 and carries a *Cre* gene under the control of the arabinose-inducible promoter, P_{BAD}. The expression of Cre was induced for 1 hr in arabinose containing media prior to transformation with the targeted plasmid. As a result, the removal of the PGKNeo cassette would result in the bacteria being Amp^r but Kan^s. The transformed bacteria were plated into Amp or Kan plates. No colonies were obtained from the Kan plate and those that grew on the Amp plate were tested for their Kan sensitivity. Twenty Amp^r/Kan^s

colonies were obtained and screened by *EcoRI* digestion, all of which appeared to contain the correctly constructed plasmid. One clone was selected that gave the correct digest fragment pattern and was designated pLM106 (Figure 6b, lane 4).

The 3' mini-targeting cassette was designed to introduce a second *loxP* site approximately 300 bp 3' of exon 1 of *Sgce*. The GH and IJ homology arms were PCR amplified from the BAC clone Rp22-237K16 with primers which added *NotI* and *EcoRI* or *BamHI* and *SalI* restriction sites respectively. As with the 5' mini-targeting cassette these restriction sites allowed for the directional cloning of the homology arms to flank a *floxed frt-PGKNeo*, *loxP-frt-PGKNeo-frt*, cassette from plasmid pL451. These 370 bp and 812 bp homology arms were cloned into pBluescript along with the *floxed frt-PGKNeo* cassette. Kan^r clones were screened by sequencing from the Primer E and Primer J sites to ensure that they had been correctly constructed. Of the 3 clones screened in this manner, all appeared to be correct. This plasmid was designated pLM105. To generate the 3' targeting cassette, pLM105 was digested with *NotI* and *SalI* restriction enzymes to excise the *loxP-frt-PGKNeo-frt* cassette along with the GH and IJ homology arms.

Integration of the targeting cassette was accomplished by homologous recombination in DY380 cells that carried pLM106. DY380 cells that were either induced by heat shock or uninduced to express the λ Red recombination proteins were transformed with 100 ng of the 3' mini-targeting cassette and selected for Amp^r/Kan^r. More than 1000 Amp^r/Kan^r clones were obtained from the induced DY380 cells and 45 were obtained from the

uninduced control. DNA from 10 induced clones was isolated and screened by digestion with *EcoRI* as there would be an additional recognition site for this enzyme as it was included in Primer H. All the plasmids screened in this manner appeared to be correctly targeted, although there was a mixed population of plasmids. The plasmid was purified by transformation and selection as described for the targeting of the first *loxP* site upstream of exon 1 of *Sgce*. This construct was designated pLM108, the CKO targeting cassette (Figure 6b, lane 5).

To test the *loxP* sites upstream and downstream of exon 1 of *Sgce* within the subcloned DNA, 1 ng of pLM108 was transformed into EL350 cells that had Cre expression induced by arabinose containing media as previously described. The cells were plated onto Amp/Kan media. DNA from Amp^r/Kan^r resistant clones was isolated and subject to digestion with *EcoRI* to confirm Cre mediated excision of the DNA between the *loxP* sites located on either side of exon 1 (Figure 6b, lane 6). All of the clones screened in this manner appeared to have undergone Cre mediated excision between the 5' and 3' *loxP* sites such that the intervening DNA was lost. Therefore subsequent expression of Cre in the ES cells or adult mouse would be expected to result in a *Sgce*-null allele.

To obtain enough CKO targeting cassette of sufficient quality and quantity it was necessary to perform large scale CsCl preparations. Approximately 1 mg of pLM108 was obtained from each large scale preparation. pLM108 was designed to contain a unique *NotI* site immediately outside the region of homology such that it could be

linearized upon digestion with this enzyme. Following digestion with an excess of *NotI*, pLM108 was purified by spin column to remove any protein and other impurities.

2.2.2 β-gal staining of HEK293 and ES cells transfected with pPR2044

To determine the transfection efficiency of HEK293 and ES cells by electroporation, these two cell types were subject to electroporation with pRP2044 and stained for β-gal activity (Figure 7). This vector has a LacZ reporter construct under the control of the highly active elongation factor 1a (*EL1F*) promoter (100). The transfection efficiency of electroporation. in the HEK293 cells was approximately 1.93% whereas the efficiency for the J1 ES cells was approximately 6%.

2.2.3 Serum toxicity testing in ES cells

A serum toxicity test was preformed for 7 days with FBS concentrations ranging from 10% to 30%, in order to determine if there was any toxicity associated with the FBS that had been purchased from Hyclone. After 7 days it was determined that there was no toxicity associated with the higher serum concentrations. However, in medium containing higher the serum concentration, the ES cells appeared to grow more quickly as they reached confluency sooner than those at a lower concentration of FBS. There did not appear to be any overt differences in morphology of differentiation status with any of the different serum concentrations.

Figure 7: Determining transfection efficiency by electroporation with HEK293 cells and J1 ES cells.

HEK293 (**A**) and J1 ES cells (B) were transfected with the vector pRP2044 by electroporation in order to assess transfection efficiency. Staining for β-gal activity was performed and the percentage of positive (blue) cells was calculated for each cell type. The percentage of b-gal positive HEK293 cells was approximately 1.93% and β-gal positive J1 ES cells were 6%.

A

B

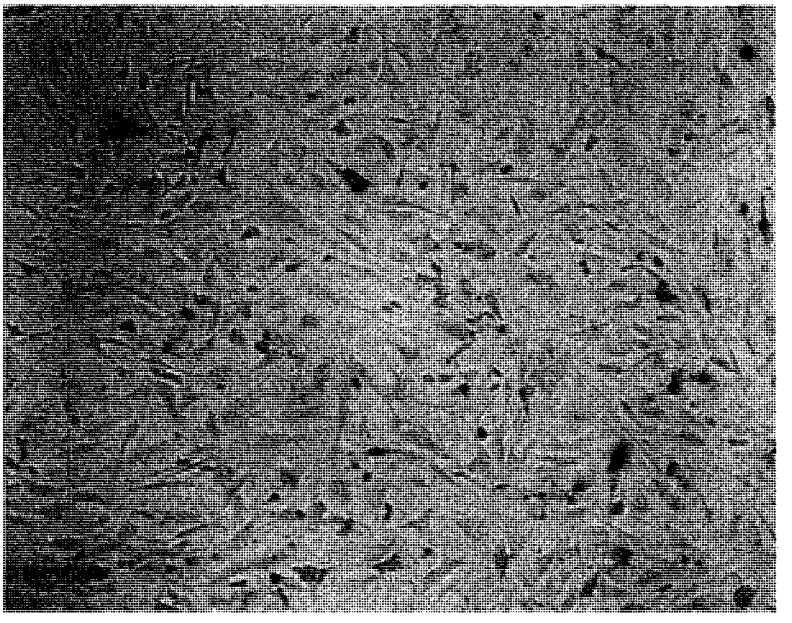

2.2.4 ES cells do not express Sgce

Total RNA was collected from passage 19 J1 and passage 25 J1 clone B3 cells and subject to random-primed RT-PCR to generate first-strand cDNA. This cDNA was then used for multiplex PCR with primers designed to amplify the *Sgce* and *Gapdh* transcripts (Figure 8). A band corresponding to the *Gapdh* PCR product, 600 bp was observed for both J1 and J1 clone B3 ES cells (Figure 8 lanes 2 & 3); however the *Sgce* PCR product, 400 bp was not detected. Lane 4 is the PCR products from a mouse cell line which is known to express *Sgce* and *Gapdh*, N1E-115.

2.2.5 Gene targeting in ES cells

J1 (129S4/SvJae) and V6.5 (129S4 x C57BL/6) were obtained and cultured as described. In each targeting experiment approximately $1X10^6$ cells were subject to electroporation with the linearized CKO targeting cassette. The transformants were selected for $G418^r$/$Ganciclovir^r$ for 7 to 8 days. There were two possible outcomes for gene targeting, the more commonly occurring is random integration of the cassette and the less common being homologous integration of the CKO cassette at exon 1 of *Sgce*. Homologous recombination may occur anywhere along the targeting cassette and the corresponding region of the genome. The presence of the positive selection marker, the 3' PGKNeo cassette, confers resistance to G418, which is likely to be retained in both random and homologous integration events. The *MC1-TK* gene, which lies outside of the region of homology, provides negative selection in the case of random integration of the CKO

Figure 8: ES cells do not express *Sgce*.

Total RNA was isolated from passage 19 J1 ES cells, lane 2, passage 25 J1 ES cell clone B3, lane 3, and the mouse neuroblastoma cell line which is known to express *Sgce*, N1E-115, lane 4. I performed multi-plex PCR to amplify the *Gapdh* transcript (600bp product), as a positive control for the RT-PCR and PCR, and *Sgce* transcript (400bp). The product for *Gapdh* is visible in all lanes; however the *Sgce* product is visible only in the N1E-115 lane.

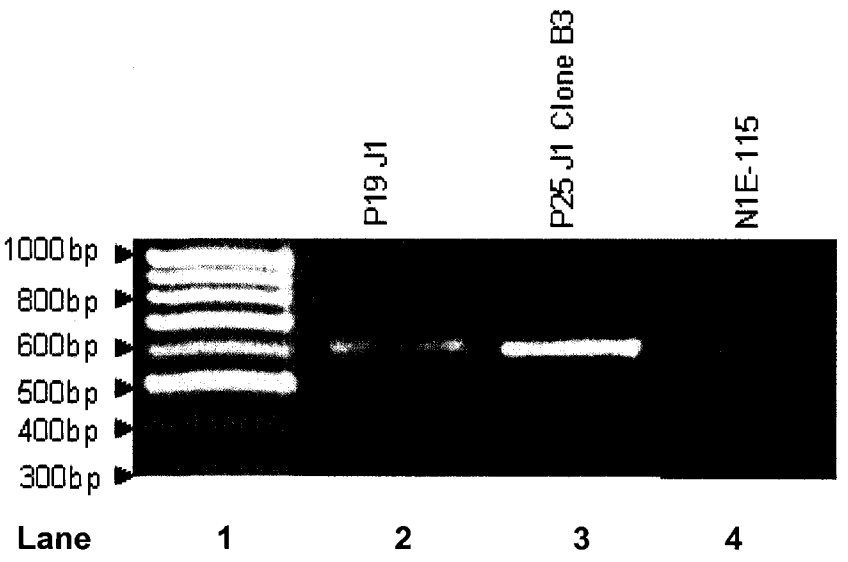
P19 J1
P25 J1 Clone B3
N1E-115
1000bp
800bp
600bp
500bp
400bp
300bp
Lane
1
2
3
4

cassette by conferring sensitivity to Ganciclovir. Homologous incorporation of the CKO targeting cassette results in the retention of the positive selection cassette, while the *MC1-tk* gene is lost because of lack of homology. This double selection strategy reduced the number of surviving clones by 5 to 10-fold. After 6 successful electroporation experiments, 126 G418^r/Ganciclovir^r clones were obtained. Due to the size of the homology arms, it was necessary to screen the G418^r/Ganciclovir^r clones by Southern blot. The resistant clones were initially screened by Southern blot following digestion with *XbaI* and using a probe located 1.8Kbp upstream of exon 1 of *Sgce*. As this did not allow for discrimination between clones that had undergone homologous integration versus random integration of the CKO targeting cassette, it was necessary to do a secondary screening by Southern blot (Figure 9a). A new probe was designed that hybridized immediately adjacent to the 3' homology arm of the targeting cassette. With this new probe, and when the genomic DNA was digested with *BglII*, the wildtype allele gave rise to a band 6.5 Kbp whereas the CKO allele a 4.5Kbp band. Those clones that had appeared to be positive for the homologous integration of the CKO targeting cassette were screened by digestion with *BglII* and the new probe. Of the original 126 G418^r/Ganciclovir^r clones, 3 gave the correct banding pattern. These three clones were expanded and re-frozen for blastocyst injection or morula aggregation experiments. Yves De Repentigny, of the laboratory of Dr. Rashmi Kothary, OHRI, performed 3 separate blastocyst injection experiments; one experiment for each of the CKO positive clones and obtained 2 chimeric male mice. These two mice were derived from FVB (white) donor embryos that had been injected with three to five V6.5 (brown) clone 3.6 ES cells. The contribution of the donor embryo and the ES cells can be seen as the white and brown

Figure 9: Screening by Southern Blot of genomic DNA was isolated from G418 and Gangciclovir resistant ES cell clones.

(**A**) Genomic DNA was digested with *XbaI* and probed with probe 2. The wild type allele is present in all lanes at approximately 7.0Kbp. The other bands present indicate that the targeting cassette has integrated. Those with * were subject to a secondary screening.

(**B**) Genomic DNA from those clones indicated with a * in A was digested with *BglII* and probed with probe 1. The wildtype allele is approximately 6.5Kbp whereas the correctly targeted CKO allele is 4.5Kbp. Only one clone, lane 5, appears to have the correctly integrated CKO allele.

A

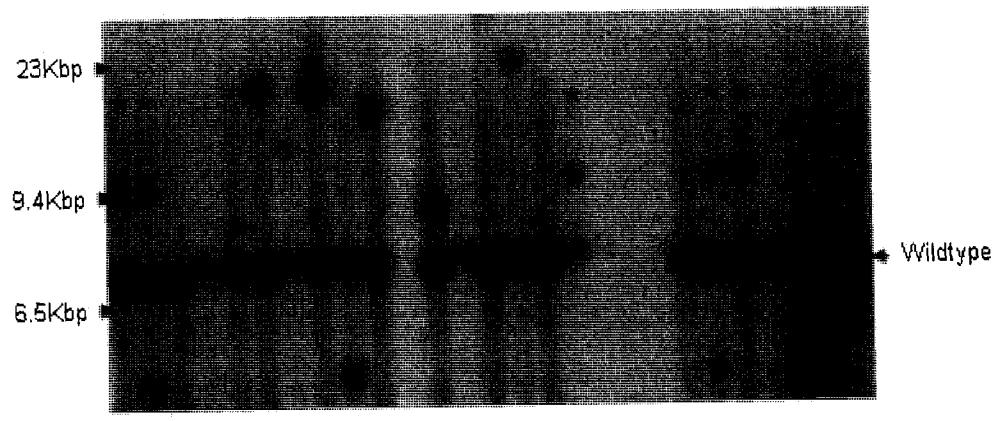
23Kbp
9.4Kbp
6.5Kbp
Wildtype

B

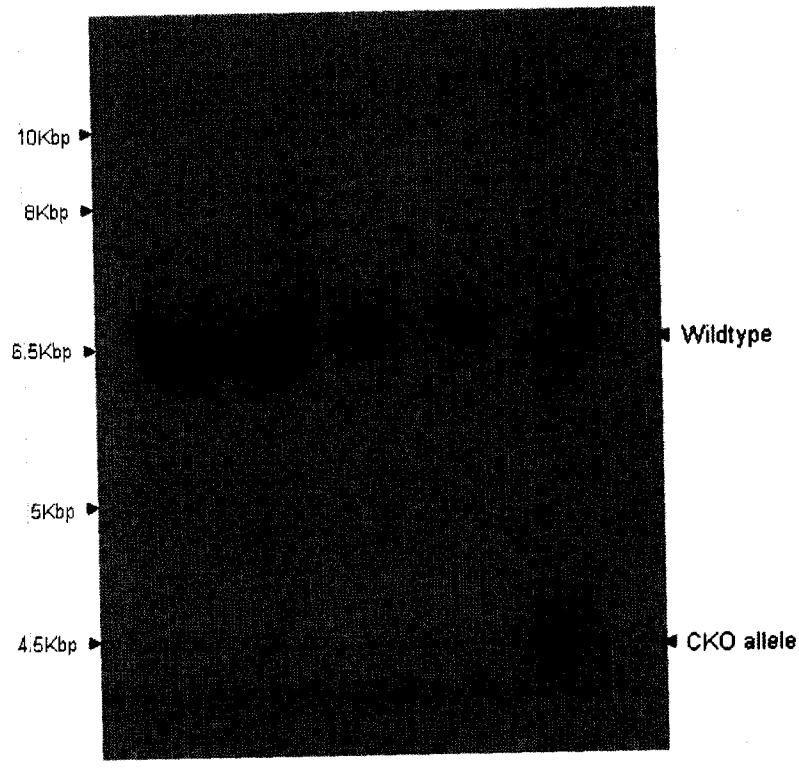
10Kbp
8Kbp
6.5Kbp
5Kbp
4.5Kbp
Wildtype
CKO allele

coat color of the animals (Figure 10). These male mice were bred to CD1 white female mice at 5 weeks of age in order to determine if germline transmission of the CKO allele had occurred. If the ES cells were able to contribute to the germ cells of the animal, the resulting pups will have a brown coat color. Ban al Jabouri, of the laboratory of Dr. Michael Rudnicki, OHRI, attempted one blastocyst injection experiment with V6.5 clone 2.5 but was unsuccessful.

2.2.6 Morula aggregation experiments

One alternative approach to generating chimeric mice is morula aggregation. Morula aggregation is generally less technically demanding and provides roughly the same success rate as blastocyst injection. In one experiment, 18 morula stage embryos were harvested from 2.5 dpc CD1 female mice and aggregated with 5 to 10 ES cell aggregates. The following day, of the original 18 embryos, 16 had progressed to the blastocyst stage and were suitable to embryo transfer. The embryos were then transferred to one 3.5 dpc pseudo-pregnant CD1 female mouse. However, no chimeric pups were obtained. Dr. Josee Coloumbe of Dr. Doug Gray's laboratory, OHRI, was successful in implanting 45 aggregated embryos into two 3.5 dpc pseudo-pregnant CD1 female mice. From this experiment, 11 pups were born in total, 6 female and 5 male. Of the male pups, two chimeras were obtained, one that was ~50% and the other that was less than 20% chimeric. The stronger chimeric mouse was placed with CD1 females at 5 weeks of age to determine if germline transmission of the CKO allele had occurred.

Figure 10: Chimeric male pups obtained from blastocyst injection experiments by Yves De Repentigny.

Two male chimeric pups (left) were derived from the injection V6.5 clone 3.6 (agouti) into FVB (albino) donor embryos. The percentage of chimerism was determined to be 60-70% for each animal by visual inspection. The white mouse on the right is a wildtype littermate.

2.3 Discussion

At the outset of this project there was no *in vivo* model of Myoclonus Dystonia (MD), therefore I propose to generate a conditional knock-out (CKO) of the mouse *Sgce* gene. Although the creation of a CKO is considerably longer and more labor intensive process than that used to generate a traditional knock-out (KO), a CKO gets around some of the limitations of the latter. Firstly, it may bypass potential embryonic lethal mutations as the gene is still "functional" until Cre mediated excision of the target exon or exons occurs. Secondly, tissue or temporal specific control of the KO is possible through controlled expression of Cre offered by many different Cre transgenic mouse lines that are available. However, in August 2003, a group based at the Beckman Institute for Advanced Science and Technology published a knock-out of exon 4 of *Sgce* (59, 101). It was decided that I would continue with our exon 1 CKO as I had already commenced ES cell targeting experiments.

Exon 1 of *Sgce* was chosen because this is the 5' most exon of the gene (52), it contains the translation initiating ATG, it is not known to be alternatively spliced *in vivo* and there are no other alternative promoters for this gene; and its removal should result in a complete null allele. I planned to insert two *loxP* sites, one 5' and one 3' of exon 1, such that when Cre mediated recombination takes place between the two *loxP* sites, an1800bp sequence of DNA would be excised, resulting in the removal of exon 1 and much of the 5' untranslated region (UTR) of *Sgce*. I did not believe that a CKO of *Sgce* would be embryonic or perinatal lethal as this gene is not expressed in ES cells and humans with null mutations in this gene have a normal life span. One complicating factor in creating a

"floxed" *Sgce* exon 1 allele is that the gene, *paternally expressed gene 10* (*Peg10*) lies approximately 6 Kbp 5' of the transcriptional start site of the *Sgce* in mouse and 300bp in human. This leaves open the possibility that there are regulatory elements required for the correct expression of *Peg10* within the introns and exons of *Sgce*. With that in mind, I chose the shortest possible target to flox in order to avoid altering those potential regulatory elements. However, this is still a possibility with the CKO cassette that was designed and could complicate the characterization of *Sgce* CKO mice as I would be effectively dealing with a double knock-out.

I utilized a highly efficient *E.coli* chromosomal engineering method, termed recombineering, to generate a CKO cassette of exon 1 of *Sgce*. This method is a variation on the lambda red system that bypasses the need to use restriction enzymes by using gap repair and recombination to clone and insert segments of DNA. This is a highly efficient method for the generation of such cassettes within a matter of weeks (97). By generating a CKO mouse for *Sgce*, I hoped to provide a model for function studies of the Sgce molecule; thus providing insight into the sarcoglycan complex within the brain and its role in the pathogenesis of MD.

A BAC clone derived from the SV129 mouse strain was chosen as most of the commonly used ES cell lines are derived from this strain of mice. It was thought important to obtain isogenic DNA to that of the ES cells, as strain polymorphisms may have had an effect on the targeting efficiency following transfection. However, the mouse genome build 35.1, available on the NCBI database, was based on the sequencing of the C57BL6 strain,

making primer design and the interpretation of sequencing results complicated. Luckily, these differences did not seem to decrease the efficiency of any of the recombineering or targeting experiments. After downloading the sequence of the region surrounding the *Sgce* gene, a region was chosen, 10.9Kbp in size, which would encompass exon 1.

The region chosen to be subcloned by gap-mediated repair was asymmetrical with respect to exon 1, with the 5' (left) homology arm being ~4Kbp in size and the 3' (right) homology arm being ~6Kbp. The reasoning behind this was to facilitate screening of targeted ES cell clones by PCR across the shorter of the two arms. The subcloning by gap repair of the 10.9Kbp target DNA was relatively simple following heat shock of the recombination competent DY380 bacteria. The number of Amp^r resistant colonies obtained, approximately 55 in one experiment, agreed with previously reported results for this protocol.

The two mini-targeting cassettes were designed to insert via recombineering 1000bp 5' and 300bp 3' of exon 1. It was possible to direct the insertion of these cassettes to a single base-pair within the target sequence and the two vectors generated for this set of experiments were designed with this in mind as to disrupt or remove as little of the endogenous sequence as possible. The insertion of the 5' targeting cassette was straightforward as it followed an identical protocol to that of subcloning via gap excision repair to generate the retrieved vector, pLM103. This step in the construction of the CKO cassette appeared to be quite efficient as 5000 Amp^r/Kan^r colonies were obtained. However, although the colonies were Amp^r/Kan^r, they carried a significant number of

non-targeted plasmids as determined by restriction digest. This was due to these non-targeted plasmids being replicated along with those that did carry the *PGKNeo* cassette. This problem was solved by transformation of a minute amount of mixed DNA into DH5α cells and selection for Amp^r/Kan^r as suggested by Copeland *et al* (2003).
The removal of the *PGKNeo* cassette by Cre mediated recombination was necessary for two reasons: (1) it would provide a region of homology for the 3' mini-targeting cassette which contains an identical *PGKNeo* cassette and (2) following the insertion of the 3' *loxP* site; this would leave three *loxP* sites within the subcloned DNA. Cre mediated recombination can take place between any two of the three *loxP* sites present, resulting in three possible products, two of which are undesirable. Cre mediated excision is an efficient process as 20 correctly constructed plasmids were obtained.

The 3' mini-targeting cassette was designed such that it would integrate one *loxP* site 3' of exon 1 in the same orientation as the 5' *loxP* site. This was important for removal of the intervening sequence following Cre mediated recombination. Although useful for some applications, inversion of the target DNA will take place if the *loxP* sites are in the opposite orientation and was unfavorable for this study. The *PGKNeo* cassette was flanked by two *frt* sites to allow for removal of the *PGKNeo* following Flp mediated recombination in ES cells or mice. One *loxP* site was situated 3' of the *loxP-frt-PGKNeo-frt* cassette providing the second *loxP* site to "flox" exon 1. The *loxP-frt-PGKNeo-frt* cassette was integrated, screened for and purified in the same manner as the 5' mini-targeting cassette. This was the CKO targeting cassette.

After purifying the CKO targeting cassette by CsCl buoyant density gradient, it was digested with *NotI*. The unique *NotI* site was located on Primer A and was originally used to clone the AB homology arm into the retrieval vector. The linearized CKO vector was then transfected into ES cells by electroporation, a method employed when working with cell lines that are difficult to transfect. Positive and negative selection was used to enrich the number of correctly targeted ES cells clones. The number of $G418^r$/$Ganciclovir^r$ clones obtained, 126 from 6 experiments, is in line with previous reports (64, 99).

As previously mentioned, I had intended to screen for correctly targeted clones by PCR across the shorter of the two homology arms. However, this was not feasible due to the highly repetitive nature of the region 5' of exon 1 making it refractory to PCR. I turned to a very reliable, albeit slower and more labor intensive, screening by Southern blot. The original screening was performed with a probe that was within the region of homology and this narrowed down the number of clones that could be correctly targeted, however, it was necessary to do a secondary screen with a probe outside the region of homology arms. This is due to the possibility that the CKO targeting cassette may have integrated randomly within the genome and coincidentally given the correct banding pattern. Those clones that appeared to be correctly targeted by the primary screen were screened again by via Southern blotting and of those only 3 were correct by the secondary screen. The number of clones obtained gives a targeting efficiency of 2.4%. Most reports give an efficiency of between 1% and 5% depending on the locus being targeted (99).

There are several different methods to generate chimeric mice from a donor embryo and ES cells, of which I chose to use two. The first method was blastocyst injection and the second was morula aggregation. ES cells are capable of behaving like normal embryonic cells when they are returned to the embryonic environment; acting like primitive ectoderm or epiblast cells. These cells are able to contribute to all cell lineages of the developing fetus including the extraembryonic tissues such as the amnion (99). Blastocyst injection was performed on FVB blastocyst stage embryos, approximately 4 days post-fertilization; where 5 to 10 ES cells of the V6.5 (129S4 x C57BL/6) were injected into the blastocoele cavity of the donor embryo using microinjection pipettes and micromanipulators. Those were then implanted into pseudopregnant FVB "foster" mothers and were born approximately 16 days later. This method is considered the standard for most ES cell chimera experiments and results in approximately 50% live births of those embryos injected. Of those that are born 50% will be chimeras (Dr. J. Coloumbe, personal communication).

The alternative approach that I used to generate chimeric mice was morula aggregation. This method has approximately the same level of success, in terms of the number of live births, as blastocyst injection and has the advantage of being less technically demanding. Morula stage embryos, approximately 2 days post-fertilization, are composed of 12 to 32 cells and have not yet reached the blastocyst stage of development (99). The cleavage stage embryos were flushed from the oviduct; their zona pellucida removed and placed into an aggregation depression in the presence of 5 to 10 ES cell aggregates. Those were

allowed to develop in culture to the blastocyst stage and were then transferred to pseudopregnant female mice to complete their development. As this method does not require as much technical expertise as blastocyst injection it is possible to aggregate a large number of embryos; up to 40 embryos injected versus 120 aggregations. However, the percentage of live births from this method is lower than that of blastocyst injection. For example, of 45 embryos that were transferred to foster females from the first experiment with Dr. Josee Coloumbe, 11 pups in total were born; 6 female and 5 male. Of the 5 males born, 2 were chimeric and only 1 strongly so.

It is known that there are some ES cells lines, such as D3 and AB1, that have not been successfully used to generate germline transmitting chimeras by morula aggregation (99). J1 (129Sv4/SVJae), from the laboratory of Dr Rudolf Jaenisch, have been successfully used for blastocyst injection to generate chimeras however, there is some discrepancy in the literature as to whether or not they are suitable for morula aggregation (102). Josee and I were able to obtain 2 chimeric male mice from aggregations of J1 ES cells and CD1 derived donor embryos indicating that it is possible to obtain viable fetus's from these cells using this approach. However, the male that appeared to be strongly chimeric was significantly smaller in size than his less chimeric or wildtype littermates. Although the embryo donor strain is important for the generation of chimeras in this fashion, CD1's are considered to be very well suited and thus it is likely that J1 ES cells are sub-optimal for this technique.

The two chimeras obtained by blastocyst injection appeared to be highly ES cell line derived. This observation was based on the amount of brown coat color which indicates the approximate contribution of the ES cells to the mouse; between 50% and 60% for each male. Generally, the degree of coat color chimerism can be correlated to the degree which the ES cells contributed to the germline of the animal. Male chimeras were chosen because the almost all ES cell lines, including J1 and V6.5, are derived from male embryos and as such carry and X and Y chromosome. There are several reasons for choosing male derived ES cells lines. For example male ES cell lines are known to be more genetically stable than female derived ES cells line; and give a higher proportion of phenotypically male offspring which can in turn produce more offspring in a given time period than a female could. It is possible to obtain phenotypic male chimeras that were derived from a female donor embryo if the ES cells were able to contribute to the tissues which contribute to determining the sex of the fetus. Likewise it is possible to obtain germline transmitting female chimeric mice. This is thought to occur when the male ES cells lose the Y chromosome and effectively become XO, and are thus capable of undergoing oogensis. Whether or not the ES cells have contributed to the germline tissues of the mice can be determined by the color of the pups obtained from matings between the chimeric males and females of the donor strain (99).

2.3.1 Future Directions:

Germline transmission of the CKO allele can be done by analyzing the coat color of the pups from the mating of the chimeric male with an appropriate female. The V6.5 ES cell line is derived from the 129S4 and C57BL/6 mouse strains, and is heterozygous for the

agouti allele, A^w/a and homozygous wildtype $+^{Tyr\text{-}c}/+^{Tyr\text{-}c}$, for the albino coat color allele. The FVB strain of mice is homozygous wildtype, A^w/A^w, for the agouti allele and homozygous albino, Tyr^c/Tyr^c (The Jackson Laboratory website, www.jax.org). FVB mice are albino despite being homozygous wildtype for the agouti allele due to the epistatic dominant albino mutation (99). If the resulting pups are albino, the germline tissues of the chimeric mice were derived from the donor embryo and the genotype of the pups for the coat color alleles will be A^w/A^w and Tyr^c/Tyr^c. If they are agouti, the germline tissues were derived from the ES cells and the genotype of the pups for the coat color alleles will be A^w/A^w or A^w/a and $+^{Tyr\text{-}c}/Tyr^c$. It is possible for there to be mosaicism of the germline in addition to the somatic tissues as is observed in the spotted coat color. If this is the case for the germline tissue, a mixture of agouti and albino pups will be born.

The agouti, F_1 generation will be composed of heterozygous, $+/sgce^{cko}$ and homozygous wild-type, +/+. Genotyping by Southern blot will be necessary to distinguish between these two possibilities. Those mice that are determined to be heterozygous, $+/sgce^{cko}$, will be mated together to produce the F_2 litters that will be composed of +/+, $+/sgce^{cko}$ and homozygous $sgce^{cko}/sgce^{cko}$ mice. As these animals have not yet been crossed to Cre expressing transgenic mice and thus "knocked out" for *Sgce*, they should appear to be normal. At this point there are two different possible breeding schemes that should be explored.

The first will allow for the rapid characterization of the *Sgce* null phenotype. Male homozygous $sgce^{cko}/sgce^{cko}$ mice from the intercrossing of the F_2 generation can be

mated to females of a transgenic Cre expressing strain in order to remove the "floxed" exon 1 and obtain the true *Sgce* knockout. The Cre expressing strains that would be of interest in this crossing scheme are Tg(Pcp2-cre)2Mpin which expresses Cre under the direction of the *purkinje cell protein 2* (*Pcp2*) gene and this directs expression to the purkinje cells, an area which has high expression of *Sgce*. The Tg(CMV-cre)1Cgn strain may also be of interest as Cre is expressed from the *human cytomegalovirus* (*hCMV*) promoter and is found in all tissues and throughout development. Both of these transgenic Cre expressing strains are available from The Jackson Laboratory, Bar Harbor, Maine.

It is important to use male $sgce^{cko}/sgce^{cko}$ mice and female transgenic Cre mice for the rapid characterization of the Sgce knockout phenotype. The *Sgce* gene is subject to maternal imprinting and as a result the female allele is silenced. The offspring of the male $sgce^{cko}/sgce^{cko}$ and female +/+ transgenic will express the paternally inherited $sgce^{cko}$ allele as opposed to the maternally inherited wildtype, +, allele. If Cre mediated excision of the paternal $sgce^{cko}$ allele has taken place, the offspring will be *Sgce* null, $sgce^{null}$, despite having a wildtype maternal *Sgce* allele. These F_3 generation mice can then be utilized to conduct behavioral and physiological studies to determine the role of *Sgce* in MD.

The second breeding scheme should be pursued in order to establish the $sgce^{cko}$ allele on a homogeneous genetic background and allow more precise characterization of the *Sgce* null phenotype and long term maintenance of the $sgce^{cko}$ allele. Genetic background can have a significant affect on the penetrance and expression of a given phenotype such as is

the case for epidermal growth factor (*Egfr*) null mice. The mutation of *Egfr* results in three different phenotypes depending on the genetic background being used (99). In order to establish the $sgce^{cko}$ allele on a homogeneous genetic background it will be necessary to breed either the chimeric F_0 or heterozygous F_1 generation to a 129 strain which the ES cells were derived such as 129P1, available from The Jackson Laboratory. Bar Harbor, Maine. Alternatively the $sgce^{cko}$ allele can be established on a different genetic background by crossing the $sgce^{cko}$ allele into a different strain of mice such as C57BL/6, which is used as the genetic background for a large number of mutations. A total of 10 to 12 backcrosses will be necessary to obtain a strain which is 99.9% pure and is carrying the $sgce^{cko}$ allele. This breeding scheme to establish the $sgce^{cko}$ allele on a pure genetic background is also possible for the $sgce^{null}$ mice from the F3 generation described in the previous paragraph. This may actually be desirable as this will eliminate the need to "purify" the strain again following being crossed to a Cre transgenic strain.

The phenotypic characterization of the $sgce^{null}$ mice will involve various experiments which will test the animal's motor function in addition to their ability to survive and thrive. The proposed experiments to gauge the affect of the $sgce^{null}$ allele will include gait assessment using a transparent gait box (103, 104), coordination using a Rotorod apparatus (Columbus Instruments, Columbus, Ohio)(105), and locomotion by measuring the level of activity of the $sgce^{null}$ mice when compared to wildtype counterparts (106). These experiments will validate whether or not I was able to recapitulate the human disease, MD, in mice.

2.3.2 Conclusions:

Our laboratory is interested in the architecture of the central nervous system and various disorders that arise due to mutations in genes required for this to take place correctly. The generation of the *Sgce* CKO allele will allow us to pursue functional studies of the molecular biology of Sgce in the mammalian nervous system and allow for a greater understanding of the sarcoglycan complex of proteins and of the DGC in this context. I was able to successfully employ bacterial recombineering to generate a *Sgce* CKO allele in *E.coli*. I was then able to use this CKO targeting cassette in ES cells to obtain 3 clones that had correctly incorporated the cassette via homologous recombination. Two of the clones, one from each ES cell line employed, were used to generate chimeras. Two chimeric male mice were obtained by blastocyst injection of the V6.5 clone 3.6 and were bred to white FVB female mice to determine if germline transmission had taken place. One male mouse was obtained by morula aggregation of the J1 clone B3. If germline transmission of the CKO allele has occurred in one or more of the chimeric male mice, the establishment of a *Sgce* CKO colony should be relatively straight forward. The crossing of the Sgce CKO mice to a Cre expressing transgenic mouse strain will allow create an $Sgce^{null}$ and hopefully will recapitulate the phenotype of patients with MD.

Although there is already a *Sgce* KO model, there will be areas of research that cannot be addressed by a single group. There have been two papers published to date describing the characterization of their *Sgce* KO mice, neither of which have addressed the function of Sgce within the central nervous system. Future experiments involving the use of the $sgce^{null}$ mice will include crossing to the $sgca^{null}$ mice that are currently being studied in

the laboratory of Dr. Micheal Rudnicki to determine the role of Sgce in cardiac and skeletal muscle. *In vitro* RNAi experiments against Sgce in a mouse neuroblastoma cell line, which will be discussed in the following chapter, have been found to have decreased neuronal nitric oxide synthase (nNos1), and increased proliferation as compared to controls. If the same is found to be true for the $sgce^{null}$ mice, this could explain the mechanism behind MD.

Chapter 3: Generation of an *In vitro* model for Myoclonus Dystonia

3.1 Materials and Methods

3.1.1 shRNA design and cloning

The rat *Sgce* mRNA NM_001002023:1 was downloaded from the NCBI database and entered into Invivogen's siRNA Wizard V2.5 webtool (www.sirnawizard.com). The specificity of each shRNA that was selected by the siRNA Wizard program was assessed by basic local alignment search tool (BLAST) against the mouse genome build 36.1 on the NCBI website. The algorithm used by the siRNA Wizard program chooses shRNA oligos based on the following criteria; the starting nucleotide is an A or a G, avoid sequences of greater than 4 A's or T's, the GC content be 30-50% and to have optimal internal stability. Three shRNA's were selected from those that those were designed by the webtool based on their specificity and their binding site within the *Sgce* mRNA. *BamHI* and *HindIII* cut sites were added to the 5' end of each oligo to facilitate cloning into the pEXPRESS-GFP vector (Nyrion Ltd, Edinburgh, UK).

The shRNA oligos were annealed and cloned into the pEXPRESS-GFP vector using the following protocol: 25 μM of each forward and reverse shRNA oligo dissolved in TE, 6 μl of 0.5 M NaCl in ddH_2O to a final volume of 30 μl was heated to 95°C for 2 min and cooled by 1°C per minute until the temperature reached 35°C then stored at 4°C. The pEXPRESS-GFP vector was digested with *BamHI* and *HindIII* restriction enzymes, purified by spin column and quantified by gel electrophoresis and quantification as previously described. The 20 μl ligation reaction was set up as follows: 100 ng of the digested pEXPRESS-GFP vector, 1 μl of the annealed shRNA oligos, 1 U of T4 DNA

ligase (Invitrogen, Carlsbad, CA), 1 μl of 10X ligase buffer and ddH_2O. The ligation reaction was allowed to incubate at 16°C O/N and transformed into MAX Efficiency Stbl2 (Invitrogen, Carlsbad, CA) competent cells according to the manufacturer's protocol and selected for Kan^r. DNA from Kan^r colonies was collected and screened for the correct insertion of the shRNA oligo by both digestion with *RsaI* (New England Biolabs, Ipswich, MA) and electrophoresis on a 10% polyacrylamide gel and by DNA sequencing.

3.1.2 Cell culture reagents and conditions

The N1E-115 mouse neuroblastoma cell line was a gift from Dr. David Picketts, OHRI and were cultured in maintenance media composed of DMEM with glucose, 10% FBS, 1X glu and 1X A/A at 37°C and 5% CO_2, unless otherwise noted. Differentiation media, which was used for neurite outgrowth studies, was composed of DMEM with glucose, 1% FBS, 1X glu, 1X A/A and 1% DMSO. For neurite outgrowth and cell proliferation assays, pooled clones of each construct that had been selected for 10 days in 400 μg/ml of G418 were used as stable clones could not be established.

3.1.3 Determining the selective G418 concentration for the N1E-115 cell line

In order to determine the appropriate concentration of G418 required to kill greater than 50% of cells in 48hrs, N1E-115 cells were exposed to a range of different concentrations of G418 from 100 μg/ml to 600 μg/ml. N1E-115 cells were plated at a starting concentration $1.0X10^5$ cells per well in a 6 well tissue culture dish in maintenance media.

The following day, the media was changed to G418 containing maintenance media, a different concentration in each of the 6 wells. Every 24 hrs, observations were made as to the health of the culture and the relative cell density for a total of 6 days.

3.1.4 Assessment of shRNA knockdown of Sgce by each shRNA construct

Twelve micrograms of each shRNA construct; shRNA1, shRNA2 and shRNA3, lacZ and empty vector (GFP) were transfected into $1.0X10^5$ non-differentiated N1E-115 cells in 35 mm dishes a total of 5 times. The transfections were performed using the Lipofectamine 2000 Transfection Reagent (Invitrogen, Carlsbad, CA) in a ratio of 3:1 to DNA according the manufacturer's protocol. Transfection efficiency was measured by fluorescence microscopy to detect the expression of the *CMV-GFP* marker present on the pEXPRESS-GFP vector. For the establishment of pooled stable clones, 24hrs post-transfection, the media was switched to selective media which contained 400 μg/ml of G418. The pooled stable clones were cultured in maintenance media for all follow up experiments.

Transient transfection experiments were used to determine the level of *Sgce* knockdown by each construct. Forty-eight hours post-transfection, the cells were trypsinized, pelleted in 1.5 ml eppendorf tubes by centrifugation at 3000 rpm for 4min at room temperature. The cells were then lysed with 300 μl of Tri-Reagent (Sigma-Aldrich, Oakville, ON) and total RNA was isolated according to the manufacturer's protocol. The RNA isolated was then quantified by spectrophotometry and frozen at -80°C for long term storage. One microgram of the total RNA isolated from 3 transfections which appeared to have similar transfection efficiency were then subject to random-primed

reverse-transcriptase PCR (RT-PCR) using the following protocol; 1 μg of RNA and 1 ng of random hexamers were mixed, incubated at 70°C for 10 min then quickly cooled on ice. Then 20 μl RT-PCR contained 10 mM dithiothreitol (DTT), 5 ng/μl of dNTPs and 200 U of Superscript II Reverse Transcriptase (Invitrogen, Carlsbad, CA). The samples were incubated at 42°C for 45 min and 95°C for 10min and stored at -20°C until required.

The complementary DNA (cDNA) was then subject to multiplex semi-quantitative PCR (Q-PCR). Primers were designed to detect the transcript of *Gapdh*, and of *Sgce*, as previously described (table). The PCR conditions for each primer set was determined individually, then combined and re-optimized in order to establish conditions necessary to detect any changes in the amount of *Sgce* cDNA present in each sample relative to *Gapdh* cDNA. The greatest sensitivity in detecting changes of *Sgce* cDNA levels to that of *Gapdh* cDNA was obtained with; 10 mM Tris-HCl pH 8.3, 0.5 M KCl, 0.15 mM $MgCl_2$1, 25 mM dNTPs, 0.35 μM Gapdh forward/reverse primers, 1.35 μM Sgce forward/reverse primers, 2 μl random-primed cDNA, 1 μl of TAQ DNA polymerase and ddH_2O to a total volume of 30 μl. The amplification conditions were (1) 95°C for 5 min; (2) 95°C for 30 sec; (3) 55°C for 30 sec; (4) 72°C for 30 sec; (5) 72°C for 2 min with steps 2 through 4 being repeated for 25 cycles. Each multiplex Q-PCR was performed in triplicate and the PCR products were subject to gel electrophoresis prior to being prepared for denaturing high performance liquid chromatography (dHPLC) by spin column.

Five microliters of each sample was injected into a Transgenomic Wave dHPLC System which utilizes a DNASep Prep HT column (Transgenomic Inc, Omaha, NE) under non-denaturing conditions at a flow rate of 0.9 ml/min at a temperature of 50°C. The data was analyzed using Transgenomic's Navigator Software (Transgenomic Inc, Omaha, NE) and images were processed using Adobe Photoshop V7.0. The number value of the area under each peak, which is calculated by the Navigator Software, was entered into a Microsoft Office Excel 2003 (Excel) (Microsoft Corporation, Redmond, WA) spreadsheet for statistical analysis. The relative amount of PCR product was determined by dividing the area under the peak for *Sgce* by that of *Gapdh*. The mean, standard deviation and student's *t*-distribution value were calculated using the functions present in Excel.

3.1.5 Differentiation and neurite outgrowth in N1E-115 cells

LacZ, GFP, shRNA3 and non-transfected N1E-115 cells were thawed from frozen stocks into 10 cm dishes and allowed to recover for 48 hrs. After the recovery period, cells were trypsinized, counted by hemacytometer and plated at a density of $1.0X10^5$ per 35 mm dishes and allowed to recovery for 24 hrs. The following day, the media was changed to differentiation media and images were taken with a Zeiss Axioplane Microscrope and images were captured using an Axiocam Rawpro camera. The images were processed using Adobe Photoshop V7.0 software. Images were taken every 24 hrs until the cells had completely differentiated at 96 hrs. Neurite length was assessed based on the following criteria; the neurite must be greater than twice the width of the cell and the

neurite must belong to what appeared to be a live cell. The data obtained was entered into an Excel spreadsheet for statistical analysis.

3.1.6 Cell Proliferation

To assess changes in cell proliferation, LacZ, GFP, shRNA3 cells were split from previously thawed stocks. The cells were plated at a starting density of $1.0X10^5$ per 35 mm dish in maintenance media. Every 48 hrs, the cells were collected by trypsinization, counted by hemacytometer and discarded. This procedure was repeated at 96 hr and 144 hr time points. Data obtained was inputted into an Excel spreadsheet for statistical analysis.

3.1.7 Collection and analysis of Affymetrix data

Affymetrix data from the Gene Expression Omnibus (GEO) database was obtained from the NCBI website. This data was made publicly available on November 11, 2004 and was submitted to the GEO database by Dr Timothy York of Virginia Commonwealth University, Richmond, Virginia. The platform used was the Affymetrix GeneChip Mouse Expression Array 430A (Affymetrix, Santa Clara, CA) which represents approximately 14,000 well-characterized mouse genes. This data was analyzed by Paul Krzyzanowski of the laboratory of Dr Miguel Andrade, OHRI. The Affymetrix package in Bioconductor (PMID: 15461798) was used to generate the expression values and the Present/Absent (P/A) calls. The MOE430 chip annotations dated April 11^{th}, 2006 were acquired from NetAffx, available from the Affymetrix website (www.affymetrix.com).

Data obtained was used to determine which dystrophin glycoprotein complex (DGC) members are expressed in the N1E-115 cell line.

3.1.8 PCR protocols and conditions

The cDNA sequences of each of the following genes was downloaded from the University of California Santa Cruz (UCSC) Genome Browser (http://genome.ucsc.edu/); *Synapsin 1* (*Syn1*), *Glial Fibrillary Acidic Protein* (*GFAP*), *Beta-sarcoglycan* (*Sgcb*), *Laminin Alpha 4* (*Lama4*), *neuronal Nitric Oxide Synthase 1* (*nNos1*), *Gamma-sarcoglycan* (*Sgcg*) and *Zeta-sarcoglycan* (*Sgcz*). The Refseq ID numbers for each gene are: *Sgcb* NM_011890.2, *Sgcg* NM_011892.2, *Sgcz* AK136779, *nNos1* NM_008712.1, *Lama4* NM_010681.1. Primer pairs were selected that lay within different exons in order to detect the transcript of each gene using the Primer 3 webtool (frodo.wi.mit.edu/cgi-bin/primer3/primer3_www.cgi) (Table 4). The PCR conditions for each primer pair were determined individually, and for *nNos1, Lama4* and *Sgcb*, combined with the primers for *Gapdh* in preparation for multiplex Q-PCR. The cDNA was prepared as previously described from pooled stable clones of each construct and each PCR was done in triplicate. Five microliters of each PCR product was subject to gel electrophoresis with the remainder being purified by spin column and subject to dHPLC to quantify any changes in gene expression.

Multiplex Q-PCR of *Sgcb* with *Gapdh* was performed as follows: 10 mM Tris-HCl pH8.3, 0.5 M KCl, 0.15 mM $MgCl_2$, 25 mM dNTPs, 0.35 μM Gapdh forward/reverse

primers, 1.35 μM Sgcb forward/reverse primers, 2 μl random-primed cDNA, 1.0 μl of TAQ DNA polymerase and ddH_2O to a total volume of 30 μl. The amplification conditions were; (1) 95°C for 5 min; (2) 95°C for 1 min; (3) 55°C for 1 min; (4) 72°C for 1 min; (5) 72°C for 2 min with steps 2 through 4 being repeated for 30 cycles.

Multiplex Q-PCR of *nNos1* with *Gapdh* was performed as follows: 10 mM Tris-HCl pH 8.3, 0.5 M KCl, 0.15 mM $MgCl_2$, 25 mM dNTPs, 0.35 μM Gapdh forward/reverse primers, 1.35 μM nNos1 forward/reverse primers, 2 μl random-primed cDNA, 1.0 μl of TAQ DNA polymerase and ddH_2O to a total volume of 30 μl. The amplification conditions were; (1) 95°C for 5 min; (2) 95°C for 1 min: (3) 66°C for 1 min; (4) 72°C for 1 min; (5) 95°C for 1 min; (6) 55°C for 1 min; (7) 72°C for 1 min; (8) 72°C for 2 min with steps 2 and 4 being repeated for 10 cycles with the temperature of step 6 being dropped by 1°C each cycle. Steps 5 through 7 were repeated for a total of 15 cycles, for a total of 25 cycles.

The PCR protocol for the amplification of *Lama4* was performed as follows: 10 mM Tris-HCl pH 8.3, 0.5 M KCl, 0.15 mM $MgCl_2$, 25 mM dNTPs, 1.35 μM Lama4 forward/reverse primers, 3 μl random-primed cDNA, 1.0 μl of TAQ DNA polymerase and ddH_2O to a total volume of 25 μl. The amplification conditions were (1) 95°C for 5 min; (2) 95°C for 1 min; (3) 66°C for 1 min; (4) 72°C for 1 min; (5) 95°C for 1 min; (6) 55°C for 1 min; (7) 72°C for 1 min; (8) 72°C for 2 min with steps 2 and 4 being repeated for 10 cycles with the temperature of step 6 being dropped by 1°C each cycle. Steps 5 through 7 were repeated for a total of 17 cycles, for a total of 27 cycles.

The PCR protocol for the amplification of *Sgcg* is as follows: 10 mM Tris-HCl pH 8.3, 0.5 M KCl, 0.15 mM $MgCl_2$, 25 mM dNTPs, 1.35 μM Sgcg-forward/reverse primers, 2 μl of random-primed cDNA, 5% Formamide, 1.0 μl of TAQ DNA polymerase and ddH_20 for a total volume of 25 μl. The amplification conditions were; (1) 95°C for 5 min; (2) 95°C for 1 min; (3) 50°C for 1 min; (4) 72°C for 1 min; (5) 72°C for 2 min with steps 2 through 4 being repeated for 35 cycles.

The PCR protocol for the amplification of *Sgcz* is as follows: 10 mM Tris-HCl pH 8.3, 0.5 M KCl, 0.15 mM $MgCl_2$, 25 mM dNTPs, 1.35 μM Sgcg-forward/reverse primers, 2 μl of random-primed cDNA, 5% DMSO, 1.0 μl of TAQ DNA polymerase and ddH_20 for a total volume of 25 μl. The amplification conditions were; (1) 95°C for 5 min; (2) 95°C for 1 min; (3) 50°C for 1 min; (4) 72°C for 1 min; (5) 72°C for 2 min with steps 2 through 4 being repeated for 35 cycles.

The PCR protocol for the amplification of *Syn1* was as follows: 10 mM Tris-HCl pH 8.3, 0.5 M KCl, 0.15 mM $MgCl_2$, 23 mM dNTPs, 0.4 μM Syn1 forward and reverse primers, 2 μl of random-primed cDNA, 1.0 μl of TAQ DNA polymerase and ddH_2O to a total volume of 25 μl. The amplification conditions were; (1) 95°C for 5 min; (2) 95°C for 30 sec; (2) 55°C for 30 sec; (3) 72°C for 30 sec (4)72°C for 30 sec; (5) 72°C for 2 min with steps 2 through 4 being repeated for 30 cycles.

Gene Name	Primer Name	Primer Sequence
Gapdh	M-Gadph-F 032106	5'-AACTTTGGCATTGTGGAAGG-3'
	M-Gadph-R 032106	5'-TGTGAGGGAGATGCTCAGTG-3'
Sgce	M-SGCE-F	5'-CGCCATAAATCATCACGTCAG-3'
	M-SGCE-R	5'-AGCCAGGGTAACGAGGAAATC-3'
Gfap	M-Gfap-F 032106	5'-CACGAACGAGTCCCTAGAGC-3'
	M-Gfap-R 032106	5'-CCTTCTGACACGGATTTGGTG-3'
Syn1	M-Syn1-F 032106	5'-CAGCACAACATACCCTGTGG-3'
	M-Syn1-R 032106	5'-AGTTCCACGATGAGCTGCTTG-3'
Gapdh	M-Gadph-F 032106	5'-AACTTTGGCATTGTGGAAGG-3'
	M-Gadph-R 032106	5'-TGTGAGGGAGATGCTCAGTG-3'
Sgcg	sgcg-F-051606	5' -TGCCCAGATGGTAGAAGTCC- 3'
	sgcg-R-051606	5' -CAACTTGGTCAAACCCACAG- 3'
Sgcz	sgcz-F-051606	5' -GAAAGAAATTCATTCCCGAAAGG- 3'
	sgcz-R-051606	5' -GAATCAGGAAAGGTGAAGGCCAA- 3'
Sgcb	sgcb-F-051606	5'-GCAACTTAGCCATCTGCGTG- 3'
	sgcb-R-051606	5' -TCTCATAGTCCGTGCTGAAC- 3'
Lama4	lama4-F-051606	5' -GATGGAAGCGAAAGACAAGC- 3'
	lama4-R-051606	5' -CAGGGGCACATCTTTCACAG- 3'
nNos1	nos1-F-051606	5' -AGGAATCCAGGTGGACAGAG- 3'
	nos1-R-051606	5' -TCCTTGAGCTGGTAGGTGCT- 3'

Table 4 PCR primers designed to amplify "hit-list" cDNA sequences

"Hit-list" of genes was selected from those listed as expressed in the Affymetrix downloaded from the NCBI Geo database. The cDNA sequences of each of the following genes was downloaded from the University of California Santa Cruz (UCSC) Genome Browser (http://genome.ucsc.edu/); *Synapsin 1* (*Syn1*), *Glial Fibrillary Acidic Protein* (*GFAP*), *Beta-sarcoglycan* (*Sgcb*), *Laminin Alpha 4* (*Lama4*), *neuronal Nitric Oxide Synthase 1* (*nNos1*), *Gamma-sarcoglycan* (*Sgcg*) and *Zeta-sarcoglycan* (*Sgcz*). The Refseq ID numbers for each gene are: *Sgcb* NM_011890.2, *Sgcg* NM_011892.2, *Sgcz* AK136779, *nNos1* NM_008712.1, *Lama4* NM_010681.1. Primer pairs were selected that lay within different exons in order to detect the transcript of each gene using the Primer 3 webtool.

The PCR protocol for the amplification of *Gfap* was as follows: 10 mM Tris-HCl pH 8.3, 0.5 M KCl, 0.15 mM $MgCl_2$, 25 mM dNTPs, 0.4 μM Gfap forward and reverse primers, 2 μl of random-primed cDNA, 1.0 μl of TAQ DNA polymerase and ddH_2O to a total volume of 25 μl. The amplification conditions were; (1) 95°C for 5 min; (2) 95°C for 30 sec; (2) 55°C for 30 sec; (3) 72°C for 30 sec (4)72°C for 30 sec; (5) 72°C for 2 min with steps 2 through 4 being repeated for 30 cycles.

3.1.9 Western blotting

Total protein was collected from N1E-115 cell lysates using a radioimmunoprecipitation (RIPA) buffer isolation protocol. The RIPA lysis buffer was modified from the standard protocol and was composed of the following ingredients: 0.125 M Tris-HCl pH6.4, 1% glycerol, 4 M urea, 5% sodiumdodecylsulfate (SDS) and ddH_2O and stored at 4°C until required. LacZ, GFP and shRNA3 pooled clones and non-transfected N1E-115 cells were thawed from frozen stocks, plated into 35 mm dishes and allowed to recover for 48 hrs prior to lysis. Immediately prior to use, 10 μl of phenylmethylsulfonyl fluoride (PMSF) was added per 1 ml of RIPA buffer. All cell lysates were stored at -80°C until required. Protein concentrations were determined by Bradford assay using the Bio-Rad Protein Assay Dye Reagent Concentrate (Bio-rad Laboratories, Hercules, CA). Fifty micrograms of protein from each sample was subject to electrophoresis on a 12% SDS-polyacrylamide gel electrophoresis (SDS-PAGE) gel. The running buffer used contained 20 mM Tris-HCl, 0.2 M Glycine and 0.1% SDS. The protein was transferred to Immuno-blot polyvinylidene difluoride (PVDF) membrane (Bio-rad Laboratories, Hercules, CA) using a Trans-Blot SD Semi-dry Electrophoretic Transfer Cell (Bio-rad Laboratories,

Hercules, CA) in a transfer buffer containing 4 mM Tris-HCl, 4 mM Glycine and 0.4% SDS at 45 mA for approximately 90 min.

Membranes were blocked in 5% milk 1X Tris-Borate Saline Tween-20 (TBST) containing 10 mM Tris-HCl pH 8.0, 0.15 M NaCl, 0.05% Tween-20, at room temperature for 1 hr. The membranes were probed with the one of the following primary antibodies anti-nNos1 (Invitrogen, Carlsbad, CA) a gift from Dr. Bernard Jasmin, OHRI, anti-Sgcg (Novacastra Laboratories Ltd, Newcastle, UK), a gift from Dr. Rashmi Kothary, OHRI, anti-Sgce, a gift from Dr. Joshua Sanes, Harvard University and anti-β-Actin (Sigma-Aldrich, Oakville, ON) as a loading control. All antibodies were incubated with the membrane at room temperature for 1hr. The membranes were then washed for 45 min at room temperature with 1X TBST prior to and after being probed with either anti-mouse or anti-rabbit HRP conjugated secondary antibody (Sigma-Aldrich, Oakville, ON). Detection of the secondary antibody was performed with the Amersham ECL Plus Western Blotting Detection Reagent (Amersham Biosciences, Fairfield, CT).

3.2 Results

3.2.1 N1E-115 cells express Sgce and neuronal markers

The N1E-115 mouse neuroblastoma cell line was established in 1973 and is considered to be a valid model for studying neurons *in vitro* as this cell line exhibits many of the characteristics of differentiated neurons. This adrenergic cell type exhibits high levels of activity of the enzymes tyrosine hydroxylase and acetylcholinesterase, which are necessary for neurotransmitter synthesis, but are almost devoid of choline acetyltransferase. N1E-115 cells differentiate in the presence of 1% DMSO and 1% FBS by ceasing cell proliferation and establishing cell polarity such that they are able to extend neurites (107). To validate whether or not the N1E-115 cell line would be suitable for an *in vitro* RNAi model of MD, I needed to confirm the expression of *Sgce* and other cell type markers. Total RNA was isolated from N1E-115 cells that were either undifferentiated or differentiated for 24 hr, 48 hr, 72 hr and 96 hrs, and subject to random-primed RT-PCR. The first strand cDNA was used for PCR with primers designed to amplify the transcripts of *Sgce*, *Synapsin-1* (*Syn1*), a marker for neurons (108), and *Glial Fibrillary Acidic Protein* (*Gfap*), a marker for astrocytes (109). The expression of *Sgce* and *Syn1* was detected in both undifferentiated and differentiated cells at all time points. The expression of *Gfap* was not detected (data not shown). These result were confirmed by the Affymetrix data obtained (Table 6).

3.2.2 shRNA design and characterization

The rat *Sgce* cDNA sequence was used to design the shRNA sequences as originally the rat pheochromocytoma cell line, PC12, was to be used. However, expression of *Sgce* in PC12 cells could not be reliably detected by either RT-PCR or western blot. The rat and mouse *Sgce* mRNA's are 94% identical and I thought it was likely that shRNA's designed against the rat *Sgce* mRNA would also be effective in silencing the mouse *Sgce* transcript. The rat *Sgce* cDNA sequence, NM_001002023, was entered into Invivogen's siRNA Wizard V2.5 webtool and three shRNA sequences were obtained. The algorithm used by this webtool searches for suitable siRNA sequences using established criteria and each sequence was subject to BLAST search to ensure its specificity. shRNA 1 is located within exon 1, shRNA 2 within exon 5 and shRNA 3 within the 3' untranslated region (UTR) of exon 11 of the rat *Sgce* transcript. A negative control, non-specific shRNA against *lacZ* was designed by Dr Robin Parks, OHRI (Table 5). The shRNA sequences were aligned to the mouse *Sgce* cDNA to determine if they would be suitable for knockdown studies in the mouse neuroblastoma cell line, N1E-115. The nucleotide mismatches between the shRNA sequences and the mouse cDNA are as follows: shRNA1, no differences; shRNA2, nucleotides 1, 7 and 18; shRNA3, nucleotide 7 (Figure 11). Each shRNA was cloned into the pEXPRESS-GFP vector using the *BamHI* and *HindIII* restriction sites included at the 5' and 3' ends of the annealed oligos, and screened by restriction digest and sequencing.

Target	Oligo name	Sequence
nt 124-144	shRNA1-oligo1 102705	5'-GATCCCGCGACCACTGGCACATTCTTATCAAG AGTAAGAATGTGCCAGTGGTCGCTTTTTGGAAA-3'
	shRNA1-oligo2 102705	5'-AGCTTTTCCAAAAAGCGACCACTGGCACATTCT TATCTTGATAAGAATGTGCCAGTGGTCGGG-3'
nt 672-692	shRNA2-oligo1 102705	5'-GATCCCGGTGCCACTTCCTATTAAAGATCAAGA GTCTTTAATAGGAAGTGGCACCTTTTTGGAAA-3'
	shRNA2-oligo2 102705	5'-AGCTTTTCCAAAAAGGTGCCACTTCCTATTAAA GACTCTTGATCTTTAATAGGAAGTGGCACCGG-3'
nt 1373-1393	shRNA3-oligo1 102705	5'-GATCCCGAAGCCATGAGTTTATAATCATCAAGA GTGATTATAAACTCATGGCTTCTTTTTGAAA-3'
	shRNA3-oligo2 102705	5'-AGCTTTTCCAAAAAGAAGCCATGCGTTTATAAT CACTCTTGATGATTATAAACTCATGGCTTCGG-3'
lacZ Control shRNA	sh_lacZ_1348F	5'-TCCCAAATC GTCTGACCGATGATCCGTTCAAG AGACGGATCGGTCAGACGATTTT-3'
	sh_lacZ_1348R	5'-AAAATCGTCTGACCGATCCGAGACTTGAACGG ATCATCATCGGTCAGACGATTTGGGT-3'

Table 5 shRNA sequences

The shRNA sequences that were generated by Invitrogen's siRNA Wizard webtool are listed including the shRNA against LacZ that was designed by Dr. Robin Parks. The target nucleotides (nt) within the *Sgce* mRNA are given.

Figure 11: Alignment of mouse and rat Sgce shRNA sequences.

Alignment of the mouse and rat *Sgce* shRNA sequences at the position where each shRNA will bind. The nucleotide mismatches are highlighted in green.

shRNA 1

Mouse exon 1	GCGACCACTGGCACATTCTTA
Rat exon 1	GCGACCACTGGCACATTCTTA

shRNA 2

Mouse exon 5	[redacted]GTGCC[redacted]CTTCCTATTAA[redacted]GA
Rat exon 5	[redacted]GTGCC[redacted]CTTCCTATTAA[redacted]GA

shRNA3

Mouse exon 11	GAAGC[redacted]ATGAGTTTATAATCA
Rat Exon 11	GAAGC[redacted]ATGAGTTTATAATCA

In order to determine the efficiency of *Sgce* silencing by each shRNA construct, N1E-115 cells were transiently transfected with each shRNA construct and two control plasmids, LacZ and empty vector (GFP), and total RNA and protein was collected 48hrs later.

Transfection efficiency was measured by fluorescence microscopy to detect the expression of the *CMV- GFP* marker present on the pEXPRESS-GFP vector; the transfection efficiency was between 60% and 90% for most experiments. RNA and protein from experiments where the transfection efficiency appeared to be similar were used to detect alterations in *Sgce* mRNA and protein expression. A rabbit polyclonal antibody against Sgce, a gift from Dr Joshua Sanes, was used to determine knockdown of Sgce protein expression in pooled stable shRNA3 clones as compared to control LacZ and GFP clones. It appeared that the protein level of Sgce was decreased when compared to controls; however the quality of the blots was very poor making a clear interpretation of the results impossible (data not shown).

In order to determine the decrease in *Sgce* mRNA expression, I developed a semi-quantitative multiplex reverse transcript-PCR (multiplex Q-PCR) using dHPLC procedure. Random-primed RT-PCR was used to generate first strand cDNA from 1 μg of RNA from each sample, providing a proportional representation of each RNA species present. Multiplex Q-PCR to amplify *Gapdh* and *Sgce* cDNA's was carried out for each of the different shRNA constructs and the resulting PCR products were first visualized by gel electrophoresis to determine if there was a detectable difference in the amount of *Sgce*

PCR product then prepared for dHPLC. dHPLC separates different PCR products based on size, with larger products being eluted from the column first. The retention time and width of an elution peak, expressed as the area under the peak, is proportional to the amount of PCR product present (110). Transgenomic's Navigator Software calculates the area under the peak of each elution product and by dividing the value obtained for the *Sgce* peak by that of the *Gapdh* peak, a ratio of expression is obtained (Figure 12). The average ratio of expression for non-transfected N1E-115 cells was 0.253 and for those transfected with the LacZ shRNA the ratio was 0.219. The average ratio of expression for each of the shRNA constructs was shRNA1 0.100, shRNA2 0.136 and shRNA3 0.055. The data was entered into an Excel spreadsheet and a Student's T-test was performed. When these ratios were compared to the two controls, each shRNA demonstrated a measurable knockdown of the *Sgce* transcript; shRNA1 was 61%, shRNA2 was 46% and shRNA3 was 77% (Figure 13). shRNA3 was used for the establishment of pooled stable clones. These pooled stable clones were then used for neurite outgrowth, cell proliferation and assays to determine the effect of *Sgce* knockdown on other members of the DGC.

3.2.3 Determining selective G418 concentration for the N1E-115 cell line

The survival of N1E-115 cells when exposed to G418 was determined in order to facilitate the establishment of pooled stable clones of each construct. Sub-confluent cultures of non-transfected N1E-115 cells were exposed to concentrations of G418 ranging from 100 ug/ml to 600 ug/ml for 6 days. The health of the cultures was monitored daily i.e. the approximate number of cells attached to the plate surface versus

Figure 12: dHPLC chromatograms of Q-PCR of Gadph and Sgce transcripts

Representative dHPLC chromatograms as viewed on Transgenomic Navigator software. The PCR products elute from the column in order to decreasing size, with larger fragments being eluted first and smaller fragments last. The right hand peak corresponds to the *Gapdh* PCR product which is 600bp. The left peak is of the *Sgce* PCR product which is 400bp. The number values are the area each peak as calculated by Transgenomics Navigator Software.

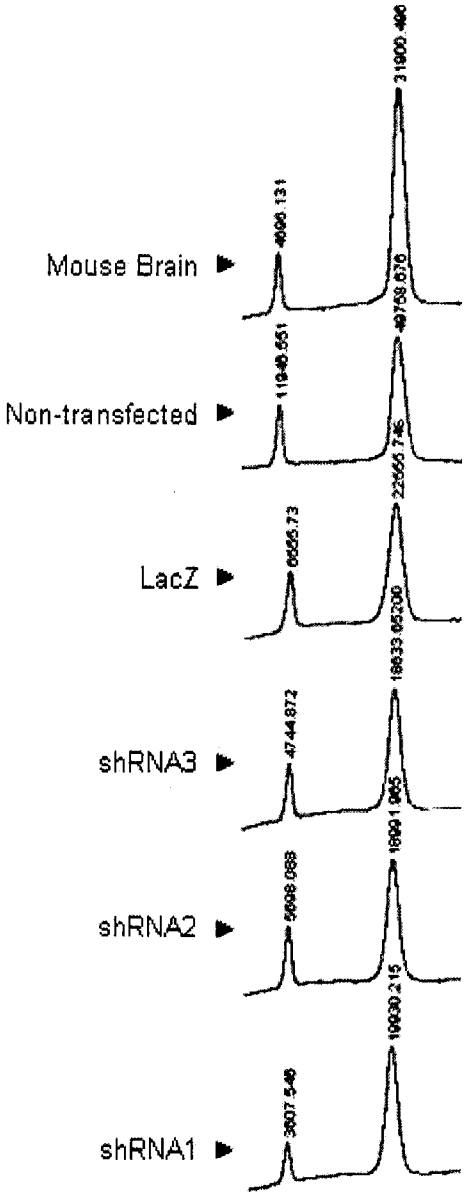
Mouse Brain
Non-transfected
LacZ
shRNA3
shRNA2
shRNA1

Figure 13: Relative knockdown of *Sgce* transcript

Area values obtained from the dHPLC chromatograms were entered into and Excel spreadsheet for statistical analysis. The ratio of *Gapdh* to *Sgce* PCR product was calculated for each sample and is represented as a number value on the Y axis. The Y error bars represent the standard deviation values obtained for each construct. The p values for shRNA1 was $p \leq 0.5$ and shRNA 3 was $p \leq 0.1$ and are indicated by * and ** respectively.

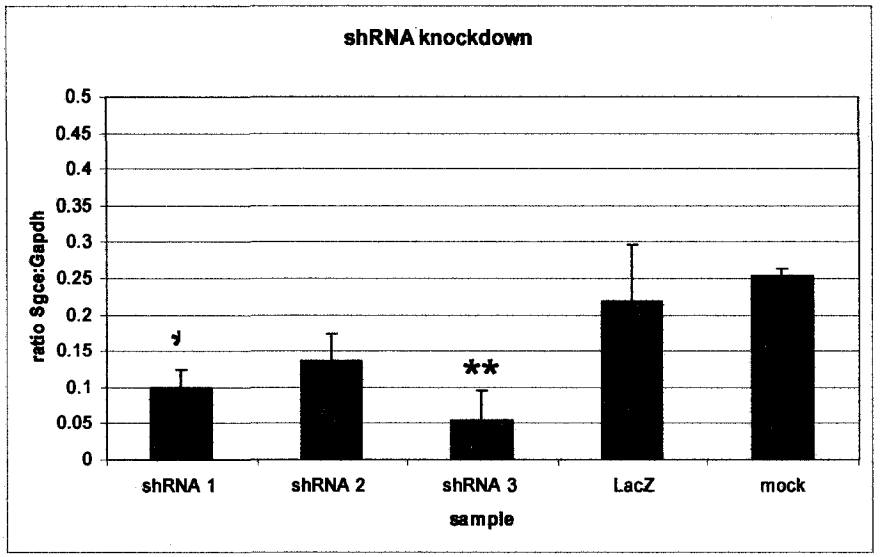
shRNA knockdown
ratio Sgce:Gapdh
0.5
0.45
0.4
0.35
0.3
0.25
0.2
0.15
0.1
0.05
0
*
**
shRNA 1
shRNA 2
shRNA 3
LacZ
mock
sample

dead and floating cells. Concentrations of G418 under 300 ug/ml did not significantly affect survival as the cells continued to proliferate and reached 100% confluency within 3 days. At concentrations between 300 ug/ml and 400 ug/ml, the cultures appeared to be less healthy as the number of cells did not increase and there was a significant amount of cell death. At concentrations higher the 400 ug/ml, the cultures started to die off within 24 hrs of culture and were dead within 4 days (Figure 14)

3.2.4 Sgce is not involved in establishing cell polarity during differentiation of N1E-115 cells

Torsin-A, encoded by the *DYT1* gene, is a member of the AAA family of adenosine triphosphatases (ATPases), associated with diverse cellular activities. Mutations in this gene result in autosomal dominant torsion dystonia, DYT1 (OMIM 128100) (4, 6). Experiments with Torsin-A have have implicated it in regulating the establishment of cell polarity and neurite outgrowth during the differentiation of the human neuroblastoma cell line, SHY- SH5Y (111). N1E-115 cells will differentiate when cultured in differentiation media by ceasing cell proliferation and producing neurites (107). In the absence of DMSO and normal FBS concentrations, most cells appeared to be rounded with few visible neurites and were growing in clusters (Figure 15a1). Culture in differentiation media resulted in increased cell body size and the extension of neurites from the cell body within 24 hrs (Figure 15a3). This process continued over a time course of 4 days, after which there was no further increase in neurite length. To quantify neurite outgrowth of the pooled stable shRNA3, LacZ, GFP and non-transfected N1E-115 cells, neurite length was measured over a period of 4 days of culture in differentiation media. Neurites

Figure 14: Determining the concentration of G418 required to kill N1E-115 cells.

N1E-115 cells were plated at a density of $1x10^5$ cells per 35mm dish. The following day, day 0, the confluency of each culture was approximately 80% and the media was switched to that which contained G418 at a range of concentrations. The confluency of each treatment was recorded for 6 days.

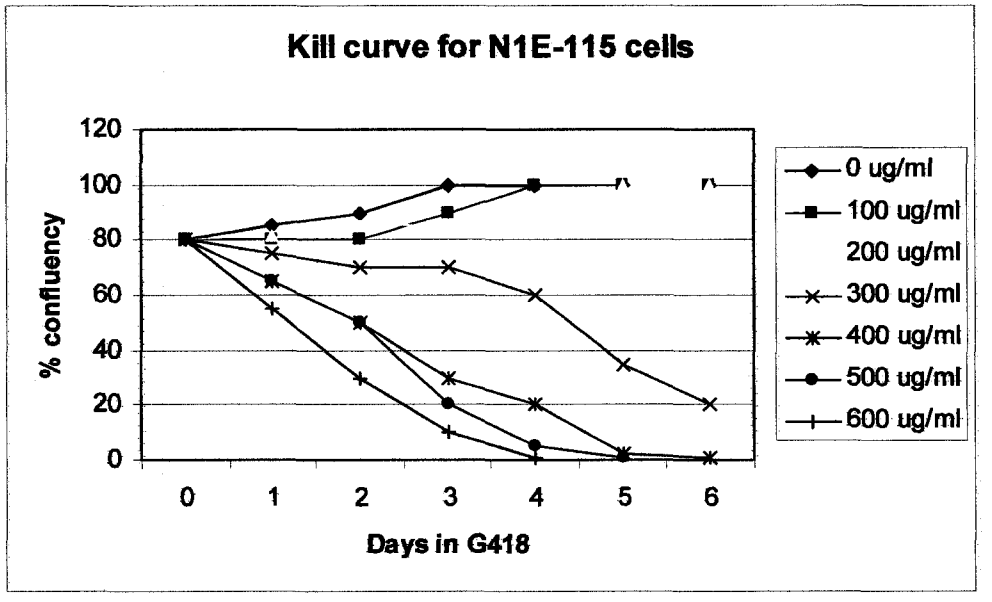
Kill curve for N1E-115 cells
% confluency
120
100
80
60
40
20
0
0
1
2
3
4
5
6
Days in G418
0 ug/ml
100 ug/ml
200 ug/ml
300 ug/ml
400 ug/ml
500 ug/ml
600 ug/ml

Figure 15: Differentiation time course of N1E-115 cells

(A) Phase contrast photographs of wildtype N1E-115 cells cultured in differentiation media containing 1% DMSO and 1% FBS.

(1) Undifferentiated N1E-115 cells have a rounded appearance and grow in clumps with few visible neurite

(2) Cells that have been cultured in differentiation media for 24hrs. The cells have a larger, flatter appearance and have ceased proliferating. Neurite outgrowths are visible.

(3) After 48hrs of culture in differentiation media, there is significant neurite extension from nearly all cells.

(4) After 72hrs in differentiation media, the process of neurite extension is nearly complete and the cells have formed a complicated network of neurites.

(B) Pooled stable clones of each construct and non-transfected N1E-115 cells were cultured for 96hrs in differentiation media. Neurite length was measured using (?) program.

15 A

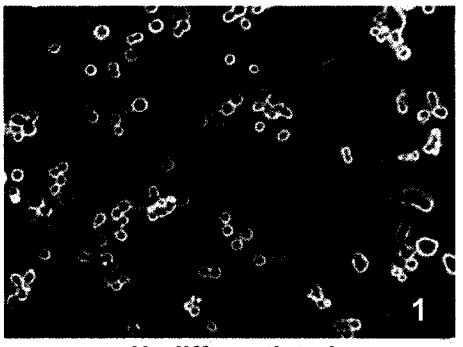

Undifferentiated

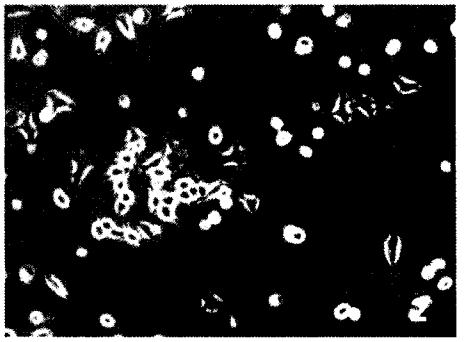

48hrs post-Diff

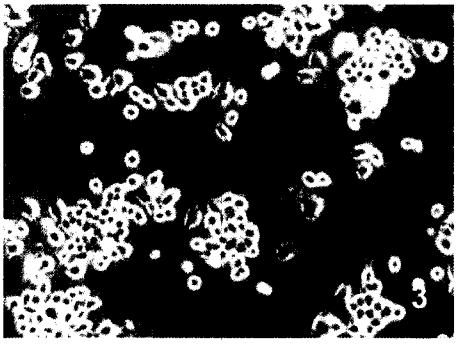

24hrs post-Diff

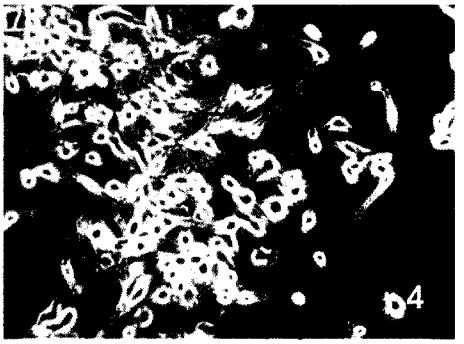

72hrs post-Diff

15 B

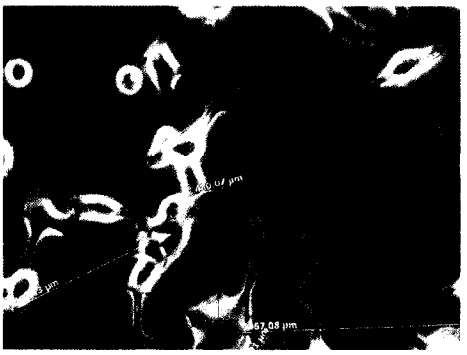

lacZ

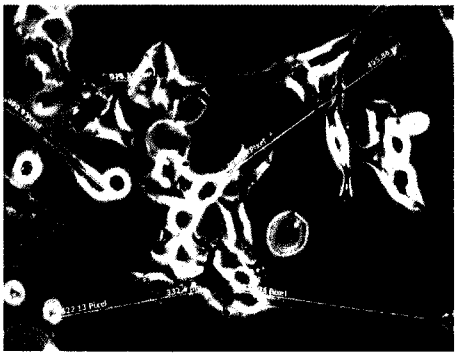

GFP

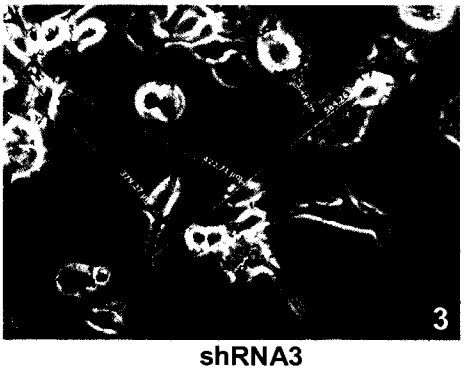

shRNA3

Non-transfected

Figure 16: Neurite outgrowth over time for LacZ. GFP and SH3 pooled stable clones.

(**A**) The data obtained from the neurite measurements was entered in Excel and subject to statistical analysis. The average neurite length was calculated and was found to increase over time for each construct and non-transfected cells.

(**B**) Neurite length at 96hrs. There was no significant difference in neurite length at this time point for each construct and non-transfected cells.

A

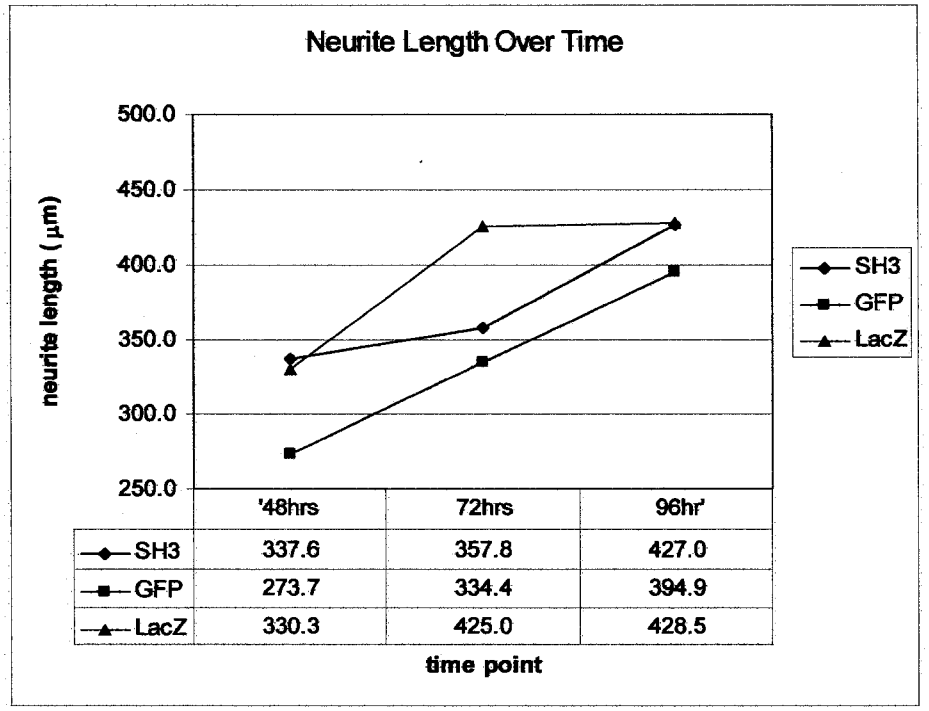
Neurite Length Over Time
500.0
450.0
400.0
350.0
300.0
250.0
neurite length (µm)
SH3
GFP
LacZ
'48hrs
72hrs
96hr'
SH3 337.6 357.8 427.0
GFP 273.7 334.4 394.9
LacZ 330.3 425.0 428.5
time point

B

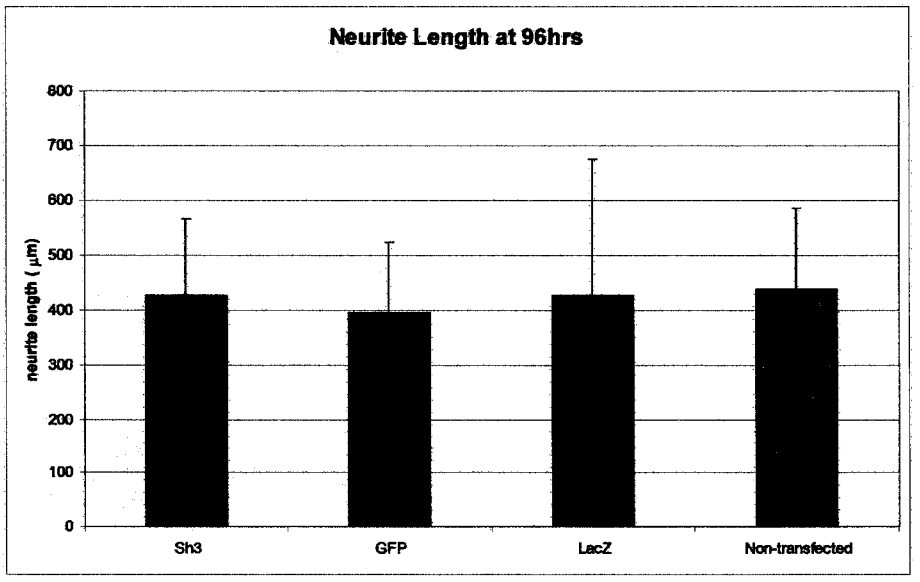
Neurite Length at 96hrs
800
700
600
500
400
300
200
100
0
neurite length (µm)
Sh3
GFP
LacZ
Non-transfected

were qualified as being greater than two times the width of the cell, and associated with a live cell. There was an increase in neurite length over time for each of the different constructs at each of the time point measured. However, pooled stable clones expressing shRNA3 were not compromised in their ability to establish cell polarity during differentiation as compared to LacZ and GFP controls (Figure 15b 1, 2, 3)

3.2.5 Sgce knockdown results in increased cell proliferation

It is not known if Sgce plays a role in cell cycle progression however, the knockdown of *Sgce* expression by RNAi increased cell proliferation in pooled stable clones by 39% at 48 hrs post-plating and 62% at 96hrs post-plating as compared to controls. A known number of cells were plated on day 1 and the number of cell per milliliter of culture was counted every 2 days for a total of 6 days for the shRNA3, LacZ and GFP cell types. There was a steady

increase in the number of cells for each cell type assayed over the course of the experiment. The number of LacZ and GFP cell types increased at approximately the same rate for the first 4 days, after which the number of GFP cells increased faster than that of LacZ cells. There were significantly more shRNA 3 cells present at 48 hr and 96 hr time points. At the 144 hr time point, the number of GFP and shRNA3 cells was approximately equal (Figure 17).

Figure 17: Increased proliferation of SH3 pooled stable clones.

Pooled stable clones of each construct were plated at a density of $1x10^5$ per 35mm dish. The number of cells was counted every 48hrs with a hemacytometer. There was approximately 50% more cells at 48hr and 96hr time point for shRNA3 cells than for lacZ and GFP cells. This difference was not observed at the 144hr time point. ** p value = 0.052

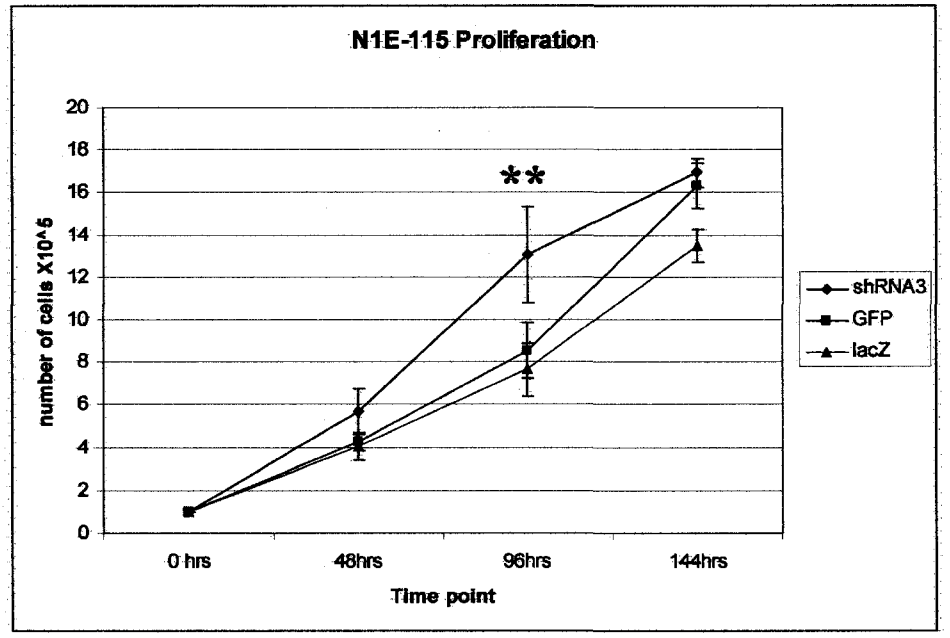
N1E-115 Proliferation
20
18
16
14
12
10
8
6
4
2
0
number of cells X10^5
**
0 hrs
48hrs
96hrs
144hrs
Time point
shRNA3
GFP
lacZ

3.2.6 Expression of DGC components in N1E-115 cells

Affymetrix data that was obtained from the NCBI GEO database and analyzed with the goal of identifying which components of the DGC are present or absent in this cell line. A "hit list" of genes was compiled from the data based on whether they are known components of the DGC in muscle or brain. Key genes of interest that are expressed in this cell line include dystroglycan-1 (*Dag1*), integrin beta 1 (*Itgb1*), laminin alpha 4 (*Lama4*), β-sarcoglycan *(Sgcb*), γ-sarcoglycan (*Sgcg*), sarcospan (*Sspn*), utrophin (*Utrn*), neuronal nitric oxide synthase (*nNos1*) and ε-sarcolygcan (*Sgce*). Those that were not detected include dystrophin 427 (*Dp427*), δ-sarcoglycan (*Sgcd*), α-sarcoglycan (*Sgca*) and caveolins 1,2 and 3 (*Cav1, 2, 3*) (Table 6). The expression of those genes that appeared to be present based on the. Affymetrix data was confirmed by RT-PCR for the following genes: *Sgcb*, *Sgcg*, *Sgcz*, *Lama4*, and *NosI* (Figure 18).

3.2.7 Sgce knockdown does not affect the expression of Sgcb or Sgcg

In muscle, the sarcoglycan proteins come together to form a heterotetrameric complex that is thought to stabilize the DGC. Humans and animals deficient in Sgcb, Sgcd, Sgca or Sgcg have greatly decreased or absence of the other sarcoglycan proteins and exhibit a musclular dystrophy phenotype (61). Multiplex Q-PCR with *Gapdh* was performed to determine if a) there were changes in the relative amounts of *Sgcb* transcript in undifferentiated and differentiated N1E-115 cells at all time points and b) to determine there was any change in the expression of *Sgcb* in response to *Sgce* knockdown. The

	Gene Name	Symbol	P/A call
Cell lineage markers	Glial Fibrillary Acidic Protein	*Gfap*	A
	Synapsin I	***Syn1***	**P**
	Tubulin Beta 3	***Tubb3***	**P**
	Myelin Basic Protein	*Mbp*	A
DGC Proteins	Alpha-dystrobrevin	*Dtna*	A
	Dystroglycan 1	***Dag1***	**P**
	Dystrophin	*Dmd*	A
	Integrin Beta 1	***Itgb1***	**P**
	Laminin alpha 1	*Lama1*	A
	Laminin alpha 4	***Lama4***	**P**
	Neuronal, Nitric Oxide Synthase 1	***Nos1***	**P**
	Macrophage, Nitric Oxide Synthase 2	*Nos2*	A
	Alpha Sarcoglycan	*Sgca*	A
	Beta Sarcoglycan	***Sgcb***	**P**
	Delta Sarcoglycan	*Sgcd*	A
	Epsilon Sarcoglycan	***Sgce***	**P**
	Gamma Sarcoglycan	***Sgcg***	**M**
	Sarcospan	***Sspn***	**P**
	Utrophin	***Utrn***	**P**

Table 6 "hit-list" of genes selected from Affymetrix data

A "hit-list" of genes was identified from the Affymetrix data obtained from the NCBI Geo database. Two classes of genes were selected from, those that are considered to be cell lineage markers and those known to be components of the DGC. Those that are expressed are in **bold**.

Figure 18: RT-PCR results for "hit-list" genes.

RT-PCR products of *Lama4*, *nNos1*, *Sgcg*, *Sgcz*, *Sgcb* and *Sgce* to confirm the Affymetrix data obtained from the NCBI website. PCR primers for each gene were designed to detect only the mRNA transcript.

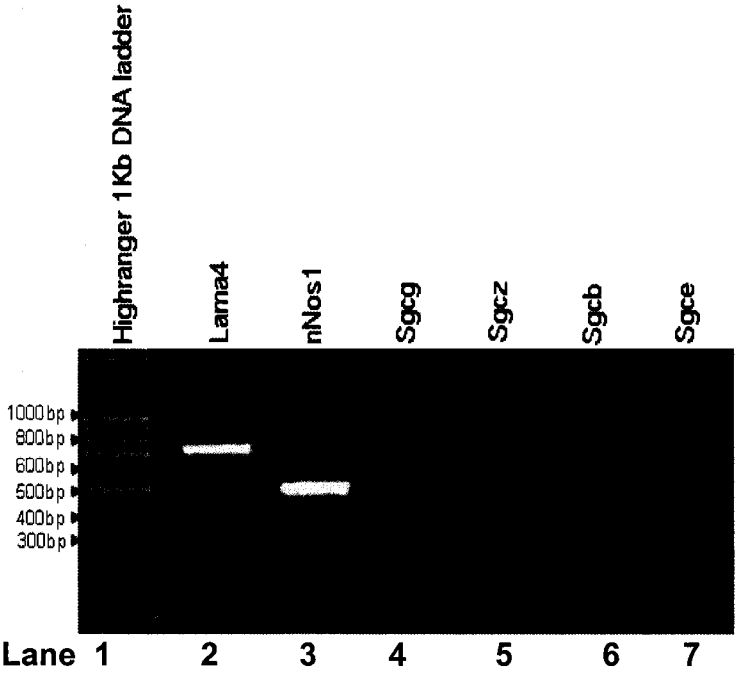
Highranger 1Kb DNA ladder
Lama4
nNos1
Sgcg
Sgcz
Sgcb
Sgce
1000bp
800bp
600bp
500bp
400bp
300bp
Lane 1
2
3
4
5
6
7

Figure 19: The affect of *Sgce* knockdown on Sgcg, *Sgcb* and nNos1

(**A**) Western blot of Sgcg in whole mouse brain homogenate, pooled stable clones of lacZ, GFP and shRNA3 constructs. The Ponceau S stain is below to serve as a loading control. The knockdown of *Sgce*, does not appear to affect the expression of Sgcg.

(**B**) Multi-plex PCR of *Sgcb* with *Gapdh*. The expression of *Sgcb* does not appear to change during the differentiation of N1E-115 cells. Knockdown of *Sgce* does not appear to affect the expression of the *Sgcb* transcript when compared to non-transfected N1E-115 cells.

(**C**) Western blot of nNos1 in whole mouse brain homogenate, pooled stable clones of lacZ, GFP and shRNA3 constructs. The amount of nNos1 is decreased by 50% during Sgce knockdown when compared with lacZ and GFP controls.

A

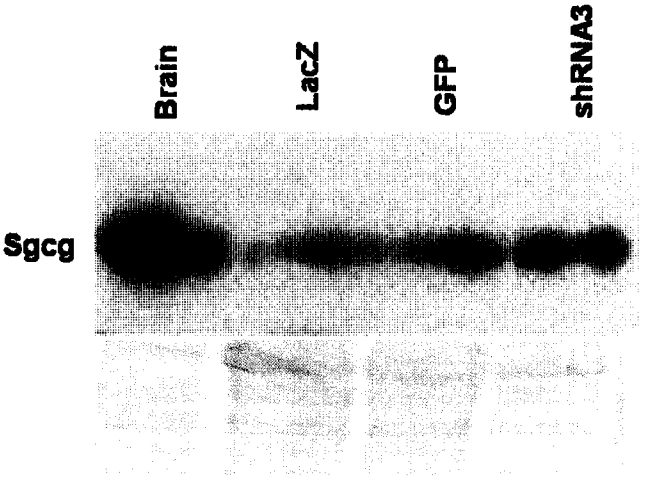
Brain
LacZ
GFP
shRNA3
Sgcg

B

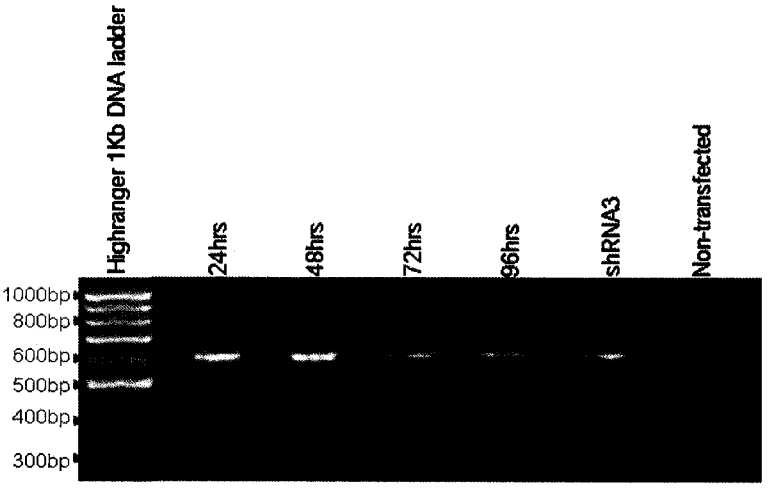
Highranger 1Kb DNA ladder
24hrs
48hrs
72hrs
96hrs
shRNA3
Non-transfected
1000bp
800bp
600bp
500bp
400bp
300bp

C

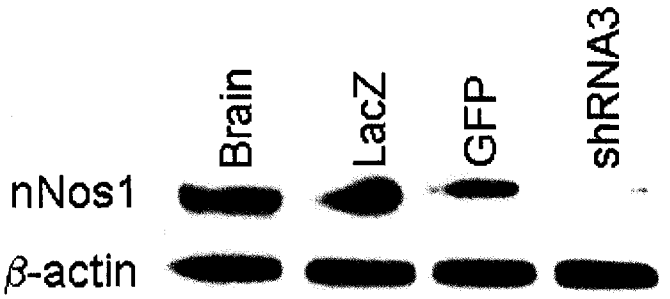
Brain
LacZ
GFP
shRNA3
nNos1
β-actin

relative levels of *Sgcb* compared to *Gapdh* was determined for undifferentiated, differentiated 24, 48, 72 and 96 hr time points and for shRNA3 stable clones in the same manner as for changes in *Sgce* expression. *Sgcb* is expressed in undifferentiated cells and also in differentiated cells at all time points. The expression of *Sgcb* in pooled stable clones for *Sgce* knockdown compared to non-transfected N1E-115 cells does not appear to be significantly different (Figure 19). RT-PCR experiments confirmed the presence of he Sgcg transcript from the Affymetrix data (Figure 18 lane 4). An antibody was obtained from Dr. Rashmi Kothary for the detection of Sgcg. N1E-115 whole cell lysates and mouse brain homogenate were subject to western blot (Figure 19a). The presence of the Sgcg transcript in the central nervous system has been previously reported, however its protein expression has not been confirmed (44).

3.2.8 Sgce knockdown results in decreased levels of nNos1

Neuronal nitric oxide synthase (nNos1) is anchored to the sarcolemma through its interactions with the DGC. It has been shown that animals lacking the sarcoglycan-sarcospan complex have significantly decreased levels of nNos1 and this is thought to contribute to the pathology of the muscular dystrophy (80, 81, 92). In order to determine if knockdown of Sgce had any effect on the expression of nNos, multiplex Q-PCR and western blotting was performed. The presence of the nNos1 transcript in N1E-115 cells was confirmed by RT-PCR (Figure 18 lane 3). Whole cell lysates from pooled stable clones of LacZ, GFP and shRNA3 and mouse brain homogenate were subject to western blotting with a polyclonal antibody against nNos1. A 160Kda band corresponding to

nNos1 was detected in each of the lanes. However, in shRNA3 pooled stable clones, the amount of nNos1 detected was decreased by 50% compared to controls (Figure 19c).

3.3 Discussion

To complement our *in vivo* model of MD I sought to develop an *in vitro* model of this disease using RNA interference (RNAi) against *Sgce*, allowing us to determine at the cellular and molecular level the affect that the absence of *Sgce* had. By designing shRNA oligos that would specifically target the Sgce mRNA transcript for degradation by the RNAi pathway, a cellular environment where the presence of Sgce would be greatly reduced or absent would be created (112). I hoped to be able to use any information that was obtained from these experiments to allow us to more efficiently characterize the CKO mouse model of MD.

There are two methods to achieve gene silencing by RNAi *in vitro*. The first method is the use of short interfering RNA (siRNA) oligos that are directly transfected into the cell and mediate transient knockdown of the target gene for 3 to 5 days. The second method is to generate 60 to 65 bp DNA oligos that are cloned into a vector that directs its expression from an appropriate promoter. These DNA oligos are complementary in sequence and form a hairpin structure after being transcribed. These short hairpin RNA (shRNA) molecules are then processed by cellular machinery and subsequently silence the expression of the target gene. The latter method has the advantage in that it provides for the establishment of stable clones that express the shRNA and allows for long term studies into the function of the target gene (112).

Three shRNA oligos, shRNA1, shRNA2, and shRNA3, were designed to target the rat *Sgce* mRNA, however I decided to use a mouse cell line. Fortunately there was a

significant amount of conservation between the rat and mouse orthologues of this gene and there appeared to be few mismatches between the shRNA oligo sequences and the mouse *Sgce* mRNA (Figure 11). Other studies have shown that mismatches do not necessarily decrease the silencing ability of an oligo and in fact, mismatches in the 5' end may actually increase silencing ability. The pEXPRESS-GFP vector was chosen for this study as it contains a *CMV-GFP* cassette in order to track transfection, a neomycin resistance gene and the expression of the shRNA is directed from the human H1 promoter. The H1 transcipt is a component of the human nuclear RNAseP enzyme that cleaves tRNA precursors to produce their mature form. The H1 promoter is relatively simple in its structure as it lies immediately upstream of the sequence to be transcribed and therefore does not require the presence of additional promoter elements within the shRNA or the vector. RNApolIII is chosen to drive shRNA expression in many different shRNA vectors as it expresses large amounts of small RNAs in mammalian cells and it terminates transcription upon incorporating a string of 3–6 uridines. Each shRNA designed contained a string of 4 thymidine residues that when transcribed would provide the termination sequence (Table 5) (113). The shRNA oligos were each directionally cloned into the pEXPRESS-GFP vector prior to being transfected into N1E-115 cells.

The N1E-115 cell line was chosen because it is of neuronal origin, is capable of producing neurite outgrowths under the appropriate conditions, is relatively easy to maintain in culture, was found to express *Sgce* and has been used extensively in models of neurological disease (114-116). Following the transfection of the shRNA oligos into this cell line, I collected total RNA and protein in order to ascertain the efficiency of

knockdown of *Sgce* of each oligo when compared to control, scrambled LacZ, and empty vector (GFP). This provided a unique obstacle as a reliable antibody against Sgce was proving difficult to obtain and I did not have the protocols required for real time or semi-quantitative RT-PCR established in our laboratory. As we already were performing dosage analysis to determine gene copy number at the genomic level using PCR and our dHPLC machine, I thought it might be possible to use a slightly modified protocol for determining mRNA levels as well.

In order to accurately quantify the amount of *Sgce* transcript present, it was necessary to use a random-primed RT-PCR approach. Random primed RT-PCR uses non-specific random hexamer oligonucleotides to prime the generation of the first strand complementary DNA by the reverse transcriptase enzyme. As this technique does not preferentially reverse transcribe any one transcript, there is a proportional representation of each mRNA species in the sample. I chose to use *Gapdh* as an internal control for the following PCR because it is a 'house keeping gene' that is expressed in all cell types and its levels did not appear to fluctuate during differentiation, which can be a drawback to using other typical controls such as *Actin* (117). After optimizing the conditions for each primer set individually, I determined the conditions necessary for the amplification of both products in the same reaction. It was found that approximately 25 cycles were sufficient to obtain a measurable amount of both PCR products prior to reaching the "plateau phase" of amplification (118).

After visualization of the products on an agarose gel using ethidium bromide staining, I was able to see that there appeared to be a decrease in the amount of *Sgce* product present as compared to the control *Gapdh* product for each. However, I was unable to assign a value to the decrease in *Sgce* transcript and the efficiency of silencing by each shRNA oligo. In order to determine this value, I then subjected the PCR products to dHPLC to provide a much more sensitive means of determining the amount of each product present as opposed to visualization followed by densitometry analysis. The retention time and width of an elution peak, expressed as the area under the peak, is proportional to the amount of PCR product present (110). Using this technique I was able to reliably determine the amount of knockdown of the *Sgce* transcript by each of the shRNA oligos as compared to the control LacZ and non-transfected cells. I found that shRNA3 had the greatest silencing efficiency compared to shRNA1 and shRNA2; 77% versus 61% and 46% respectively (Figure 13). This method is a novel way to measure changes in the amount of transcript present in a sample, and may prove useful to investigators who do not have easy access to real-time PCR reagents and equipment, yet still wish to accurately quantify silencing by RNAi at the mRNA level.

After determining which of the 3 shRNA oligos was most efficient at silencing the expression of *Sgce*, I went on to establish stable pooled clones for cells that had been transfected with shRNA3, LacZ and GFP vectors. These were then used to characterize the affect of Sgce knockdown on a number of different variables. It has been previously described that alterations in the expression of TorA result in changes in the establishment of cell polarity and neurite outgrowth during the differentiation of SHY-SH5Y cells

(111). As mutations in TorA results in a movement disorder which is clinically similar to MD, I sought to determine if neurite outgrowth was affected by the knockdown of *Sgce* (1) . I examined neurite outgrowth for pooled stable clones of the three vectors and also non-transfected cells every 24 hrs for 4 days and found that there wasn't a significant difference between the different cell lines (Figure 16). This indicates that although DYT1 and MD are clinically similar, their phenotypes do not arise from the same cellular dysfunction.

It was noted that during routine culture that the shRNA3 pooled stable cell line appeared to grow much quicker than either the LacZ or GFP cell lines. Follow up experiments to quantify this difference in growth rate indicated that shRNA3 clones grew between 39% and 62% faster than controls (Figure 17). There have been no previous reports of the DGC or other sarcoglycan proteins being involved in cell cycle progression or cell proliferation. However, in neurons, nNos1 is known to be involved in regulating many cellular activities such as apoptosis, differentiation and proliferation and appears to be reduced in the N1E-115 clones silenced for *Sgce* (79). This protein is also known to interact with the DGC and sarcoglycans (80).

Nitric oxide (NO) and L-citruline are the products of nNos1 as it breaks down L-arginine and O_2 in the presence of nicotinamide adenine dinucleotide phosphate (NADPH) (75, 119) (Figure 20). Although NO has many diverse functions, in the central nervous system NO functions as a paracrine signaling molecule to negatively regulate neuronal precursor cell (NPC) proliferation and positively regulate differentiation (79, 88, 89,

120). In neurons, nNos is localized to the post-synaptic density where it interacts with the post-synaptic density protein 95 (PSD-95) and nitric oxide synthase interacting protein (NOSIP) (82). This protein interacts with cytoskeletal elements such as PSD-95 through its PDZ domain which in turn tethers nNos1 to a functional complex containing N-methyl-D-aspartic acid (NMDA) subtype of glutamate receptor (83, 87, 91). The activation of the NMDA receptors by glutamate results in an increase in intracellular Ca^{2+} concentrations which in turn activates nNos1 through calmodulin (CALM). The highest levels of expression of nNos1 in the mammalian brain are the olfactory bulb and the granule cells of the cerebellum (79).

It has been previously reported that nNos is a positive regulator of neural progenitor cell (NPC) proliferation in a pathway that also includes brain-derived neurotrophic factor (BDNF) and N-Myc (89, 120). Animals deficient in nNos1 have a decrease in the number of immature neurons in the olfactory epithelium and are decreased in the complexity of the dendrites in developing motor neurons (79). Humans and animals that are deficient in dystrophin and the other sarcoglycan proteins also appear to have a great decrease or complete absence of nNos1 (80, 92). However, this is the first evidence that there may be a link between ε-sarcoglycan and nNos1 levels. The increase in proliferation observed in the *Sgce* silenced N1E-115 cells may be related to the decrease in the presence of the nNos1 protein and a concurrent decrease in NO production (Figure 19c). It is not clear whether there is a direct or indirect interaction between these two molecules that is being disrupted leading to an increase in the turnover of the nNos1 protein. Or whether or not the amount of NO produced is in fact decreased. It will be

Figure 20: The production of NO by Nos.

Nitric oxide (NO) and L-citruline are produced by a nitric oxide synthase as it breaks down L-arginine in the presence of O2 and NAPDH. Adapted with modification from Voet et al (*121*)

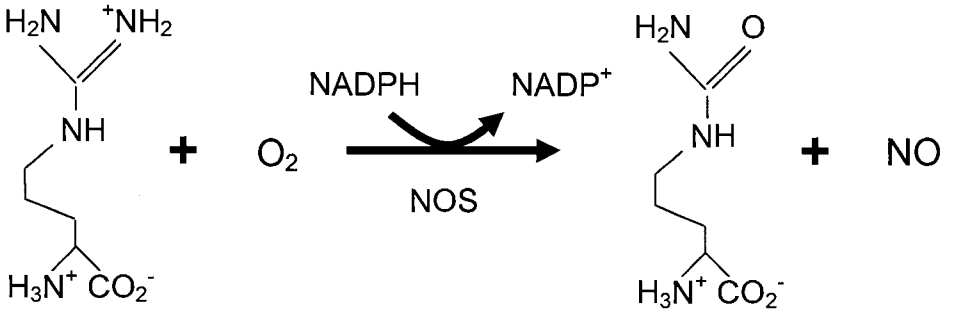
H2N
+NH2
NH
H3N+ CO2-
+
O2
NADPH
NADP+
NOS
H2N
O
NH
H3N+ CO2-
+
NO

necessary to quantify the amount of NO produced by the Sgce silenced cells when compared to controls. Alternatively, it may be feasible to treat non-transfected, LacZ and GFP N1E-115 cells with the Nos inhibitor, N-ω-nitro-L-arginine methylester (L-NAME) and compare any changes observed in their proliferation to the Sgce silenced cells (79).

The LacZ and GFP cells eventually caught up with the shRNA3 cells by 144hrs in culture. This can be attributed to this particular cell lines ability to tolerate high cell densities for a long period of time. It was observed during routine culture, that this cell line did not appear to tolerate being kept at confluency for extended periods of time before the cells appeared to form aggregates and detach from the cell surface. This intolerance did not appear to be different between each of the different cell lines (data not shown).

It has been reported that the correct expression and localization of the other DGC protein and sarcoglycans is necessary for the assembly of the complex at the sarcolemma. This affect manifests itself clinically as muscular dystrophy i.e. Duchenne muscular dystrophy or LGMD (41). However, the presence of ε-sarcoglycan does not appear to be required for the correct assembly of the DGC or SGC at the sarcolemma in skeletal muscle despite its being expressed in this tissue. Although the presence of a sarcoglycan complex of proteins in the brain has not been described I have found transcriptional evidence of *Scgb*, *Sgcg* and *Sgcz* and protein evidence of Sgcg in both mouse brain and the N1E-115 cell line. Therefore it is likely that a sarcoglycan complex exists within the mammalian brain and is composed of β, γ, ζ and ε. This would be the third such complex, the first of

which is found in skeletal and cardiac muscle and is composed of α, β, δ and γ and the second, which is found in smooth muscle, is composed of ε, β, δ and ζ (41, 44). This finding is interesting as it paints a more complete picture of the DGC and associated proteins within the brain, although it does raise some questions as well. For example, what is the function of the DGC and sarcoglycan complex within the brain and why is it that mutations in *Sgce* results in a neurological disorder whereas mutations in the other sarcoglycans results in muscular dystrophy? Further experimentation will be needed to answer these questions.

3.3.1 Future Directions

These results provide tantalizing clues into the presence of an SGC complex within the CNS which will require further experimentation to confirm. The results of our *in vitro* model of MD using RNAi in a cell line of neuronal origin will be useful for the characterization of the CKO mouse model. Valuable time and labor will be saved by focusing experiments on the mouse model on the expression and function of nNos1. That there is an increase in cell proliferation *in vitro* could provide an explanation for the defect present in MD. It is hoped that the results of this study, in combination with the CKO mouse model of MD, that I will gain insight into the function of the Sgce molecule within the mammalian central nervous system.

Chapter 4: General Directions

The long term goal of this project is to provide knowledge and insight into the pathogenesis of MD. The establishment of an *in vivo* and *in vitro* model of MD was important in achieving this goal as it will provide valuable information not only with regards to this disease but also into the function of the mammalian CNS. I was able to employ methods that were relatively new to our laboratory to generate the CKO targeting cassette, to isolate 3 correctly targeted ES cell clones and to obtain 3 chimeric male mice. The establishment, biochemical and behavioral characterization of the *sgce*^{null} mouse colony will be the responsibility of present and future members of the Bulman laboratory. The results of the *in vitro* RNAi experiments against this molecule provided novel information into the function of ε-sarcoglycan and the possible consequences of its absence. My results indicate that ε-sarcoglycan is required for the proper expression of nNos and therefore NO signaling resulting in increased cell proliferation. Although it has not been reported that MD patients have increased cell density within the areas of the brain that are required for motor control, this defect may be missed during routine histological examination. It is hoped that this information will be useful for the characterization of the *sgce*^{null} mice.

References

1. de Carvalho Aguiar, P.M. and Ozelius, L.J. (2002) Classification and genetics of dystonia. *Lancet Neurol,* **1,** 316-25.
2. Nemeth, A.H. (2002) The genetics of primary dystonias and related disorders. *Brain,* **125,** 695-721.
3. Ozelius, L.J., Hewett, J.W., Page, C.E., Bressman, S.B., Kramer, P.L., Shalish, C., de Leon, D., Brin, M.F., Raymond, D., Corey, D.P. *et al.* (1997) The early-onset torsion dystonia gene (DYT1) encodes an ATP-binding protein. *Nat Genet,* **17,** 40-8.
4. Konakova, M., Huynh, D.P., Yong, W. and Pulst, S.M. (2001) Cellular distribution of torsin A and torsin B in normal human brain. *Arch Neurol,* **58,** 921-7.
5. Gerace, L. (2004) TorsinA and torsion dystonia: Unraveling the architecture of the nuclear envelope. *Proc Natl Acad Sci U S A,* **101,** 8839-40.
6. Naismith, T.V., Heuser, J.E., Breakefield, X.O. and Hanson, P.I. (2004) TorsinA in the nuclear envelope. *Proc Natl Acad Sci U S A,* **101,** 7612-7.
7. Nolte, D., Niemann, S. and Muller, U. (2003) Specific sequence changes in multiple transcript system DYT3 are associated with X-linked dystonia parkinsonism. *Proc Natl Acad Sci U S A,* **100,** 10347-52.
8. Segawa, M., Nomura, Y. and Nishiyama, N. (2003) Autosomal dominant guanosine triphosphate cyclohydrolase I deficiency (Segawa disease). *Ann Neurol,* **54 Suppl 6,** S32-45.
9. Werner-Felmayer, G., Golderer, G. and Werner, E.R. (2002) Tetrahydrobiopterin biosynthesis, utilization and pharmacological effects. *Curr Drug Metab,* **3,** 159-73.
10. Fink, J.K., Rainer, S., Wilkowski, J., Jones, S.M., Kume, A., Hedera, P., Albin, R., Mathay, J., Girbach, L., Varvil, T. *et al.* (1996) Paroxysmal dystonic choreoathetosis: tight linkage to chromosome 2q. *Am J Hum Genet,* **59,** 140-5.
11. Walker, E.S. (1981) Familial paroxysmal dystonic choreoathetosis: a neurologic disorder simulating psychiatric illness. *Johns Hopkins Med J,* **148,** 108-13.
12. Muller, U. and Kupke, K.G. (1990) The genetics of primary torsion dystonia. *Hum Genet,* **84,** 107-15.
13. Rainier, S., Thomas, D., Tokarz, D., Ming, L., Bui, M., Plein, E., Zhao, X., Lemons, R., Albin, R., Delaney, C. *et al.* (2004) Myofibrillogenesis regulator 1 gene mutations cause paroxysmal dystonic choreoathetosis. *Arch Neurol,* **61,** 1025-9.
14. Asmus, F., Zimprich, A., Tezenas Du Montcel, S., Kabus, C., Deuschl, G., Kupsch, A., Ziemann, U., Castro, M., Kuhn, A.A., Strom, T.M. *et al.* (2002) Myoclonus-dystonia syndrome: epsilon-sarcoglycan mutations and phenotype. *Ann Neurol,* **52,** 489-92.
15. Doheny, D.O., Brin, M.F., Morrison, C.E., Smith, C.J., Walker, R.H., Abbasi, S., Muller, B., Garrels, J., Liu, L., De Carvalho Aguiar, P. *et al.* (2002) Phenotypic features of myoclonus-dystonia in three kindreds. *Neurology,* **59,** 1187-96.
16. Zimprich, A., Grabowski, M., Asmus, F., Naumann, M., Berg, D., Bertram, M., Scheidtmann, K., Kern, P., Winkelmann, J., Muller-Myhsok, B. *et al.* (2001)

Mutations in the gene encoding epsilon-sarcoglycan cause myoclonus-dystonia syndrome. *Nat Genet,* **29,** 66-9.
17. Asmus, F., Salih, F., Hjermind, L.E., Ostergaard, K., Munz, M., Kuhn, A.A., Dupont, E., Kupsch, A. and Gasser, T. (2005) Myoclonus-dystonia due to genomic deletions in the epsilon-sarcoglycan gene. *Ann Neurol,* **58,** 792-7.
18. Grimes, D.A., Han, F., Lang, A.E., St George-Hyssop, P., Racacho, L. and Bulman, D.E. (2002) A novel locus for inherited myoclonus-dystonia on 18p11. *Neurology,* **59,** 1183-6.
19. Brashear, A., DeLeon, D., Bressman, S.B., Thyagarajan, D., Farlow, M.R. and Dobyns, W.B. (1997) Rapid-onset dystonia-parkinsonism in a second family. *Neurology,* **48,** 1066-9.
20. de Carvalho Aguiar, P., Sweadner, K.J., Penniston, J.T., Zaremba, J., Liu, L., Caton, M., Linazasoro, G., Borg, M., Tijssen, M.A., Bressman, S.B. *et al.* (2004) Mutations in the Na+/K+ -ATPase alpha3 gene ATP1A3 are associated with rapid-onset dystonia parkinsonism. *Neuron,* **43,** 169-75.
21. Nygaard, T.G., Raymond, D., Chen, C., Nishino, I., Greene, P.E., Jennings, D., Heiman, G.A., Klein, C., Saunders-Pullman, R.J., Kramer, P. *et al.* (1999) Localization of a gene for myoclonus-dystonia to chromosome 7q21-q31. *Ann Neurol,* **46,** 794-8.
22. Caviness, J.N., Alving, L.I., Maraganore, D.M., Black, R.A., McDonnell, S.K. and Rocca, W.A. (1999) The incidence and prevalence of myoclonus in Olmsted County, Minnesota. *Mayo Clin Proc,* **74,** 565-9.
23. Quinn, N.P., Rothwell, J.C., Thompson, P.D. and Marsden, C.D. (1988) Hereditary myoclonic dystonia, hereditary torsion dystonia and hereditary essential myoclonus: an area of confusion. *Adv Neurol,* **50,** 391-401.
24. Maloudji, M., Gordon, A.M. and Scott, C.I., Jr. (1971) Hereditary essential myoclonus. *Birth Defects Orig Artic Ser,* **7,** 226-7.
25. Korten, J.J., Notermans, S.L., Frenken, C.W., Gabreels, F.J. and Joosten, E.M. (1974) Familial essential myoclonus. *Brain,* **97,** 131-8.
26. Kyllerman, M., Forsgren, L., Sanner, G., Holmgren, G., Wahlstrom, J. and Drugge, U. (1990) Alcohol-responsive myoclonic dystonia in a large family: dominant inheritance and phenotypic variation. *Mov Disord,* **5,** 270-9.
27. Daube, J.R. and Peters, H.A. (1966) Hereditary essential myoclonus. *Arch Neurol,* **15,** 587-94.
28. Mahloudji, M. and Pikielny, R.T. (1967) Hereditary essential myoclonus. *Brain,* **90,** 669-74.
29. Klein, C., Liu, L., Doheny, D., Kock, N., Muller, B., de Carvalho Aguiar, P., Leung, J., de Leon, D., Bressman, S.B., Silverman, J. *et al.* (2002) Epsilon-sarcoglycan mutations found in combination with other dystonia gene mutations. *Ann Neurol,* **52,** 675-9.
30. Klein, C., Gurvich, N., Sena-Esteves, M., Bressman, S., Brin, M.F., Ebersole, B.J., Fink, S., Forsgren, L., Friedman, J., Grimes, D. *et al.* (2000) Evaluation of the role of the D2 dopamine receptor in myoclonus dystonia. *Ann Neurol,* **47,** 369-73.
31. Wahlstrom, J., Ozelius, L., Kramer, P., Kyllerman, M., Schuback, D., Forsgren, L., Holmgren, G., Drugge, U., Sanner, G., Fahn, S. *et al.* (1994) The gene for

familial dystonia with myoclonic jerks responsive to alcohol is not located on the distal end of 9q. *Clin Genet,* **45,** 88-92.
32. Gasser, T., Bereznai, B., Muller, B., Pruszak-Seel, R., Damrich, R., Deuschl, G. and Oertel, W.H. (1996) Linkage studies in alcohol-responsive myoclonic dystonia. *Mov Disord,* **11,** 363-70.
33. Klein, C., Schilling, K., Saunders-Pullman, R.J., Garrels, J., Breakefield, X.O., Brin, M.F., deLeon, D., Doheny, D., Fahn, S., Fink, J.S. *et al.* (2000) A major locus for myoclonus-dystonia maps to chromosome 7q in eight families. *Am J Hum Genet,* **67,** 1314-9.
34. Fahn, S. and Sjaastad, O. (1991) Hereditary essential myoclonus in a large Norwegian family. *Mov Disord,* **6,** 237-47.
35. Kurlan, R., Behr, J. and Shoulson, I. (1987) Hereditary myoclonus and chorea: the spectrum of hereditary nonprogressive hyperkinetic movement disorders. *Mov Disord,* **2,** 301-6.
36. Lundemo, G. and Persson, H.E. (1985) Hereditary essential myoclonus. *Acta Neurol Scand,* **72,** 176-9.
37. Kurlan, R., Behr, J., Medved, L., Shoulson, I., Pauls, D. and Kidd, K.K. (1987) Severity of Tourette's syndrome in one large kindred. Implication for determination of disease prevalence rate. *Archives of neurology,* **44,** 268-9.
38. Okita, C., Meguro, M., Hoshiya, H., Haruta, M., Sakamoto, Y.K. and Oshimura, M. (2003) A new imprinted cluster on the human chromosome 7q21-q31, identified by human-mouse monochromosomal hybrids. *Genomics,* **81,** 556-9.
39. Ono, R., Shiura, H., Aburatani, H., Kohda, T., Kaneko-Ishino, T. and Ishino, F. (2003) Identification of a large novel imprinted gene cluster on mouse proximal chromosome 6. *Genome Res,* **13,** 1696-705.
40. Grabowski, M., Zimprich, A., Lorenz-Depiereux, B., Kalscheuer, V., Asmus, F., Gasser, T., Meitinger, T. and Strom, T.M. (2003) The epsilon-sarcoglycan gene (SGCE), mutated in myoclonus-dystonia syndrome, is maternally imprinted. *Eur J Hum Genet,* **11,** 138-44.
41. Lapidos, K.A., Kakkar, R. and McNally, E.M. (2004) The dystrophin glycoprotein complex: signaling strength and integrity for the sarcolemma. *Circulation research,* **94,** 1023-31.
42. Wheeler, M.T. and McNally, E.M. (2003) Sarcoglycans in vascular smooth and striated muscle. *Trends Cardiovasc Med,* **13,** 238-43.
43. Fort, P., Estrada, F.J., Bordais, A., Mornet, D., Sahel, J.A., Picaud, S., Vargas, H.R., Coral-Vazquez, R.M. and Rendon, A. (2005) The sarcoglycan-sarcospan complex localization in mouse retina is independent from dystrophins. *Neurosci Res,* **53,** 25-33.
44. Ozawa, E., Mizuno, Y., Hagiwara, Y., Sasaoka, T. and Yoshida, M. (2005) Molecular and cell biology of the sarcoglycan complex. *Muscle Nerve,* **32,** 563-76.
45. Ettinger, A.J., Feng, G. and Sanes, J.R. (1997) epsilon-Sarcoglycan, a broadly expressed homologue of the gene mutated in limb-girdle muscular dystrophy 2D. *J Biol Chem,* **272,** 32534-8.
46. Hack, A.A., Lam, M.Y., Cordier, L., Shoturma, D.I., Ly, C.T., Hadhazy, M.A., Hadhazy, M.R., Sweeney, H.L. and McNally, E.M. (2000) Differential

requirement for individual sarcoglycans and dystrophin in the assembly and function of the dystrophin-glycoprotein complex. *J Cell Sci,* **113 (Pt 14),** 2535-44.

47. Chen, J., Shi, W., Zhang, Y., Sokol, R., Cai, H., Lun, M., Moore, B.F., Farber, M.J., Stepanchick, J.S., Bonnemann, C.G. *et al.* (2006) Identification of functional domains in sarcoglycans essential for their interaction and plasma membrane targeting. *Exp Cell Res,* **312,** 1610-25.
48. Holt, K.H. and Campbell, K.P. (1998) Assembly of the sarcoglycan complex. Insights for muscular dystrophy. *J Biol Chem,* **273,** 34667-70.
49. Shi, W., Chen, Z., Schottenfeld, J., Stahl, R.C., Kunkel, L.M. and Chan, Y.M. (2004) Specific assembly pathway of sarcoglycans is dependent on beta- and delta-sarcoglycan. *Muscle Nerve,* **29,** 409-19.
50. Imamura, M., Mochizuki, Y., Engvall, E. and Takeda, S. (2005) Epsilon-sarcoglycan compensates for lack of alpha-sarcoglycan in a mouse model of limb-girdle muscular dystrophy. *Hum Mol Genet,* **14,** 775-83.
51. Crosbie, R.H., Lim, L.E., Moore, S.A., Hirano, M., Hays, A.P., Maybaum, S.W., Collin, H., Dovico, S.A., Stolle, C.A., Fardeau, M. *et al.* (2000) Molecular and genetic characterization of sarcospan: insights into sarcoglycan-sarcospan interactions. *Hum Mol Genet,* **9,** 2019-27.
52. McNally, E.M., Ly, C.T. and Kunkel, L.M. (1998) Human epsilon-sarcoglycan is highly related to alpha-sarcoglycan (adhalin), the limb girdle muscular dystrophy 2D gene. *FEBS letters,* **422,** 27-32.
53. Nishiyama, A., Endo, T., Takeda, S. and Imamura, M. (2004) Identification and characterization of epsilon-sarcoglycans in the central nervous system. *Brain Res,* **125,** 1-12.
54. Xiao, J. and LeDoux, M.S. (2003) Cloning, developmental regulation and neural localization of rat epsilon-sarcoglycan. *Brain Res,* **119,** 132-43.
55. Holt, K.H., Lim, L.E., Straub, V., Venzke, D.P., Duclos, F., Anderson, R.D., Davidson, B.L. and Campbell, K.P. (1998) Functional rescue of the sarcoglycan complex in the BIO 14.6 hamster using delta-sarcoglycan gene transfer. *Mol Cell,* **1,** 841-8.
56. Yoshida, T., Pan, Y., Hanada, H., Iwata, Y. and Shigekawa, M. (1998) Bidirectional signaling between sarcoglycans and the integrin adhesion system in cultured L6 myocytes. *J Biol Chem,* **273,** 1583-90.
57. Chan, P., Gonzalez-Maeso, J., Ruf, F., Bishop, D.F., Hof, P.R. and Sealfon, S.C. (2005) Epsilon-sarcoglycan immunoreactivity and mRNA expression in mouse brain. *J Comp Neurol,* **482,** 50-73.
58. Chou-Green, J.M., Holscher, T.D., Dallman, M.F. and Akana, S.F. (2003) Compulsive behavior in the 5-HT2C receptor knockout mouse. *Physiol Behav,* **78,** 641-9.
59. Yokoi, F., Dang, M.T., Li, J. and Li, Y. (2006) Myoclonus, Motor Deficits, Alterations in Emotional Responses and Monoamine Metabolism in {varepsilon}-Sarcoglycan Deficient Mice. *J Biochem (Tokyo),* **140,** 141-6.
60. Warner, T.T. and Schapira, A.H. (2003) Genetic and environmental factors in the cause of Parkinson's disease. *Ann Neur,* **53 Suppl 3,** S16-23; discussion S23-5.

61. Campbell, K.P. (1995) Three muscular dystrophies: loss of cytoskeleton-extracellular matrix linkage. *Cell,* **80,** 675-9.
62. Anderson, J.L., Head, S.I., Rae, C. and Morley, J.W. (2002) Brain function in Duchenne muscular dystrophy. *Brain,* **125,** 4-13.
63. Blake, D.J. and Kroger, S. (2000) The neurobiology of duchenne muscular dystrophy: learning lessons from muscle? *Trends Neurosci,* **23,** 92-9.
64. Grady, R.M., Wozniak, D.F., Ohlemiller, K.K. and Sanes, J.R. (2006) Cerebellar synaptic defects and abnormal motor behavior in mice lacking alpha- and beta-dystrobrevin. *J Neurosci,* **26,** 2841-51.
65. Knuesel, I., Mastrocola, M., Zuellig, R.A., Bornhauser, B., Schaub, M.C. and Fritschy, J.M. (1999) Short communication: altered synaptic clustering of GABAA receptors in mice lacking dystrophin (mdx mice). *Eur J Neurosci,* **11,** 4457-62.
66. Moore, S.A., Saito, F., Chen, J., Michele, D.E., Henry, M.D., Messing, A., Cohn, R.D., Ross-Barta, S.E., Westra, S., Williamson, R.A. *et al.* (2002) Deletion of brain dystroglycan recapitulates aspects of congenital muscular dystrophy. *Nature,* **418,** 422-5.
67. Imamura, M., Araishi, K., Noguchi, S. and Ozawa, E. (2000) A sarcoglycan-dystroglycan complex anchors Dp116 and utrophin in the peripheral nervous system. *Hum Mol Genet,* **9,** 3091-100.
68. Tinsley, J.M. and Davies, K.E. (1993) Utrophin: a potential replacement for dystrophin? *Neuromuscul Disord,* **3,** 537-9.
69. Korpi, E.R., Kleingoor, C., Kettenmann, H. and Seeburg, P.H. (1993) Benzodiazepine-induced motor impairment linked to point mutation in cerebellar GABAA receptor. *Nature,* **361,** 356-9.
70. Radel, M., Vallejo, R.L., Iwata, N., Aragon, R., Long, J.C., Virkkunen, M. and Goldman, D. (2005) Haplotype-based localization of an alcohol dependence gene to the 5q34 {gamma}-aminobutyric acid type A gene cluster. *Arch Gen Psychiatry,* **62,** 47-55.
71. Papadimitriou, G.N., Dikeos, D.G., Karadima, G., Avramopoulos, D., Daskalopoulou, E.G., Vassilopoulos, D. and Stefanis, C.N. (1998) Association between the GABA(A) receptor alpha5 subunit gene locus (GABRA5) and bipolar affective disorder. *Am J Med Genet A,* **81,** 73-80.
72. Ma, D.Q., Whitehead, P.L., Menold, M.M., Martin, E.R., Ashley-Koch, A.E., Mei, H., Ritchie, M.D., Delong, G.R., Abramson, R.K., Wright, H.H. *et al.* (2005) Identification of significant association and gene-gene interaction of GABA receptor subunit genes in autism. *Am J Med Genet A,* **77,** 377-88.
73. Wagstaff, J., Knoll, J.H., Fleming, J., Kirkness, E.F., Martin-Gallardo, A., Greenberg, F., Graham, J.M., Jr., Menninger, J., Ward, D., Venter, J.C. *et al.* (1991) Localization of the gene encoding the GABAA receptor beta 3 subunit to the Angelman/Prader-Willi region of human chromosome 15. *Am J Med Genet A,* **49,** 330-7.
74. Cossette, P., Liu, L., Brisebois, K., Dong, H., Lortie, A., Vanasse, M., Saint-Hilaire, J.M., Carmant, L., Verner, A., Lu, W.Y. *et al.* (2002) Mutation of GABRA1 in an autosomal dominant form of juvenile myoclonic epilepsy. *Nat Genet,* **31,** 184-9.

75. Alderton, W.K., Cooper, C.E. and Knowles, R.G. (2001) Nitric oxide synthases: structure, function and inhibition. *Biochemic J,* **357,** 593-615.
76. Kadekaro, M. and Summy-Long, J.Y. (2000) Centrally produced nitric oxide and the regulation of body fluid and blood pressure homeostases. *Clin Exp Pharmacol Physiol,* **27,** 450-9.
77. Lee, K.H., Baek, M.Y., Moon, K.Y., Song, W.K., Chung, C.H., Ha, D.B. and Kang, M.S. (1994) Nitric oxide as a messenger molecule for myoblast fusion. *J Biol Chem,* **269,** 14371-4.
78. Kobzik, L., Reid, M.B., Bredt, D.S. and Stamler, J.S. (1994) Nitric oxide in skeletal muscle. *Nature,* **372,** 546-8.
79. Esplugues, J.V. (2002) NO as a signalling molecule in the nervous system. *Br J Pharmacol,* **135,** 1079-95.
80. Brenman, J.E., Chao, D.S., Xia, H., Aldape, K. and Bredt, D.S. (1995) Nitric oxide synthase complexed with dystrophin and absent from skeletal muscle sarcolemma in Duchenne muscular dystrophy. *Cell,* **82,** 743-52.
81. Crosbie, R.H., Barresi, R. and Campbell, K.P. (2002) Loss of sarcolemma nNOS in sarcoglycan-deficient muscle. *Faseb J,* **16,** 1786-91.
82. Dreyer, J., Schleicher, M., Tappe, A., Schilling, K., Kuner, T., Kusumawidijaja, G., Muller-Esterl, W., Oess, S. and Kuner, R. (2004) Nitric oxide synthase (NOS)-interacting protein interacts with neuronal NOS and regulates its distribution and activity. *J Neurosci,* **24,** 10454-65.
83. Christopherson, K.S., Hillier, B.J., Lim, W.A. and Bredt, D.S. (1999) PSD-95 assembles a ternary complex with the N-methyl-D-aspartic acid receptor and a bivalent neuronal NO synthase PDZ domain. *J Biol Chem,* **274,** 27467-73.
84. Jaffrey, S.R., Benfenati, F., Snowman, A.M., Czernik, A.J. and Snyder, S.H. (2002) Neuronal nitric-oxide synthase localization mediated by a ternary complex with synapsin and CAPON. *Proc Natl Acad Sci U S A,* **99,** 3199-204.
85. Govers, R. and Oess, S. (2004) To NO or not to NO: 'where?' is the question. *Histol Histopathol,* **19,** 585-605.
86. Albrecht, D.E. and Froehner, S.C. (2002) Syntrophins and dystrobrevins: defining the dystrophin scaffold at synapses. *Neuro-Signals,* **11,** 123-9.
87. Sattler, R., Xiong, Z., Lu, W.Y., Hafner, M., MacDonald, J.F. and Tymianski, M. (1999) Specific coupling of NMDA receptor activation to nitric oxide neurotoxicity by PSD-95 protein. *Science,* **284,** 1845-8.
88. Cheng, A., Wang, S., Cai, J., Rao, M.S. and Mattson, M.P. (2003) Nitric oxide acts in a positive feedback loop with BDNF to regulate neural progenitor cell proliferation and differentiation in the mammalian brain. *Dev Biol,* **258,** 319-33.
89. Matarredona, E.R., Murillo-Carretero, M., Moreno-Lopez, B. and Estrada, C. (2004) Nitric oxide synthesis inhibition increases proliferation of neural precursors isolated from the postnatal mouse subventricular zone. *Brain Res,* **995,** 274-84.
90. Phung, Y.T., Bekker, J.M., Hallmark, O.G. and Black, S.M. (1999) Both neuronal NO synthase and nitric oxide are required for PC12 cell differentiation: a cGMP independent pathway. *Brain Res,* **64,** 165-78.
91. Brenman, J.E., Chao, D.S., Gee, S.H., McGee, A.W., Craven, S.E., Santillano, D.R., Wu, Z., Huang, F., Xia, H., Peters, M.F. *et al.* (1996) Interaction of nitric

oxide synthase with the postsynaptic density protein PSD-95 and alpha1-syntrophin mediated by PDZ domains. *Cell,* **84,** 757-67.
92. Crosbie, R.H. (2001) NO vascular control in Duchenne muscular dystrophy. *Nat Med,* **7,** 27-9.
93. Barton, E.R., Morris, L., Kawana, M., Bish, L.T. and Toursel, T. (2005) Systemic administration of L-arginine benefits mdx skeletal muscle function. *Muscle & nerve,* **32,** 751-60.
94. Nelson, R.J., Demas, G.E., Huang, P.L., Fishman, M.C., Dawson, V.L., Dawson, T.M. and Snyder, S.H. (1995) Behavioural abnormalities in male mice lacking neuronal nitric oxide synthase. *Nature,* **378,** 383-6.
95. Huang, Z., Huang, P.L., Panahian, N., Dalkara, T., Fishman, M.C. and Moskowitz, M.A. (1994) Effects of cerebral ischemia in mice deficient in neuronal nitric oxide synthase. *Science,* **265,** 1883-5.
96. Braissant, O., Gotoh, T., Loup, M., Mori, M. and Bachmann, C. (1999) L-arginine uptake, the citrulline-NO cycle and arginase II in the rat brain: an in situ hybridization study. *Brain Res,* **70,** 231-41.
97. Liu, P., Jenkins, N.A. and Copeland, N.G. (2003) A highly efficient recombineering-based method for generating conditional knockout mutations. *Genome Res,* **13,** 476-84.
98. Southern, E.M. (1992) Detection of specific sequences among DNA fragments separated by gel electrophoresis. 1975. *Biotechnology (Reading, Mass,* **24,** 122-39.
99. Joyner, A.L. (2000) *Gene targeting : a practical approach.* 2nd ed. Oxford University Press, Oxford ; New York.
100. Yip, D.J. and Picketts, D.J. (2003) Increasing D4Z4 repeat copy number compromises C2C12 myoblast differentiation. *FEBS letters,* **537,** 133-8.
101. Yokoi, F., Dang, M.T., Mitsui, S. and Li, Y. (2005) Exclusive paternal expression and novel alternatively spliced variants of epsilon-sarcoglycan mRNA in mouse brain. *FEBS letters,* **579,** 4822-8.
102. Orimo, A., Tominaga, N., Suzuki, M., Kawakami, T., Kuno, J., Sato, M., Minowa, O., Inoue, S., Kato, S., Noda, T. *et al.* (1999) Successful germ-line transmission of chimeras generated by coculture aggregation with J1 ES cells and eight-cell embryos. *Anal Biochem,* **269,** 204-7.
103. Clarke, K.A. and Still, J. (1999) Gait analysis in the mouse. *Physiol Behav,* **66,** 723-9.
104. Clarke, K.A. and Still, J. (2001) Development and consistency of gait in the mouse. *Physiol Behav,* **73,** 159-64.
105. Andreassen, O.A., Ferrante, R.J., Klivenyi, P., Klein, A.M., Shinobu, L.A., Epstein, C.J. and Beal, M.F. (2000) Partial deficiency of manganese superoxide dismutase exacerbates a transgenic mouse model of amyotrophic lateral sclerosis. *Ann Neurol,* **47,** 447-55.
106. Tang, X., Orchard, S.M. and Sanford, L.D. (2002) Home cage activity and behavioral performance in inbred and hybrid mice. *Behav Brain Res,* **136,** 555-69.
107. Kimhi, Y., Palfrey, C., Spector, I., Barak, Y. and Littauer, U.Z. (1976) Maturation of neuroblastoma cells in the presence of dimethylsulfoxide. *Proc Natl Acad Sci U S A,* **73,** 462-6.

108. Greengard, P., Valtorta, F., Czernik, A.J. and Benfenati, F. (1993) Synaptic vesicle phosphoproteins and regulation of synaptic function. *Science,* **259,** 780-5.
109. Inagaki, M., Nakamura, Y., Takeda, M., Nishimura, T. and Inagaki, N. (1994) Glial fibrillary acidic protein: dynamic property and regulation by phosphorylation. *Brain pathology (Zurich, Switzerland),* **4,** 239-43.
110. Kumar, J., Kumar, A., Das, S.K., Shukla, G. and Sengupta, S. (2005) Detection of differential gene copy number using denaturing high performance liquid chromatography. *J Biochem Biophys Methods,* **64,** 226-34.
111. Ferrari-Toninelli, G., Paccioretti, S., Francisconi, S., Uberti, D. and Memo, M. (2004) TorsinA negatively controls neurite outgrowth of SH-SY5Y human neuronal cell line. *Brain Res,* **1012,** 75-81.
112. Agrawal, N., Dasaradhi, P.V., Mohmmed, A., Malhotra, P., Bhatnagar, R.K. and Mukherjee, S.K. (2003) RNA interference: biology, mechanism, and applications. *Microbiol Mol Biol Rev,* **67,** 657-85.
113. Makinen, P.I., Koponen, J.K., Karkkainen, A.M., Malm, T.M., Pulkkinen, K.H., Koistinaho, J., Turunen, M.P. and Yla-Herttuala, S. (2006) Stable RNA interference: comparison of U6 and H1 promoters in endothelial cells and in mouse brain. *J Gene Med,* **8,** 433-41.
114. Kranenburg, O., Bouma, B., Gent, Y.Y., Aarsman, C.J., Kayed, R., Posthuma, G., Schiks, B., Voest, E.E. and Gebbink, M.F. (2005) Beta-amyloid (Abeta) causes detachment of N1E-115 neuroblastoma cells by acting as a scaffold for cell-associated plasminogen activation. *Mol Cell Neurosci.,* **28,** 496-508.
115. Ostlund, P., Lindegren, H., Pettersson, C. and Bedecs, K. (2001) Altered insulin receptor processing and function in scrapie-infected neuroblastoma cell lines. *Brain Res,* **97,** 161-70.
116. Ho, M. and Segre, M. (2001) Individual and combined effects of ethanol and cocaine on the human dopamine transporter in neuronal cell lines. *Neurosci Lett,* **299,** 229-33.
117. Serazin-Leroy, V., Denis-Henriot, D., Morot, M., de Mazancourt, P. and Giudicelli, Y. (1998) Semi-quantitative RT-PCR for comparison of mRNAs in cells with different amounts of housekeeping gene transcripts. *Mol Cell Probes,* **12,** 283-91.
118. Jung, R., Soondrum, K. and Neumaier, M. (2000) Quantitative PCR. *Clin Chem Lab Med,* **38,** 833-6.
119. Voet, D., Voet, J.G. and Pratt, C.W. (1999) *Fundamentals of biochemistry*. Wiley, New York.
120. Ciani, E., Severi, S., Contestabile, A., Bartesaghi, R. and Contestabile, A. (2004) Nitric oxide negatively regulates proliferation and promotes neuronal differentiation through N-Myc downregulation. *J Cell Sci,* **117,** 4727-37.